

WATCH-OVER – THE CONCEPT OF A COOPERATIVE SYSTEM FOR VEHICLE TO VULNERABLE ROAD USERS COMMUNICATION

Katrin Meinken

University of Stuttgart

Germany

Luisa Andreone

Andrea Guarise

Centro Ricerche Fiat

Italy

Axel Sikora

Steinbeis Research Institute Wireless Communications

Germany

Paper Number 07-0126

ABSTRACT

WATCH-OVER is a European Specific Targeted project co-funded by the European Commission Information Society and Media within the initiatives of the cooperative systems for traffic safety and efficiency based on communication and sensor technologies. The project, supported by EUCAR and coordinated by Centro Ricerche Fiat, includes in its consortium vehicle and motorcycle makers, technology, automotive suppliers and research centres for the design, development and testing phase.

The main goal of the WATCH-OVER project is to avoid road accidents that involve vulnerable road users such as pedestrians, cyclists and motorcyclists. The innovative system concept, presented in this paper, will be represented by the cooperation of an on-board platform and a vulnerable user module. It is based on the interaction between an in-vehicle unit and users' devices that will allow all road users to take an active part in traffic in urban and extra-urban areas. For that reason the WATCH-OVER project carries out research and development activities in order to design and develop an efficient system for accident prevention.

INTRODUCTION

The WATCH-OVER project aims at avoiding traffic accidents that involve vulnerable road users, namely pedestrians, bicyclists and motorcyclists, in urban and extra-urban areas. This objective is in line with the European Policies and the ambitious goal of halving the road fatalities in 2010. The project is co-funded by the European Commission Information Society Technology (IST) in the strategic objective "eSafety Co-operative Systems for Road Transport" and started its activity in January 2006.

In 2002 around one third of the total road accident fatalities have been vulnerable road users. This is still an unacceptable high number and needs to be reduced. WATCH-OVER will contribute to increase the safety for pedestrians, bicyclists and powered two wheeler riders. Therefore the WATCH-OVER project is carrying out research and development activities for the design and development of a cooperative system that is aiming at the circumvention of accidents involving vulnerable road users in urban and extra-urban environments. As stated in the 2005-6 Work Programme of the IST, the main objective of the WATCH-OVER project is "to develop and demonstrate cooperative systems for road transport that will make transport more efficient and effective, safer and more environmentally friendly." According to this objective, the system concept is based on the interaction of an in-vehicle module and vulnerable road user's devices. These devices will be directly integrated in powered two wheelers or in wearable objects like helmets, watches or consumer electronics. Such systems will notably enhance the support obtainable to drivers and other traffic participants.

The European funded projects PROTECTOR and SAVE-U had already been investigating accident prevention involving vulnerable road users. Both initiatives had as main objective the analysis of systems that are based on in-vehicle sensors. Different sensor technologies, such as microwave radar, near and far infrared, laser-radar and mono and stereo vision had been evaluated. The final outcome however shows that the extent to which these technologies are applicable is limited to those scenarios in which the vulnerable road users are not hidden by obstacles or located in a "blind area" of the sensors.

Thus the main difficulty in the detection of vulnerable road users in complex traffic is the limited “visibility” of car drivers and of in-vehicle sensor based systems. Additionally, the complexity of the traffic scenario presents a number of cases in which vulnerable road users are suddenly getting out from an area that was covered by other vehicles or by the infrastructure and therefore could not be seen by the driver in advance.

- The cooperative system of WATCH-OVER aims at enhancing these soft spots by focussing on advanced short range communication technologies in combination with the most promising video sensing technologies. By this combination of technologies the detection of vulnerable road users in complex traffic shall be enabled and therewith the most critical road scenarios shall be covered.

The technological challenge will be the development of a cooperative system for real time detection and relative localisation of vulnerable road users that includes innovative short range communication and video sensing technologies. The implementation challenge will be the deployment of a reliable system that is versatile for different vehicles and vulnerable road users.

The system will be limited to urban and extra-urban areas only, so traffic situations on motorways or speeds higher than a certain threshold find no consideration in this project. To ensure an expedient design and development and the technical feasibility of the co-operative vehicle-user system, the WATCH-OVER consortium consists of vehicle and PTW manufacturers, technology, automotive suppliers and research centres for its development and testing phase.

In this paper the results of the first project activities are presented. The most relevant information needed for the development of the WATCH-OVER system is given as well as an overview on the defined traffic scenarios and use cases.

OVERALL PROJECT ORGANISATION

To succeed in developing an efficient cooperative system for accident prevention, the work in the WATCH-OVER project is divided into seven different work packages (WPs). In these work packages the tasks for the involved partners in the project are defined as follows:

WP1 Project management and exploitation

WP1 deals with the management of all financial, administrative, technical and non-technical aspects of the project. Key activities of this work package are the exploitation of project results, the association to other related R&D projects and the standardisation bodies.

WP2 User requirements and scenarios

The goal of WP2 is to identify the needs and requirements of the target users as well as to analyse the most relevant scenarios of application.

WP3 Overall system specification

In WP3 the functional architecture specifications of the WATCH-OVER system is defined. Furthermore, all communication and sensor technologies as well as the warning and intervention strategy will be specified.

WP4 Communication and Sensing Technologies

WP4 deals with the major technological aspects of the project. It will analyse and adapt the selected communication and sensing technologies and will additionally work on data fusion.

WP5 System development

In WP5 the different subsystems are developed as well as the on-board and wearable devices and related software applications. A particular attention is given to the HMI design for the driver and for the VRU.

WP6 Cooperative system test and validation

In WP6 the WATCH-OVER application will be integrated in the demonstrators for testing. The demonstrators will be: the vehicles, cars and motorbike and the wearable module. Besides technical and user acceptance tests will be performed.

WP7 Deployment strategies and dissemination

WP7 deals with the strategies related to the deployment of the WATCH-OVER system. In particular, the main activities are a thorough market analysis as well as a cost/benefit analysis, the evaluation of the impact on road safety and the dissemination of the project activities.

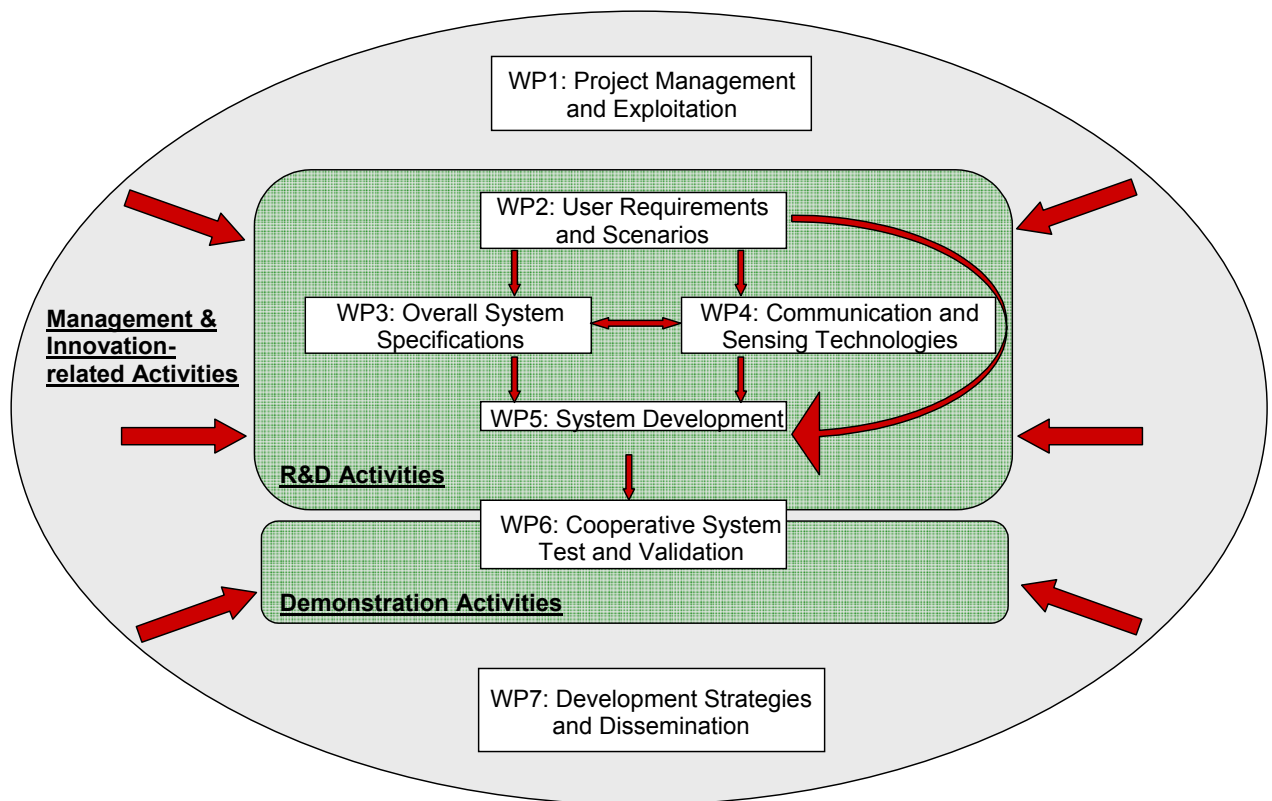


Figure 1. Overview on the WATCH-OVER project activities.

The chart visualises the organisation of the WATCH-OVER project, structured in the following main phases:

- “User Requirements and Needs” phase (WP2).
- “System Specification” phase (WP3).
- “System Development” phase (WP4 / WP5).
- “Testing and Validation” phase (WP6).
- WP1 and WP7 belong to the transversal phase that includes all horizontal activities.

THE WATCH-OVER SYSTEM CONCEPT

The WATCH-OVER system is composed of different components that are cooperating at the detection of vulnerable road users in urban or extra-urban scenarios. The system will enable the cooperation of different actors who communicate with each other in order to exchange data and share information.

While the vehicle moves along a road there are two sensing system in charge of collecting information of the external scenario, a vision sensor device and a communication module.

Vulnerable road users that are in a potentially dangerous position in front or nearby a vehicle equipped with the WATCH-OVER system will be identified with the vision sensor that recognises objects and motions and with the communication

module that gathers the responding signals in the covered area. The vision sensor device focuses on the frontal part of the car and recognises objects and their motion on the image pattern. The communication module searches for responding signals in the area covered from the antenna(s) and calculates the relative position of each answering signal. The on-board device collects the different input and evaluates the risk level for possible colliding trajectories by means of data fusion. In case the risk level passes a certain threshold there will be both an alert to the driver and to the VRU module.

The reference architecture for the WATCH-OVER system is depicted in Figure 2. It presents the different components that each specific actor shall be equipped with:

- The car shall be equipped with the vision based sensor, the communication device and an on-board unit that performs data fusion and evaluates the objects relative positioning.
- The motorcycle shall be equipped with a communication system and an on-board unit able

to collect and store information on the surrounding traffic flow.

- The pedestrian or bicyclist shall be equipped with a wearable communication module in order to be able to be recognised from vehicles equipped with the WATCH-OVER system

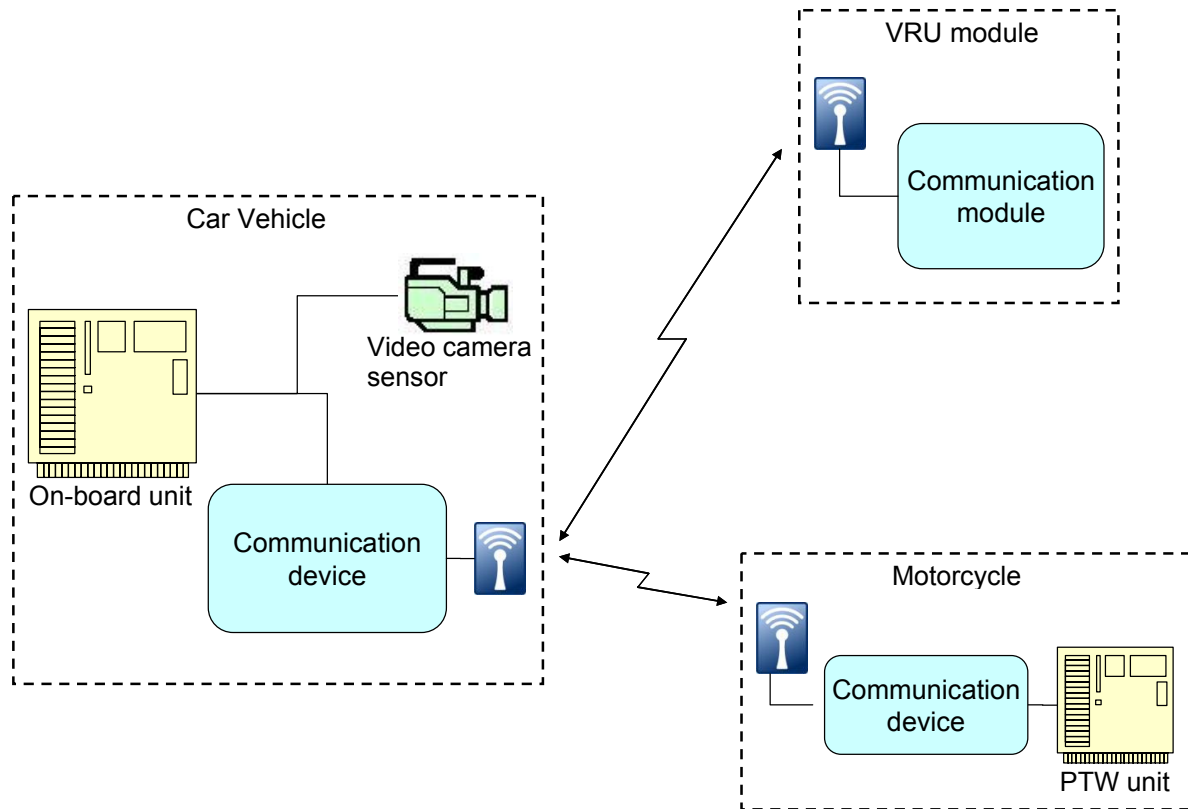


Figure 2. WATCH-OVER reference architecture scheme.

The above illustrated architecture organisation gives an overview on the used technologies for the different involved actors of the WATCH-OVER system. For general observation the video camera sensor is used on all car maker vehicles, the communication module will be present in one of the car manufacturer vehicles and in the PTW and additionally there will be a vulnerable road user module that is assembled with the communication short range technology.

The idea behind this architecture approach is that the WATCH-OVER cooperative system shall guarantee:

- a wider scenario coverage including blind spots and
- a flexible and open architecture.

Based on the use of most promising communication technologies in combination with most promising vision sensor technologies the WATCH-OVER system architecture presents the foundation for an

efficient system for accident prevention that will further advance the findings of the preceding European projects PROTECTOR and SAVE-U. In order to do so the following characteristics will account for the design of the WATCH-OVER system:

- the extension of the “protection concept” by an effective driver warning and vehicle braking strategy,
- an increased vehicle speed range (up to 50 km/h) at which the system is operable,
- high reliability and timely performances related to the detection and localisation of the vulnerable road users,
- low cost sensor and communication technologies,
- an increased processing speed (more than 10 Hz),
- an increased sensor coverage (0–20m).

Specifically, the WATCH-OVER cooperative platform is expected to perform the following tasks efficiently:

- to promptly answer to vehicle's stimulus delivering its identification parameters,
- to send back a few self-localisation parameters,
- to give feedback to the specific traffic participants with an appropriate interface.

The WATCH-OVER application, consisting of the in-vehicle control unit and the communication and image sensing modules as well as the wearable devices including communication technology, will be tested to verify technical performances and user acceptance. Therefore it will be implemented in three demonstrator vehicles. As demonstrators two cars and one motorcycle will be used. For more complex traffic scenarios simulation tools will be applied.

COMMUNICATION AND SENSOR TECHNOLOGIES FOR VEHICLES AND VULNERABLE ROAD USERS

From the preceding projects PROTECTOR and SAVE-U substantial progresses have been achieved. While the PROTECTOR project showed that sensor technologies, such as stereo vision, laser scanner or 24 GHz radar, are suitable for the detection of pedestrians, the SAVE-U project showed that the fusion of GHz radar, a far infrared and a colour-video camera improved the detection performance of the PROTECTOR system by an order of magnitude concerning the number of false classifications.

The cooperative platform of the WATCH-OVER system will not only reduce the number of false classifications and extend the actual coverage of the state of the art technologies but will also be open to integrate localisation technologies.

The huge variety of different urban and extra-urban scenarios that involve numerous vulnerable road users is one of the main challenges the project is facing. Therefore the in-vehicle system is conceived to feature the following functionalities:

- real-time detection of pedestrians, cyclists, motorcyclists equipped with the WATCH-OVER module,
- calculation of the relative positioning of the user vs. drivers,
- detection of dangerous situations,
- appropriate warning to the driver, providing information only in really dangerous situations.

The sensing technologies that support the detection of vulnerable road users can be summarised in the following categories:

- Far infrared systems
- Vision based systems
- Microwave radar
- Laser radar.

The short range wireless communication technologies that support the detection of vulnerable road users can be summarised as following:

- Wireless Fidelity (WI-FI)
- IEEE 802.15
- Bluetooth
- Radio Frequency Identification (RFID)
- Ultra Wideband (UWB).

To identify those technologies suitable for the use in users' localisation mechanisms and to enhance cooperative systems even further, a set of state of the art technologies have been examined.

The communication system shall allow a two way communication between vehicles and vulnerable road users. The vulnerable road user shall be able to communicate with several vehicles and, conversely one vehicle shall be able to communicate with several vulnerable road users.

The in-vehicle and the wearable modules shall both have identical functionality regarding their Radio-Frequency-(RF)-modules.

The two way communication is required due to the following reasons:

- It should be possible to send out data from the vulnerable road user to the vehicle, so that the in-vehicle module can receive information about the position and the activity of the vulnerable road user. In addition, the RF-waves help to determine the local position of the VRU with regard to the vehicle.
- It should also be possible to send data from the vehicle to the vulnerable road user. This data might include:
 - a) Information about the actual results of the in-vehicle module, e.g. a warning to the vulnerable road user about a potential risk.
 - b) Control information to the wearable unit, e.g. detection of presence to increase the frame frequency.

The following pictures show typical situations in which the WATCH-OVER system platform will be applied and where the communication between the in-vehicle and the vulnerable road user module is established:



Figure 3. Typical scenarios in which the WATCH-OVER system will be applied.

From the scouting activities mentioned above, the following overall situation could be derived.

- It is assessed that communication based localisation and information flow between a vulnerable road user and a vehicle provide an additional means of increasing the accuracy of detection, ranging, and localisation.
- A broad variety of technologies exist. Due to cost, size, energy consumption and availability reasons, Short Range Wireless Communication (SRWN) are a major candidate to provide communication and localisation.
- Technologies and products for SRWN rapidly evolve. A broad choice is available for communication purposes.
- From this large choice, only selected technologies are inherently suitable to offer ranging and localisation.
- The number of technologies can be further reduced when two additional parameters are regarded:
 1. The accuracy of many of the inherently location-capable systems is at a low level, so that the use cases of the WATCH-OVER project cannot be covered.
 2. Practically all RF-systems working in the GHz-range are theoretically capable to support ranging. However, for doing this they must be equipped with additional circuitry, which accesses the low-level, high-accuracy timing information at the signal input. Therefore, it is only realistic to use existing hardware.

Many of the ranging-capable systems are either only prototypes, or are addressing a different market.

- This could be observed for most of the UWB-based products, where contacts to the manufacturers showed their meagre interest in applications beyond consumer electronics.

- Unfortunately the same situation was encountered during the examination of other eSafety-related communication protocols and products.

Taking into account the above mentioned parameters and the evaluation of existing technologies, it was decided to further proceed with the following approaches Based on the evaluation done above:

- A Chirp Spread Spectrum (CSS)-based system, described in IEEE802.15.4a, turns out to provide a good trade-off between bandwidth consumption, hardware efforts and achievable accuracy. This was evaluated under real-life conditions in extensive measurement sessions. CSS-based systems are already available as an integrated circuit (IC), allowing low power, low footprint and flexible designs at reasonable cost.
- UWB-systems promise a good accuracy, if time-of-flight measurements are used. This could be affirmed through various simulations. The simulation was oriented towards an UWB-emulator. This system comes with a very generic approach and promises a very high flexibility.
- Systems for self-localisation allow accuracy well below the level of the two relative ranging systems selected above). However, due to their absolute positioning, they allow consistency checks and maps. As GPS / Galileo based systems are assumed to come for free in future product generations, it is reasonable to include their information into the sensor fusion, as well.

During all the future efforts, the aspects of security and privacy must be considered.

USER REQUIREMENTS AND RELEVANT SCENARIOS

Besides defining the technologies used for developing a cooperative system for the prevention of accidents, it is very important to analyse the needs of the future user and to describe the relevant scenarios in which the system will be applied.

The analysis of the user requirements has to be conducted at the beginning of the project as they are of crucial importance for the development and implementation of the system hardware and software architecture. In the WATCH-OVER project user requirements have been interrogated by a questionnaire that was answered by non-technical experts, who were pedestrians and drivers themselves and commute regularly with cars, motorcycles and bicycles. The questionnaire was divided into two different parts:

1. One part acquired the user requirements concerning the in-vehicle Human Machine Interface (HMI).
2. The other part retrieved the prioritisation of the before established traffic scenarios and the possibility to propose new accident situations.

The first part of the questionnaire focused on the prospective output of the WATCH-OVER system. In particular on how and when a warning or information should be given. Users were asked to specify their preferences and, according to their answers, system requirements could be derived:

In case of no accident risk,

3. the system should only inform the driver of the presence of VRUs (location, distance, etc.) on demand.
4. the visual information should appear on the head up display or on the instrument cluster.
5. the system should inform the driver of the presence of VRUs regarding the distance and the heading of the vulnerable road user on demand only.

In case of an acute accident risk due to the presence of a VRU,

6. the system should warn the driver.
7. the warning should be a tone/beep or an icon on the display.
8. secondary important information provided, are the relative position, the weather, the height of the pedestrian and the momentum.
9. These information (see item 5 and 6) should be presented by an icon on display or by a tone/beep.

In addition general conclusions concerning the set up of an efficient HMI could be derived from

previous projects and they were considered important for the WATCH-OVER project as well:

- The allowance for false alarm should be very low. If a driver perceives too many false alarms, the warning will be ignored.
- The warning should be given acoustically and therefore must be heard.
- Mere visual information is not sensible and might possibly decrease safety due to its distraction effect. A combination with acoustic information might be useful.
- The warning should be given early enough to allow the driver to react well considered.

The second part of the questionnaire displayed 16 traffic scenarios to the users and asked for a prioritisation according to the estimated frequency, the level of support needed and the conditions under which support would be needed most. The scenarios were defined beforehand by a multiple approach. First of all the available data on road accidents involving vulnerable road user were analysed as well as the outcomes of previous projects focusing on similar topics as WATCH-OVER, then an expert group of the WATCH-OVER project reviewed the systematic definition of the scenarios and assigned the final list of relevant scenarios. This list of relevant scenarios was then displayed to the external non-technical users.

The result of this user requirement survey is the selection of eight use cases that will be approached in the course of the WATCH-OVER project. The use cases are prioritised according to the estimated relevance for road safety. The key parameters that describe the use cases even further were set up by experts and evaluated by users and can be described as the following:

- Type of vehicle / vulnerable road user
- Type of road.
- Relative trajectories.
- Vehicle's / vulnerable road users' speed.
- Time to collision.
- Time of day.
- Weather.

The scenarios have been grouped according to the estimated occurrence and the relevance for road safety. Only those scenarios indicating a high estimated occurrence as well as a high relevance for road safety will be directly addressed by the WATCH-OVER system development. Scenarios with only a medium estimated occurrence and therefore with a medium expected impact on road safety were also considered but will not directly affect the WATCH-OVER project.

The following sketches demonstrate those scenarios affecting the WATCH-OVER system directly and thus being addressed in the testing phase.

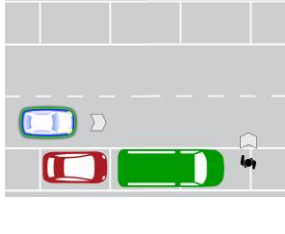
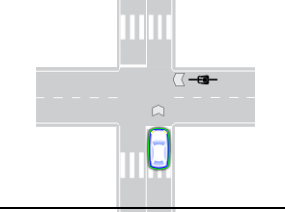
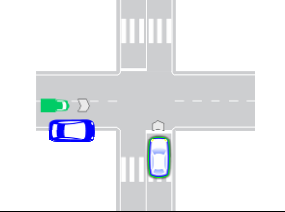
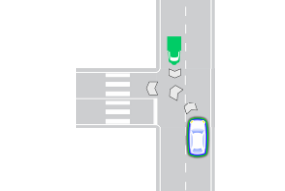
Description	Sketch
1. Pedestrian (or cyclist) crossing the road from the right to the left.	
2. Pedestrian (or cyclist) crossing the road from the right to the left (or from the left to the right) occluded from parked or stopped cars or other obstacles.	
3. Vehicle turning left at an intersection, pedestrian crossing the road from the right to the left (or from the left to the right).	
4. Vehicle turning right at an intersection, pedestrian (or cyclist) crossing the road from the right to the left (or from the left to the right).	
5. Vehicle on a crossroad, pedal cyclist crossing the road from the right (or from the left).	
6. PTW arrives from left side (or from right side) at intersection, paths perpendicular.	
7. PTW arrives from left side at intersection, paths perpendicular, occluded from parked car or other obstacles.	
8. PTW (or pedal cyclist) and vehicle travelling in opposite directions, vehicle turns in front of PTW.	

Figure 4. Scenarios addressed by the WATCH-OVER system.

WATCH-OVER HMI CONCEPT

In the WATCH-OVER expert workshop not only issues regarding the identification of traffic scenarios and user needs have been discussed, but also issues relating to the development and implementation of the WATCH-OVER Human Machine Interface (HMI). The main objective of the HMI was to diminish the number of false alarms or warnings given by the interface in order to avoid an information overload for the driver or the vulnerable road user. The best solution of course would be to evade false alarms completely. To realise a system that is efficient in driver warning it is important to be coherent throughout the warning strategy and to avoid redundancy.

To establish a coherent warning strategy, the WATCH-OVER warning concept follows the approach of Wickens et al. (2004): “The goal [of a warning] is to get the user to comply with the warning and, therefore, use the product in a safe way, or avoid unsafe behaviour.”

To achieve this professed goal four elementary requirements have to be fulfilled:

- The warning must be noticed.
- The warning must be perceived (read/heard).
- The warning must be understood.
- The warning must be accepted.

That means in detail that a warning has to draw attention of the driver or the vulnerable road user. In a second step it has to be ensured that the warning is not only noted by the addressee but moreover apprehended and then accepted. In addition the system should be able to give information about the identified risk and about recommendable actions to be taken by the driver or the vulnerable road user.

Besides defining the approach for an efficient warning strategy it is also crucial to analyse and then follow existing standards, guidelines and recommendations for HMI design as well as those still under construction in order to comply with statutory provisions.

The major requirements for HMI functionality that will be followed by the WATCH-OVER system are listed below:

- The system must comply with relevant regulation and standards.
- The system supports the driver and does not increase driver distraction from driving task.
- The system shall not require uninterruptible sequences of interaction.
- The system does not distract or visually entertain the driver.

- No part of the system should obstruct the driver's view of the road scene.
- The system response (e.g. feedback, confirmation) following driver input should be timely and clearly perceptible.
- Information which has the highest safety relevance should be given priority.
- The behaviour of the system should not adversely interfere with the display or controls required for the primary driving task and for road safety.

- The system must be error relevant.

The main goal of the WATCH-OVER HMI, as stated before, is the avoidance of misunderstandings and of an overload of the addressee, in WATCH-OVER namely the driver or the vulnerable road user. Only information assisting the driver more than distracting him in complex traffic situations should be provided by the HMI.

Thus the WATCH-OVER HMI persecutes the following approach:

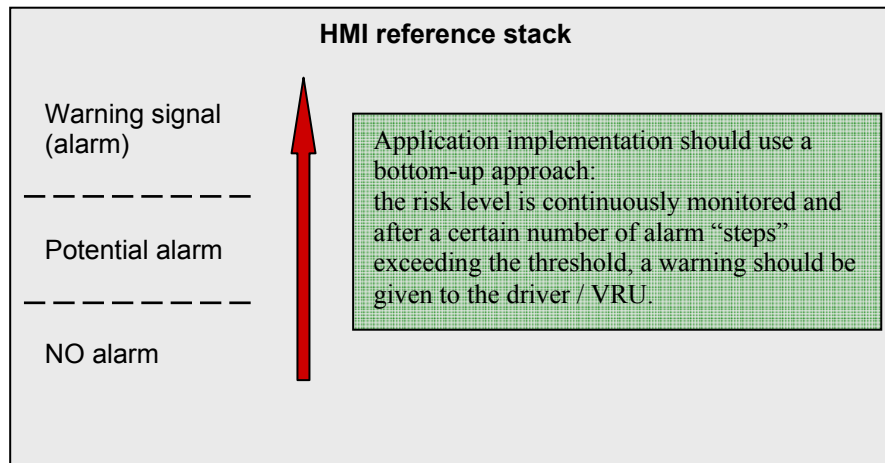


Figure 5. HMI approach followed within the WATCH-OVER project.

This concept foresees a continuous evaluation of the risk level by the WATCH-OVER system. If the risk level is approaching a certain threshold that was specified beforehand, the system will give a warning to the driver or the vulnerable road user respectively. The thresholds will be identified according to the different risk levels.

This approach is adopted because the WATCH-OVER experts assume that it will ensure a system development that does not potentially distract the driver or the vulnerable road user but will instead assist him in complex traffic situations. Intrusiveness by the system has to be prevented as it may lead to switching off the system altogether. If the HMI interface is too pervasive, with an intensive visual or acoustical output presented to the user, it will give rise to an increase of distraction of the addressee. Thus it is important to not only minimise but eliminate false alarms as well as an overload of information in all cases if possible.

CONCLUSION

WATCH-OVER is a European project that aims at the design and development of an integrated cooperative system for the accident prevention involving vulnerable road users in urban and extra-urban areas. The project is coordinated by Centro Ricerche Fiat and assembles in its consortium 13 project partners from six different European countries. The consortium presents vehicle and PTW manufacturers, automotive suppliers, technology and research centres for the development and testing phase.

The system core is the cooperation of an in-vehicle unit with a user module based on communication and sensor technologies. The in-vehicle module will locate vulnerable road users that are in potentially hazardous locations and will then give a warning signal to the driver. On the other hand the wearable user module will draw attention of the vulnerable road users to dangerous traffic situations. The interaction of the different modules rests on the exploitation of innovative wireless short range communication technologies and promising sensor technologies. With this cooperation the actual coverage of existing systems will be extended and the WATCH-OVER platform

will in addition be open to the integration of localisation technologies.

The WATCH-OVER in-vehicle platform will then be supplied with the following main functionalities:

- Real-time detection of vulnerable road users (pedestrians, bicyclists, motorcyclists).
- Relative Positioning of the vulnerable road user vs. the driving vehicle.
- Identification of dangerous situations.
- Appropriate warning to the driver.

The project activities are now focusing on the final design of the system architecture. The most appropriate communication technologies will be selected and a new generation of CMOS cameras is being developed. Furthermore, the development phase of the WATCH-OVER HMI has just started and will be further promoted within the ongoing project activities.

An important milestone has been achieved by establishing the collaboration with the European project SAFESPOT. The applicability of the WATCH-OVER system is aspired within the future framework of the cooperative system for road safety developed within the SAFESPOT project.

Such cooperative platforms will significantly help accomplish the goal of reducing the number of road fatalities and thereby to further enhance road safety

REFERENCES

Andreone, L.; Bekiaris, E.; A. Guarise, A.; Mousadakou, A. (2006), *D2.1 "Requirements and use cases"*, WATCH-OVER project, July 2006

Andreone, L.; Guarise, A.; Lilli, F.; Gavrilu, D. M.; Pieve, M. (2006), "Cooperative Systems for Vulnerable Road Users: The Concept of the WATCH-OVER Project", 13th ITS World Congress, London, 2006

Barber, C. (1994). Psychological aspects of conventional in-car warning devices. In Stanton N. (Ed.), *Human Factors in Alarm Design* (pp. 193-205). London: Taylor & Francis.

European Commission, "Commission Recommendation of 21 December 2005 on safe and efficient in-vehicle information and communication systems: A European statement of principles on human machine interface", 2006

ISO 15008: Road vehicles – "Ergonomic aspects of transport information and control systems – Specifications and compliance procedures for in-vehicle visual presentation"

Kusmann, H. et al. (2004), "Requirements for AIDE HMI and safety functions", AIDE project, March 2004

Lerner, N. D.; Kotwal, B.M.; Lyons, R.D.; Gardner-Bonneau, D.J., "Preliminary Human Factors Guidelines for Crash Avoidance Warning Devices", National Technical Information Service, Springfield, 1996

Marberger, C., Dangelmaier, M., Bekiaris, E., Nikolaou, S. (2004). "User centred HMI development for the AWAKE vigilance monitoring system", Conference Proceedings FISITA 2004.

Sikora, A. (2006), D4.1 "Communication technologies specifications", WATCH-OVER project, December 2006

WATCH-OVER web site: www.watchover-eu.org

Wickens, C. D.; Lee, J. D.; Gordon Becker, S. E.; Liu, Y., "An introduction to human factors engineering", Pearson Education, Upper Saddle River, New Jersey, 2004

DEVELOPMENT OF AN FE BIOFIDELIC FLEXIBLE PEDESTRIAN LEG-FORM IMPACTOR (FLEX-GT-PROTOTYPE) MODEL

Takahiro Issiki

Atsuhiko Konosu

Japan Automobile Research Institute

Masaaki Tanahashi

Japan Automobile Manufacturers Association, Inc.

Japan

Paper Number 07-0179

ABSTRACT

The Japan Automobile Research Institute and the Japan Automobile Manufacturers Association, Inc., have been developing a biofidelic flexible pedestrian legform impactor (Flex-PLI) since 2002, and its latest version is called Flex-GT-prototype.

Flex-GT-prototype has flexible construction like human lower limb and is equipped with many sensors to evaluate the severity of pedestrian lower limb injuries in multiple locations. In this study, an FE Flex-GT-prototype model was developed, and its fidelity to an actual Flex-GT-prototype was verified at various evaluation conditions.

INTRODUCTION

Test methods for assessing the pedestrian protection performances of motor vehicles in pedestrian-vehicle collisions (hereafter simply "pedestrian protection test methods") were developed by EEVC (European Enhanced Vehicle-safety Committee), ISO (International Organization for Standardization) and IHRA (International Harmonized Research Activity) in the past. At the present, the Pedestrian Protection Informal Group belonging to the United Nations ECE/WP29/GRSP plays the central role in the development of international pedestrian protection test methods.

In these test methods, the pedestrian lower limb protection test method is designed to collide a leg-form impactor, simulating a human lower limb, against a car, and measure the intensity of impact on a leg-form impactor. Therefore leg-form impactors are required to be highly biofidelic (i.e. having a response-to-impact characteristic equivalent to that of the human leg) and to be highly injury-assessable (i.e. enabling to accurately estimate the severity of leg injury to realworld pedestrians). However, the conventional leg-form impactor "TRL-LFI" which was developed by Transport Research Laboratory (TRL)¹⁾ cannot reproduce the bending deformation characteristics of the human long bones due to the rigid structure of long bones, and the bending characteristics of the TRL-LFI knee is more stiffer than the one of human knee. For these reasons the

appropriateness of TRL-LFI as an assessment tool has been in question^{2),3)}.

From such a background, the Japan Automobile Research Institute and the Japan Automobile Manufacturers Association, Inc., started to develop a biofidelic flexible pedestrian legform impactor (Flex-PLI) in 2002^{3),4)}, and its latest version is called Flex-GT-prototype. In this study, a computer simulation model which has high capability on reproducing the Flex-GT-prototype responses was developed. The model can be used for finalizing the Flex-GT leg-form impactor specifications and improving various car front technologies for pedestrian lower limb protection.

FE FLEX-GT-PROTOTYPE MODEL

Model Construction

Figure 1 shows the overall construction of Flex-GT-prototype and its computer simulation finite element model ("FE Flex-GT-prototype model"). FE Flex-GT-prototype model is based on the Flex-PLI 2004 model developed by Honda R&D Co., Ltd.⁵⁾. The body construction of the FE Flex-GT-prototype model consists of the thigh, leg, and knee parts.

As shown in Figure 2(a), the FE Flex-GT-prototype model has similar constructions of the actual thigh and leg of the Flex-GT-prototype. Regarding the knee, the FE Flex-GT-prototype model also has similar construction of the actual knee of the Flex-GT-prototype, then employs bar elements to simulate the knee ligaments while Flex-GT-prototype employs cables and springs to serve as the knee ligaments, as shown in Figure 2(b).

As shown in Figure 3, the FE Flex-GT-prototype model has the similar construction of the flesh of Flex-GT-prototype, so as to add the deformation characteristics of flesh.

Measurement Items

Figure 4 shows the measurement items of Flex-GT-prototype. The strain which is generated at

various points on the surface of each bone core under an impact is measured by strain gages to determine the bending moment applied to the thigh and leg. The elongation which is generated in the knee ligaments due to the bending and shear deformation of the knee is measured by potentiometers installed along the ligaments. The FE Flex-GT-prototype model was designed to produce strain of the bone core (convert to bending moments using dynamic 3-point bending simulation results) and elongation of the knee ligaments, then can compare the actual Flex-GT-prototype measurement values.

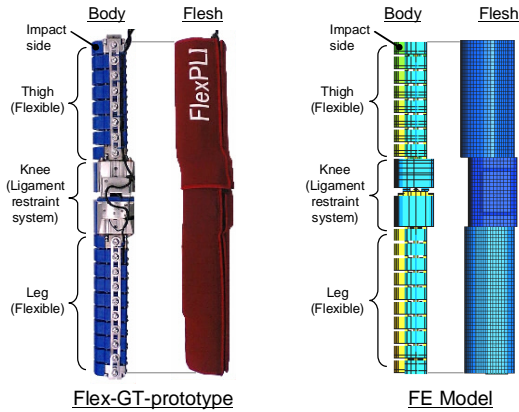


Figure 1. Overview of Flex-GT-prototype and FE Flex-GT-prototype model.

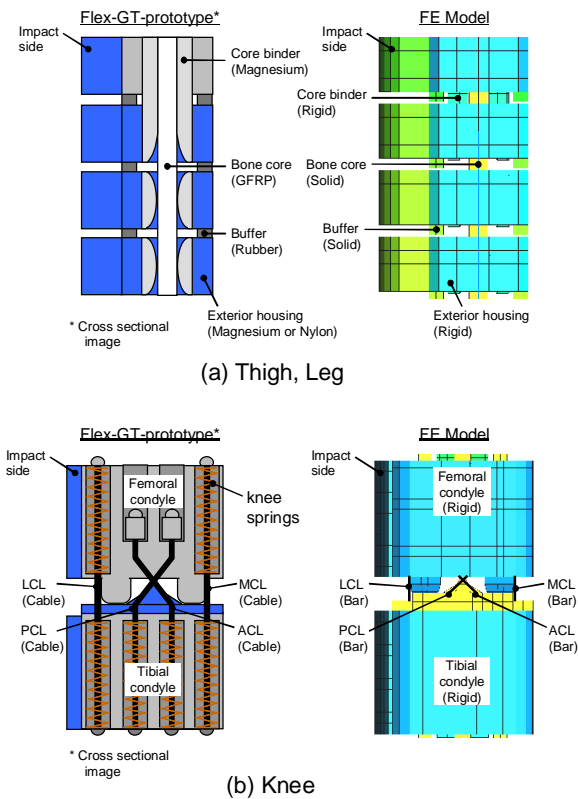


Figure 2. Body construction of Flex-GT-prototype and FE Flex-GT-prototype model.

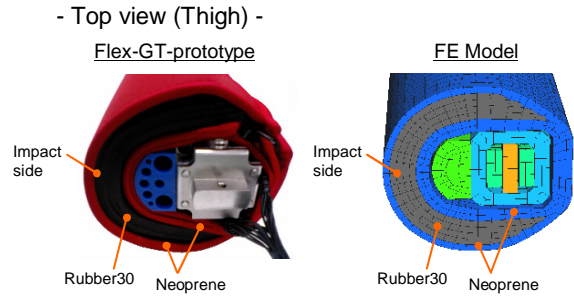


Figure 3. Flesh construction of Flex-GT-prototype and FE Flex-GT-prototype model.

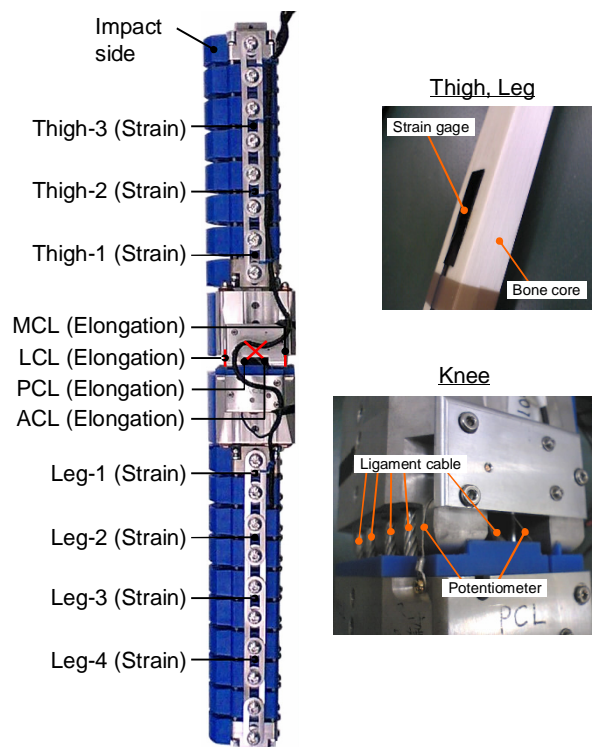


Figure 4. Measurement items of Flex-GT-prototype.

EVALUATION OF THE FE FLEX-GT-PROTOTYPE MODEL

The FE Flex-GT-prototype model was evaluated to verify its ability to simulate Flex-GT-prototype. The evaluation was conducted on the segmental models (Thigh, Leg, and Knee models), and the assembled model.

Evaluation of Segmental Models

Thigh and leg models

Figure 5 shows the dynamic 3-point bending simulation setup for evaluating the bending characteristics of the thigh and leg models. In this simulation, a solid ram was made to collide with the thigh or leg by free fall (Figures 6 and 7 shows the kinematics of thigh and leg 3-point bending), and the response characteristics of the thigh and leg models were compared with the experimental results of the Flex-GT-prototype thigh and leg.

Figures 8 and 9 compare the moment-deflection responses of the thigh and leg models with the experimental results of the Flex-GT-prototype thigh and leg in 3-point bending. The comparison indicates that, although the deformation characteristics of the thigh and leg models slightly vibrated in the early stage of deflection, the thigh and leg models both exhibited an overall deformation characteristic that is equivalent to the experimental results of the Flex-GT-prototype thigh and leg, respectively.

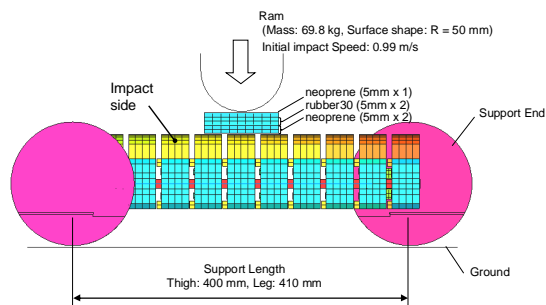


Figure 5. Dynamic 3-point bending simulation set up for thigh and leg of FE Flex-GT-prototype model.

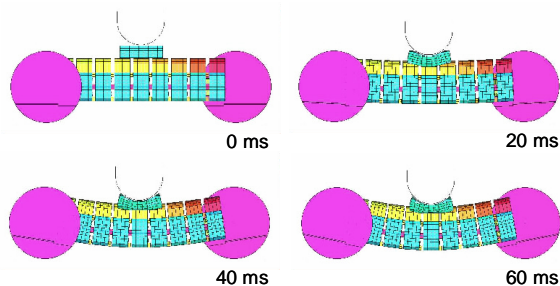


Figure 6. Thigh 3-point bending (Kinematics).

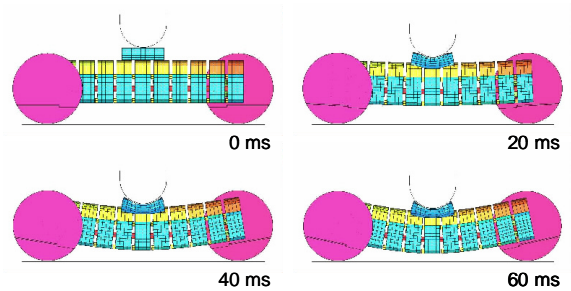


Figure 7. Leg 3-point bending (Kinematics).

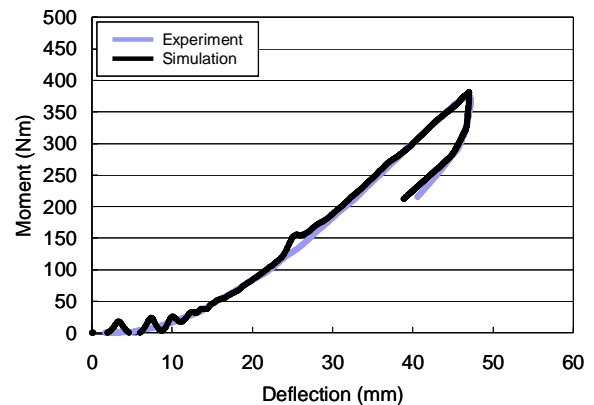


Figure 8. Comparison of moment-deflection response in dynamic thigh 3-point bending between experiment and simulation.

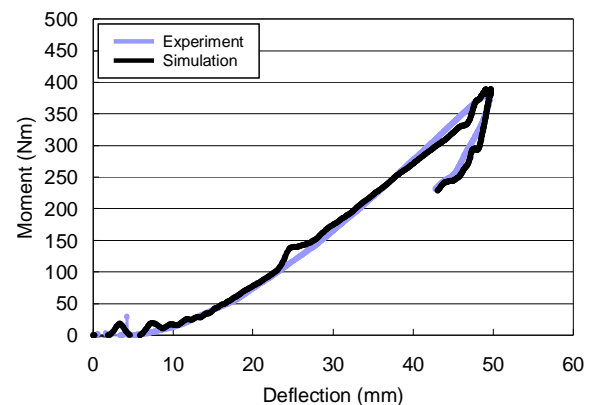


Figure 9. Comparison of moment-deflection response in dynamic leg 3-point bending between experiment and simulation.

Knee model

Figure 10 shows the dynamic 3-point bending simulation setup for evaluating the bending characteristics of the knee model. In this simulation, a solid ram was made to collide with the knee by free fall (Figures 11 shows the kinematics of knee 3-point bending), and the response characteristics of the knee model were compared with the experimental results of the Flex-GT-prototype knee.

Figure 12(a) compares the bending moment of the knee model with the experimental results of the Flex-GT-prototype knee in relation to the passage of time from the impact. Though containing some vibrations, the waveform of the knee model indicated an overall similarity to the experimental results of the Flex-GT-prototype knee.

Figure 12(b) compares the ligament elongation of the knee model with the experimental results of the Flex-GT-prototype knee in relation to the passage of time from the impact. The waveforms of the knee model indicated an overall similarity to the experimental results of the Flex-GT-prototype knee. Thus, the results reported in Figures 12(a) and 12(b) verify the equivalence of the knee model to the Flex-GT-prototype knee.

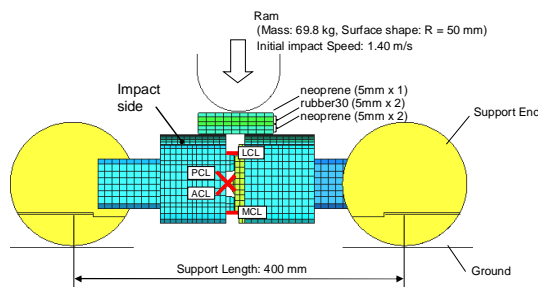


Figure 10. Dynamic 3-point bending simulation set up for knee of FE Flex-GT-prototype model.

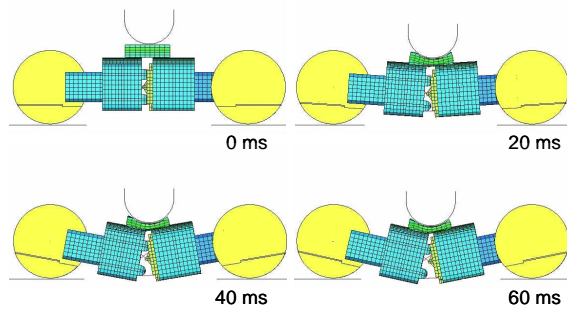
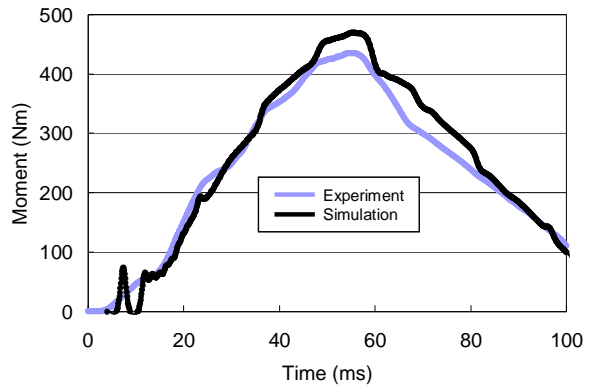
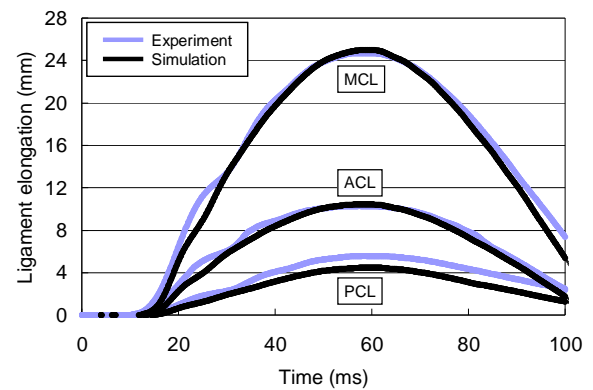


Figure 11. Knee 3-point bending (Kinematics).



(a) Moment



(b) Ligament elongation

Figure 12. Comparison of time history curve in dynamic knee 3-point bending between experiment and simulation.

Evaluation of Assembly Model

Assembly dynamic bending simulation

Figure 13 shows the dynamic bending simulation setup of the assembly model. In this simulation, the assembly model was made to collide with a rigid stopper by free fall from a rotational joint with a one degree of freedom. Then, the response characteristics of the assembly model were compared with the experimental results of Flex-GT-prototype.

Figure 14 reports the waveforms and maximum values recorded by the assembly model at its various measurement points, together with the experimental results of Flex-GT-prototype. Although the waveforms of the assembly model slightly vibrated, they proved to be similar to the measured waveforms of Flex-GT-prototype. There was also a high degree of congruence between the simulation results and experimental results relating to the maximum value and the time at which the maximum value was generated.

The above comparative results verify that the FE Flex-GT-prototype model in the dynamic bending simulation gives responses equivalent to the responses of Flex-GT-prototype in its real calibration test.

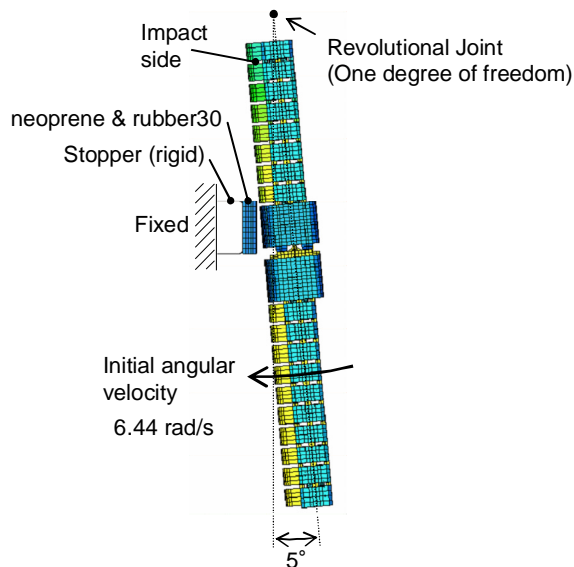
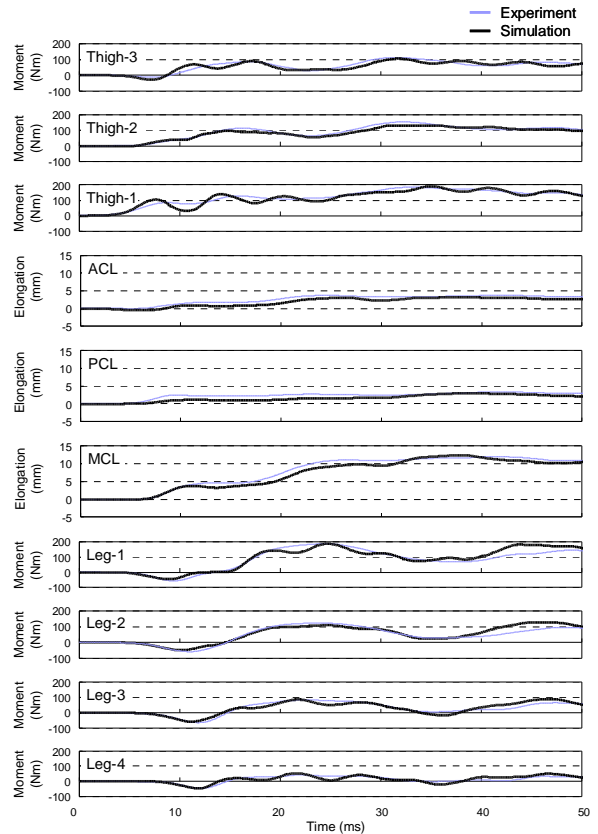
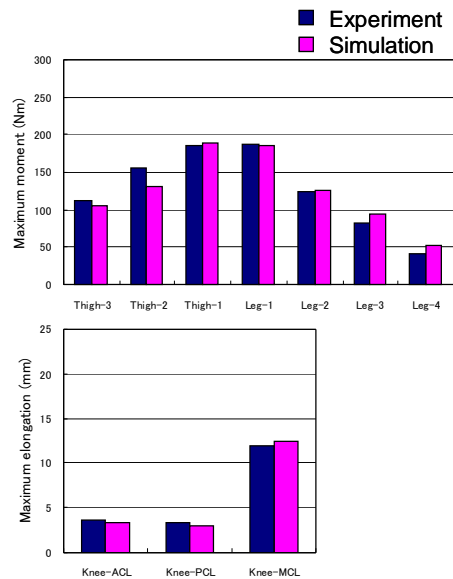


Figure 13. Dynamic bending simulation set up for FE Flex-GT-prototype model.



(a) Wave forms



(b) Maximum values

Figure 14. Results of dynamic bending simulation for FE Flex-GT-prototype model.

Simplified car collision simulation

Figure 15 shows the setup of a simplified car collision simulation. The FE Flex-GT-prototype model was made to collide with a simplified car model at an initial impact speed of 11.1 m/s. The simplified car model was composed of a BLE (bonnet leading edge) model, BP (bumper) model, and SP (spoiler) model each having shell elements for simulating the characteristics of automotive steel sheets. The responses of the FE Flex-GT-prototype model were compared with the experimental results of Flex-GT-prototype.

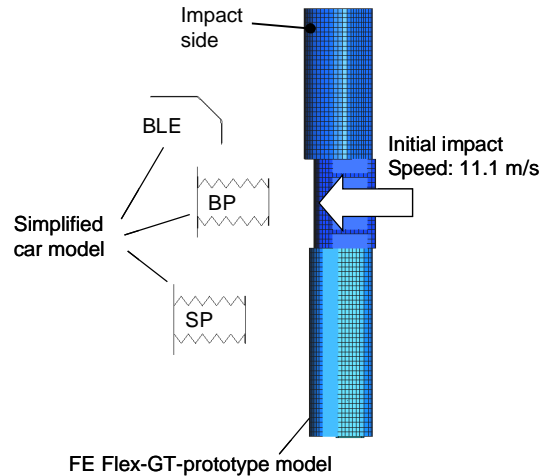


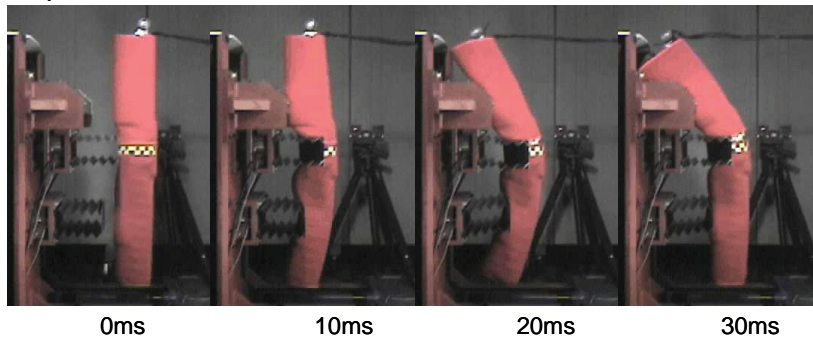
Figure 15. Collision simulation setup with Flex-GT-prototype and simplified car model.

Figure 16 shows the behavior of the FE Flex-GT-prototype model in the simplified car collision test and the behavior of Flex-GT-prototype in an actual car collision test. It is evident that the FE Flex-GT-prototype model closely simulates the flexible behavior of Flex-GT-prototype when colliding with a car.

Figure 17 compares the response waveforms and maximum values of the FE Flex-GT-prototype model with the experimental results of Flex-GT-prototype. Both indicated a high similarity in waveform shape, maximum value and the time at which the maximum value was generated.

The above comparative results verify that the FE Flex-GT-prototype model in a simulated car collision test generates responses equivalent to the responses of Flex-GT-prototype in its real collision test with a car.

Experiment



Simulation

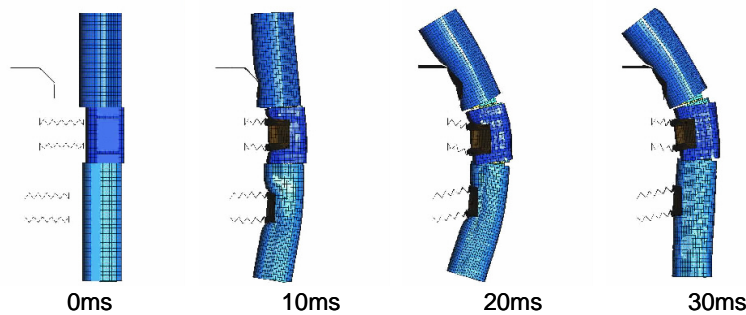
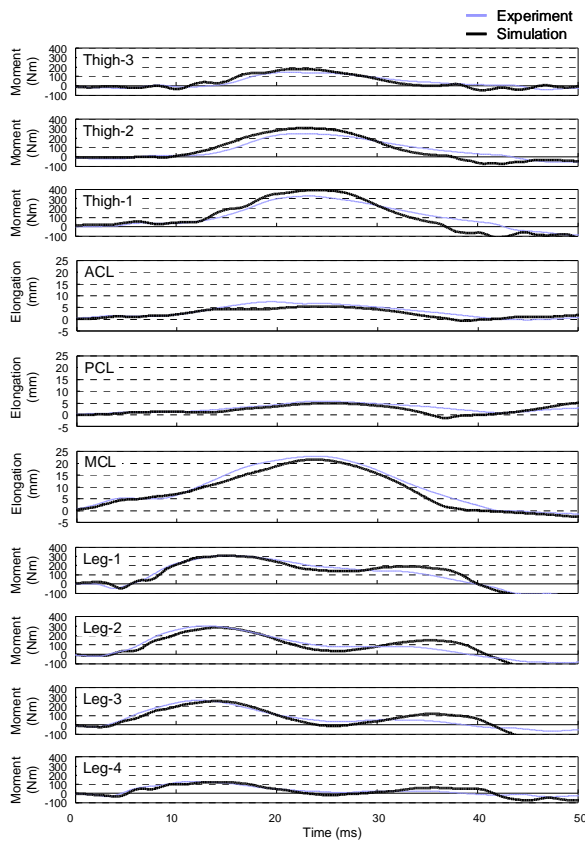
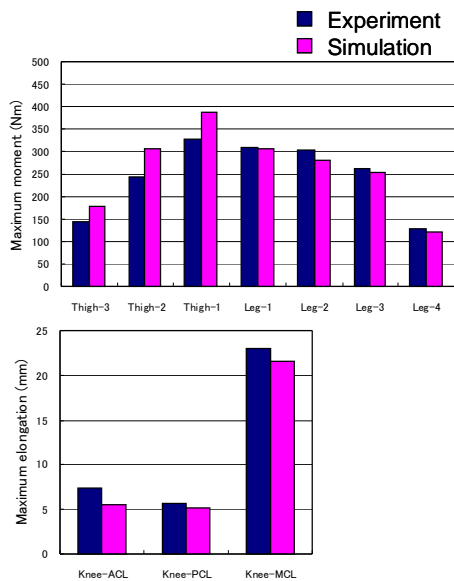


Figure 16. Collision simulation with Flex-GT-prototype and simplified car model (Kinematics).



(a) Wave forms



(b) Maximum values

Figure 17. Results of collision simulation with Flex-GT-prototype and simplified car model.

CONCLUSION

In the present study, a computer simulation model of the latest version pedestrian leg-form impactor, FE Flex-GT-prototype model, was developed, and its fidelity to an actual Flex-GT-prototype was evaluated.

Based on the evaluation results under the segmental level (thigh, leg, and knee parts) and assembly level loading conditions, it was verified the equivalence of the FE Flex-GT-prototype model to an actual one.

It is planned that this computer simulation model will be used in finalizing the Flex-GT leg-form impactor specifications and improving various car front technologies for pedestrian lower limb protection.

ACKNOWLEDGEMENT

We would like to thank the members of Honda R&D Co., Ltd. for their generous supply of a base model and valuable advice in our development of the computer simulation model for Flex-GT-prototype.

REFERENCES

- 1) European Enhanced Vehicle-safety Committee, EEVC Working Group 17 report, Improved test methods to evaluate pedestrian protection afforded by passenger cars(1998).
- 2) Bhalla K., Bose D., Madeley N.J., Kerrigan J., Crandall J., Longhitano D., and Takahashi Y., Evaluation of the Response of Mechanical Pedestrian Knee Joint Impactors in Bending and Shear Loading, 16th International Conference on the Enhanced Safety of Vehicles (ESV), Paper Number 429(2003).
- 3) Konosu A. and Tanahashi M., Development of a Biofidelic Flexible Pedestrian Legform Impactor, 2003-22-0020, Stapp Car Crash Journal, Vol. 47, Oct. (2003).
- 4) Konosu A. and Tanahashi M., Development of an FE Flexible Pedestrian Leg-form Impactor (Flex-PLI 2003R) Model and Evaluation of its Biofidelity, SAE, Paper Number 2004-01-1609(2004).
- 5) Kikuchi Y., Takahashi Y., and Mori F., Development of a Finite Element Model for Flex-PLI, 19th International Conference on the Enhanced Safety of Vehicles (ESV), Paper Number 05-0287(2005).

CONCEPT DESIGN OF A 4-DOF PEDESTRIAN LEGFORM

Qing Zhou

Michael Quade*

Huiliang Du

State Key Laboratory of Automotive Safety and Energy
Tsinghua University

China

* Exchange student from RWTH-Aachen, Germany

Paper Number 07-0196

ABSTRACT

The new European car-to-pedestrian impact safety protection regulation has prompted many research efforts in this area. For knee and lower leg protection, the current regulation requires using a legform that consists of 2 degrees-of-freedom (DOF) for injury assessment. It mimics the shear and bending about the knee joint when the lateral side of a pedestrian is impacted by a vehicle. However, in a smaller portion, non-lateral impact accidents also exist in the real world. Moreover, even in a purely lateral impact, once the legform contacts with the bumper, it could rotate towards the other directions due to the curvatures of the bumper shape and the deformation of the bumper foam, causing the legform taking load from other directions. For assessing injuries under omni-direction impact, a concept design of a 4-DOF pedestrian legform is developed. The two added DOFs represent the natural human knee rotation and the shear with respect to the knee joint when a pedestrian is impacted from the front or the back. The bio-mechanical requirements of the 4-DOF legform are adopted from the existing 2-DOF pedestrian legform and the Hybrid III dummy knee. The challenge is to design all the 4-DOF mechanisms, including the motion and stiffness mechanisms, in a limited space of the legform. Design methodology is also documented in this paper.

INTRODUCTION

Car-to-pedestrian collisions are one of the main



Figure 1. Sketch of car-to-pedestrian impact.

types of traffic accidents in cities. In the European Union more than 7,000 pedestrians are killed every year in road accidents [1]. In the US, pedestrian fatalities were over 4,700 in 2000 [2]. In China, there exists large amount of roads with mix traffic of pedestrians and vehicles in big cities. In 2003, China had 28,000 pedestrian fatalities, about 25% of the total fatalities in traffic accidents [3].

In car-to-pedestrian collisions, the lower limbs are usually struck first and the pedestrian's head arcs downward to strike the engine hood surface (see sketch in Figure 1). Head injuries are among the most life threatening form of injury for pedestrians and are predominantly caused by a direct blow to the head. Leg injuries account for more than half of the severe injuries. Although not life threatening, severe knee joint injuries often cause permanent disability.

Certain test methods are used for assessing pedestrian impact protection performance of a vehicle, in which dummy or dummy components are used as impactor forms. There has been a debate about whether standing dummy or dummy components such as headform and legform should be used in assessment test. Although using a standing dummy can account for full body kinematics similar to real world accidents, it is difficult to design test setup and control test process. For this and some other reasons, EEVC finally adopted the dummy components in the required test [1] as illustrated in Figure 2.

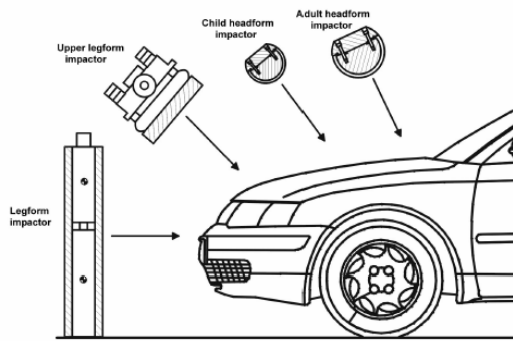


Figure 2. EEVC component tests for assessing pedestrian impact protection [1].

Common injuries of pedestrian lower leg and knee joint as the result of impact with bumper include long bone fractures, knee femoral condyle and tibial condyle fractures, knee ligament tearing and rupture, etc. A joint study by University of Virginia and Honda R&D [4] found that knee bending tests are capable of reproducing real world pedestrian injuries. Pure shear of the knee joint is an extreme case that does not occur in real world pedestrian crashes. A more recent study using cadavers by the same group in University of Virginia [5] further concluded that the real world pedestrian knee injury patterns could only be produced under combined bending and shear. It implies that the combined bending and shear is the actual loading condition that the pedestrian knees experience in real world car-to-pedestrian collisions.

For knee and lower leg protection, the current EEVC regulation [1] requires using a legform that consists of two degrees-of-freedom (2-DOF) for injury assessment. It mimics the shear and bending about the knee joint when the lateral side of a pedestrian is impacted by a vehicle. However, if pedestrian is in walking stance or impacted from an oblique direction, the 2-DOF legform may not have an appropriate response. A study by Kuehn et al [6] found that 56% of car-to-pedestrian collisions occurred when the pedestrian was in walking stance. On the other hand, even the impact is perfectly lateral, once the legform contacts with the bumper, the legform could rotate towards the other directions due to the curvatures of the bumper shape and the deformation of the bumper foam, causing the legform taking load from the other directions. The anatomy of the human knee joint also determines that the knee joint response to external impact may have some degree of coupling effect between different directions. By allowing the knee joint

appropriately responding in multi-direction impact, it may open a channel to better correlate the load transferred to the lower leg and upper leg. These manifest a need of a multiple-DOF legform.

To develop a pedestrian legform that can assess injuries from omni-direction impact, a concept design of a 4-DOF pedestrian legform has been developed and is documented in this paper. In fact, the new 4-DOF legform is a combination of the existing 2-DOF pedestrian legform (Figure 3(b)) and the Hybrid III dummy knee (Figure 3(a)), from which the joint stiffness data are also adopted. Whether superimposing the joint stiffness of different directions makes sense in biofidelity is beyond the scope of this study.

The most injury concerned DOFs already exist in the current EEVC legform (Figure 3(b)) for assessing the leg injury when the lateral side of a pedestrian (defined as the y-direction) is impacted. One is the relative shearing in the y-direction between the tibia and the femur, and the other is the relative bending about the x-direction (see the definition below).

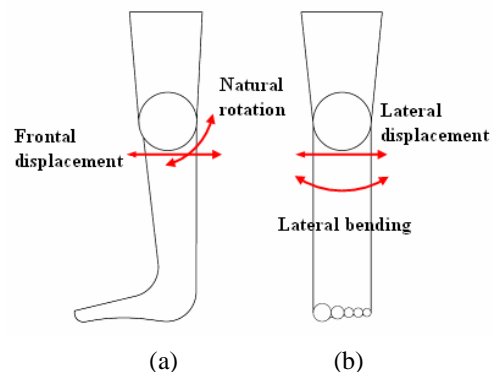


Figure 3. The 4 degrees-of-freedom of the knee joint are designed in the legform.

The 2 added DOFs represent the natural human knee rotation and the shear about the knee joint when a pedestrian is impacted from the front or the back (defined as the x-direction). This can be better explained as: when pedestrian faces to a coming car and the tibia is impacted by the bumper, the tibia may experience a shear displacement in the x-direction relative to the femur. It is the same injury displacement when a driver sits in a car and the tibia is impacted by the intruded engine in frontal impact accident. Therefore these two DOFs already exist in the Hybrid III dummy knee for assessing femur and knee injuries using the Hybrid

III dummy sitting in a car involved in frontal impact.

The challenge is to design all the 4-DOF mechanisms, including the motion and stiffness mechanisms, in a limited space of a legform. Several design options are developed and analyzed in this project. By ranking and weighting different design requirements, one of the designs is selected for further detailing it in a complete pedestrian legform.

DESIGN TASK AND REQUIREMENTS

As illustrated in Figure 3, the knee joint allows the shearing displacements along the two axes as well as the rotations about the same two axes. The design deals with a large school of requirements. The kinematic structure of the 4-DOF joint in a rather small design space is the first issue to tackle. Furthermore, except the natural knee rotation, all the other 3 DOFs are injury producing motions and need to satisfy certain stiffness and damping requirements such as bending moment vs. bending angle or shear force vs. shear displacement.

Geometry and Packaging

By referencing the overall geometrical requirements of the EEVC legform [1], it is determined that the optimal size of the 4-DOF knee joint is a cylinder with a diameter smaller than 70mm, the diameter of the femur and tibia of the EEVC legform. This size limit is actually difficult to house a 4-DOF joint, and therefore is quoted as optimal size, or a wish size. The 2-DOF EEVC knee joint is housed within the perimeter of the femur and tibia diameter, while in the 4-DOF knee joint design, in order to gain more packaging space, the knee joint is allowed to be slightly larger than the tibia and femur diameter (“extruding out”). This is more like human knee and Hybrid III dummy knee, and the flesh thickness in the knee joint area is reduced in order to maintain the overall size within a certain range. It is therefore determined that the maximum size for the design space is using a cylinder with diameter 100mm and covering it with 10mm flesh foam.

The human knee joint is like a spherical joint, in which all the axes meet at the same point. To achieve a high biofidelity, in the 4-DOF legform, all the axes should also be near each other. In fact, designing the 4-DOF knee joint as a spherical joint is one of our early options for its good similarity to the

human knee. But a spherical joint might have great disadvantages compared to non-spherical ones in mechanical sense.

Stiffness Requirement of the Joints

The natural rotation of the human knee joint is not an injury concerned DOF and defined as a rotation from 0° to 120°, which seems to be a suitable range for the purpose of being a pedestrian legform. Although no bio-fidelity requirement, the joint should have certain friction damping, and the friction magnitude may be equivalent to, for example, resisting motion under gravity loading.

Since this work is not about developing more appropriate biofidelity requirements for the human knee and leg under impact loading, the stiffness requirements of the other 3 injury concerned degrees-of-freedom are adopted from that of the existing dummies and dummy components. When more appropriate stiffness requirements become available in the future, they may be built into the mechanical mechanisms of the design of this work.

For shearing in the x-direction, based on the test data in [7] and result of a Hybrid III dummy knee slider stiffness test, the shear stiffness curve in Figure 4 is adopted.

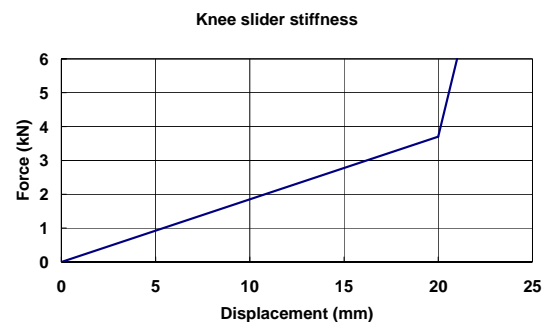


Figure 4. Frontal shear force vs. displacement of the knee joint.

For lateral impact to the legform, the EEVC document [1] has given the shear force vs. shear displacement shown in Figure 5 and the bending force vs. bending angle shown in Figure 6. Note that these requirements of the knee joint are derived from the static certification test of the EEVC legform. The bending moment can be calculated by multiplying the given force value in Figure 6 with 2m, the force arm length in the certification test.

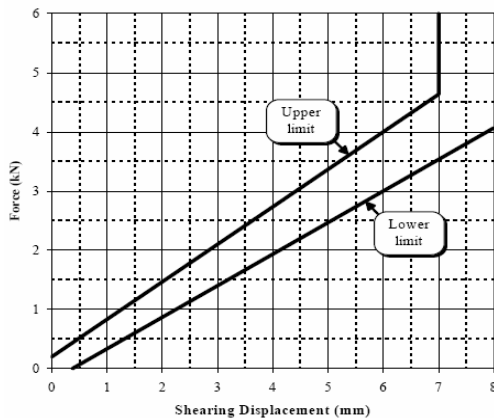


Figure 5. Lateral force vs. displacement of the knee joint [1].

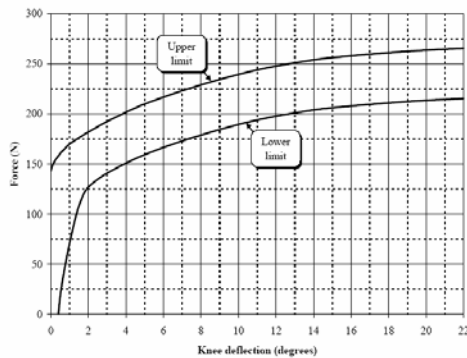


Figure 6. Lateral bending force vs. bending angle of the knee joint [1].

As the legform is used under impact loading condition, damping mechanisms must be considered when designing the kinematic structure of the joint. It is also desirable that recoverable deformation and motion mechanisms, as opposed to any destructive elements, are used in achieving the required stiffness.

Summary of Design Requirements

Other design requirements include measurement of displacements and forces needed for assessing the injury severity. Therefore, there must be space in the legform to install sensors and make measurement with high repeatability and reliability. This work is still ongoing and will be reported in future publications.

The design requirements and evaluation criteria can be summarized as follows: (a) high biofidelity, (b) flexible characteristics of stiffness and damping

mechanisms to meet different characteristic curves, (c) small design space, (d) good measurement possibilities, (e) easy use, and (f) high durability. Among them, high biofidelity and good measurement possibilities are more important.

DESIGN OF 4-DOF LEGFORM

Design Methodology

Based on the requirements and functions established above, some principle solution variants are first developed to fulfill the requirements of each of the 4 degrees-of-freedom. By this way a complex problem is divided into several simple problems, for which solutions can be found more easily. Then the kinematic chain of the knee device is considered to sort out many different possibilities of arranging the 4 degrees-of-freedom. Following that, these solutions are combined into solution concepts by analyzing their merits and drawbacks. In the last step, the concepts are evaluated according to certain criteria. The best solution emerged from this evaluation process is the solution that fulfils all the requirements best and therefore is further designed with details.

To identify rotational or translational motion mechanisms that fulfill the required stiffness and damping, the following elements are considered and their advantages and disadvantages are analyzed: pressure spring, Belleville spring, gas spring, leaf spring, friction spring, leg spring, spiral spring, torsion spring, rubber element, plastically deformable element, rolling bearing, plain surface bearing, sliding plane, ball joint, hydraulic damper, rotation brake, etc.

To realize 4-DOF, one can use 4 single joints, 2 double joints, 1 triple joint and 1 single joint, 1 quadruple joint, or any other combinations. An advantage of using triple joint or quadruple joint is that it can lead to small design space, but it is very difficult to achieve the required stiffness in a combined joint, and measurement would be nearly impossible. In contrast, it would be easy to achieve the required stiffness by using 4 single joints, but it would occupy a large space and result in complex connections between the joints. Therefore a knee structure consisting of 1 double joint and 2 single joints or 2 double joints would be appropriate. The first joint may be a translation joint, followed by a rotation-rotation double joint and another translation joint; or the first joint may be a translation-rotation

double joint, followed by a translation joint and a rotation joint; or some of their permutations.

By combining the partial solutions, matrix of different variants is established. To achieve the best combination, it is important to combine the sub-functions without creating a conflict between the solution variants. A clear arrangement of the sub-functions to prevent conflicts is using morphological matrix. The selection of solutions from the morphological matrix sometimes requires a certain kinematic chain, in which the evaluation criteria summarized in an earlier section are used. These processes lead to the following design.

Embodiment Design of Chosen Solutions

Figure 7 shows the legform in unloaded posture and Figure 8 shows the legform stances under different loadings. The mechanisms of the 4-DOF are illustrated in the following.

The lateral displacement DOF and the natural rotation DOF are realized in a double joint. It allows a lateral shear displacement of 8mm in each direction, leading to a total movement of 16mm, with the force-displacement relationship shown in Figure 5. It is achieved by a rubber element with a certain stiffness and damping characteristic. The basic idea can be seen in Figure 9 and Figure 10. This solution offers a small design space and flexibility to design the rubber element characteristic in a wide range. Additionally, although no stiffness requirement, a rotation stopper must be included to the natural rotation of the knee joint to limit range of its rotation angle to a desired value.

Similar to the displacement in the lateral shear DOF, the joint characteristic of the frontal shear (Figure 4) is achieved by a rubber element too. However, the shear displacement in the frontal direction is much larger, 20mm in front and rear directions, respectively, with a linear force-displacement relationship. With a total displacement of 40mm, it is very difficult to install a rubber element in the radial direction (only 100mm diameter cylinder by the requirement). On the other hand, there is a relatively large space available in the axial direction in the upper and lower leg tubes. By using ligament cables, it is possible to transform the radial displacement into the axial one and install rubber elements in the lower tube. Figure 11 shows such a design.



Figure 7. Legform impactor in unloaded position.

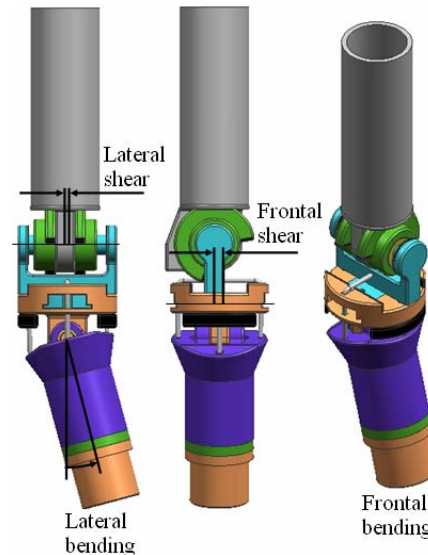


Figure 8. Legform impactor in loaded position.

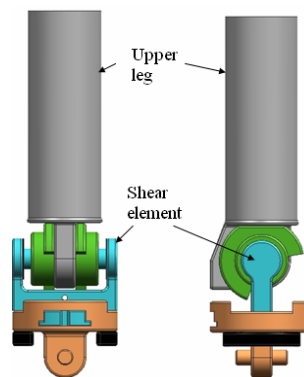


Figure 9. Double joint for lateral displacement and natural rotation.

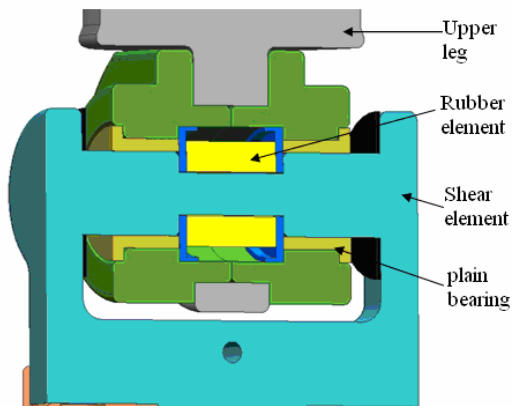


Figure 10. Interior view of lateral displacement system.

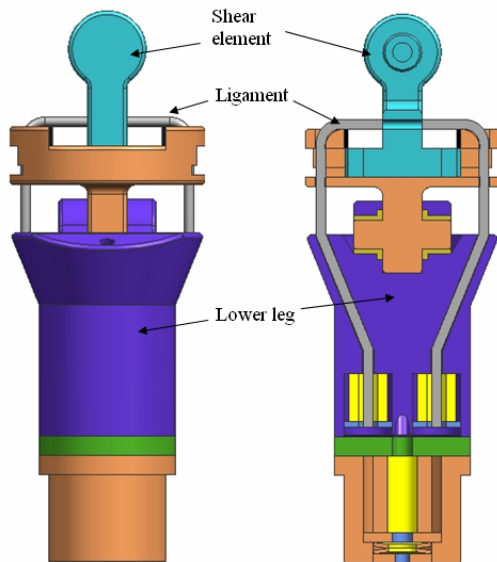


Figure 11. Frontal displacement system.

By transforming the direction of movement, the design allows a greater flexibility to change the rubber elements. It would even be possible to install a spring-damper system. When the shear element moves (Figure 11), it pulls the ligament cable to make the rubber element compressed. As the forces are relatively high, it may be necessary to calculate the resulting force-displacement curve by including the stiffness of the cable. Additionally, the friction between ligament cables and the supporting elements should be minimized (for example, using pulleys).

As shown in Figure 6, the joint characteristic of lateral bending DOF is nearly bi-linear and is more difficult to achieve than that of the lateral and frontal

shear DOFs, which are linear. In the EEVC 2-DOF legform, it is achieved by using plastically deformable elements. In this design, it is hoped not to use any destructive elements.

The design is shown in Figure 12. It uses a system consisting of a Belleville spring and a preloaded rubber element to generate the required stiffness. Again, ligament cables are used to transform rotation into translation. This is not only for using the space in the lower leg tube, but also for easy to achieve the nonlinear force-displacement characteristic in translational movement. The rubber element is preloaded to the maximum force of the Belleville spring. Thus, when the force reaches the maximum, the Belleville spring cannot be compressed any further and the rubber element is compressed instead. A difficulty with this design is to achieve the high required force to generate a bending moment as large as 500Nm.

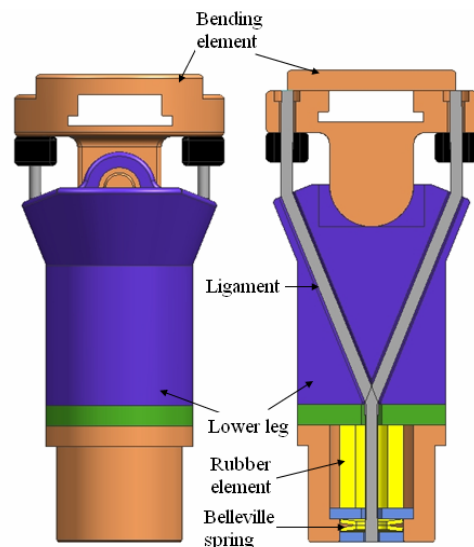


Figure 12. Lateral bending spring system.

CONCLUSIONS

A concept design of a 4-DOF pedestrian legform is documented in this paper, together with summary of the design requirements and the design methodology. This is the first phase work of the 4-DOF pedestrian legform development. The design improvements are still ongoing. The next steps include design of the measurement means of injury parameters (deformation, acceleration, force, etc.) and their packaging. For protection and damping purpose, like in all other dummies, a certain cushion envelope, especially around the knee joint, is also be needed.

A finite element model of the legform is also under development. A prototype will then be built, evaluated and tested.

ACKNOWLEDGMENT

This project is supported by National Natural Science Foundation of China under grant No. 50422284.

REFERENCES

- [1] EEVC. 2002. "Improved Test Methods to Evaluate Pedestrian Protection Afforded by Passenger Cars." European Enhanced Vehicle Safety Committee, Working Group 17. www.eevc.org.
- [2] NHTSA. 2000. "Traffic Safety Facts 2000 – Pedestrians." DOT HS 809 331. The US National Highway Traffic Safety Administration.
- [3] China Traffic Control Bureau. "2003 Data of traffic accidents in China."
- [4] Bhalla K, Bose D, Madeley NJ, Kerrigan J, Crandall J, Longhitano D, and Takahashi Y. 2003. "Evaluation of the response of mechanical pedestrian knee joint impactors in bending and shear loading." The 18th International Technical Conference on the Enhanced Safety of Vehicles, Nagoya, Japan.
- [5] Bose D, Bhalla K, Rooij LV, Millington SA, Studley AF, and Crandall JR. 2004. "Response of the Knee Joint to the Pedestrian Impact Loading Environment." SAE 2004-01-1608. SAE Congress.
- [6] Kuehn M, Froeming R, and Schindler V. 2003. "An advanced testing procedure for the pedestrian-car-collision." The 18th International Technical Conference on the Enhanced Safety of Vehicles, Nagoya, Japan.
- [7] Viano D, Culver C, Haut R, Melvin J, Bender M, Culver R, and Levine R. 1978. "Bolster impacts to the knee and tibia of human cadavers and an anthropomorphic dummy." SAE-780896.

STIFFNESS CORRIDORS OF THE EUROPEAN FLEET FOR PEDESTRIAN SIMULATIONS.

Luis Martinez
Luis J. Guerra
Gustavo Ferichola
Antonio Garcia
UPM-INSIA
Spain

Jikuang Yang
Chalmers University
Sweden
Paper Number 07-0267

ABSTRACT

Multibody simulations of pedestrian impact scenarios as well as pedestrian accident reconstructions have been used and improved through the years to enhance the pedestrian protection (Lestrelin 1980, Wismans 1982 to Van Hoof 2003, Yao 2005).

In these years, pedestrian multibody models have been developed and validated extensively but there has not been a uniform approach to the pedestrian-vehicle contact interactions. In general, the reference values used for the stiffnesses of the impacted cars were individually obtained for each car through testing (Mizuno 2000) or through FEM simulations (Van Rooij 2003).

This paper aims to define and supply to the research community appropriate and wide test based estimates on the stiffnesses of the European vehicles front parts for pedestrian simulations through the development of a set of stiffness corridors based on the pedestrian subsystem tests from EuroNCAP.

Based on the 425 tests that EuroNCAP has made available for APROSYS SP3 sub-project, this paper defines procedures to derive the vehicle stiffness out of these pedestrian tests. Moreover, these methodologies are applied extensively to these 425 tests to build a set of stiffness corridors for the different vehicle front parts areas.

Finally, some guidelines are included in the paper to use appropriately the obtained corridors to simulate properly the different current European vehicles.

INTRODUCTION AND APPROACH.

As pedestrian subsystem tests have been performed since 1998, EuroNCAP owns a huge database with

over 3,000 pedestrian tests. This dataset includes tests on at least 18 pedestrian potential impacting areas in each car, with four different impactors: adult and child headform, legform and upper legform (EuroNCAP 2004).

Considering the raw data channels of these tests, it is feasible to define procedures to process these data and derive information regarding the behaviour of the vehicle structure in those tests, that can be used as contact characteristics into pedestrian simulation models.

In a first phase, the kinematics of the different test configurations has been analysed. These analyses have led to identify a set of assumptions to define a unique methodology to obtain the force-deflection characteristics for the different impactors (headform tests, legform tests and upper legform tests).

Secondly, these methodologies have been applied extensively to the whole set of tests (425), differentiating the adult headform tests impacting on the bonnet from the ones impacting on the windscreen base.

The responses have been grouped for each test configuration (legform tests, upper legform tests, child headform tests, adult headform tests on the bonnet and adult headform tests on the windscreen base) in five vehicle groups (super mini cars SMCs, small family cars SFCs, large family cars LFCs, multi purpose vehicles MPVs and sport utility vehicles SUVs), getting 25 groups.

An analysis on these 25 groups showed the existence of different stiffness trends in the same test configurations not linked to the vehicle groups; therefore, an EuroNCAP rating variable (red, yellow, green) was included to explain these differences. Consequently, each test was rated individually, following EuroNCAP rating protocols, and a re-grouping was performed to the

whole set of tests into red, yellow and green groups in each test configuration.

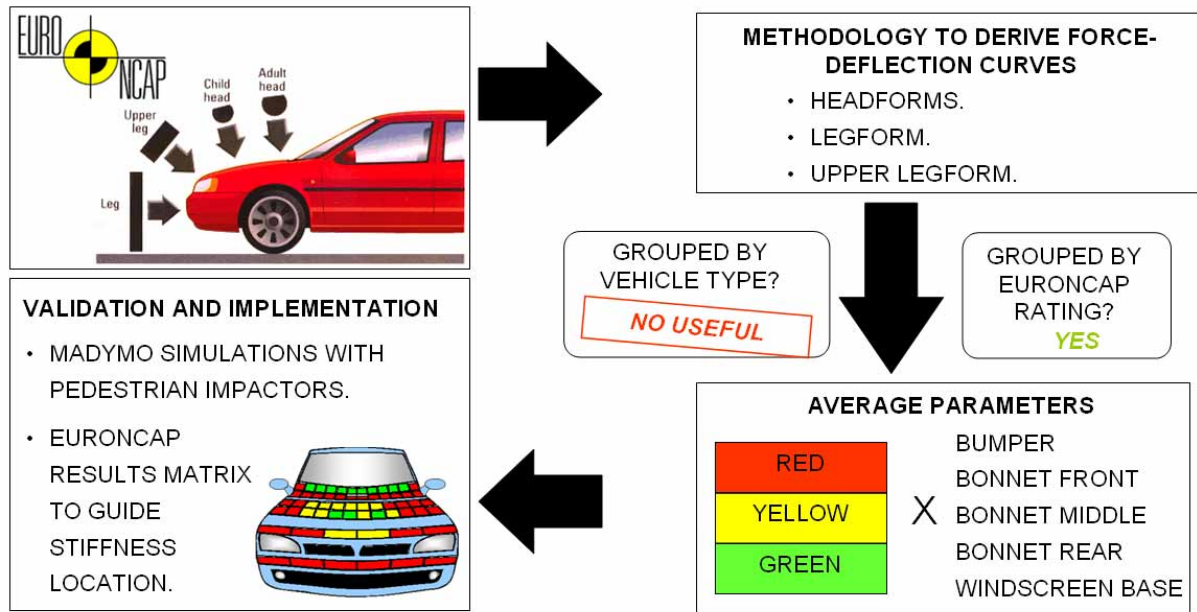


Figure 1: Approach to the development of stiffness corridors for the European fleet.

As a next step, average parameters (average curves, standard deviation and average unloading slopes) have been calculated for each of the 15 groups (red, yellow and green groups in each of the 5 test configurations defined) leading to a set of corridors, which have been simplified into straight lines to ease handling and dissemination.

The validity of these corridors have been checked with MADYMO. It has been analysed that impacts with the different pedestrian impactors, according EuroNCAP configurations, into detailed vehicle models implemented with the average contact characteristics curves obtained for the different groups do result in EuroNCAP ratings according the groups they represent.

Finally, to couple the obtained 15 corridors with the current European fleet, guidelines are given on how to implement them into simulation models based on the matrix used by EuroNCAP for defining the impact points and rating the pedestrian tests.

METHODOLOGIES TO OBTAIN CONTACT CHARACTERISTICS FROM SUB-SYSTEM PEDESTRIAN TESTS.

Objective and limitations.

Considering the kinematics of the different impactors along with the instrumentation used in each of the test configurations, it is intended to define the most suitable methods to obtain force-deflection characteristics for each of the three

pedestrian impactors (headform, legform and upper legform) in the most realistic and univocally possible way.

As in most cases no trigger signal has been available for the analysis, a t_0 has needed to be set. This t_0 has been defined as the time when the corresponding acceleration or force in the impactor exceeded a certain limit, as described in Table 1.

In order to quantify the effect of the non-zero value of the acceleration or force in t_0 in the force-deflection curve calculation, an error analysis has been performed for the three different impactors and test configurations.

The average time delay for the different channels to exceed their limits with respect its zero value has been calculated and summarized in Table 1.

Table 1: t_0 definition for the different test configurations and time delay to reach it.

Test configuration	t_0 definition	Average time delay
Headforms	Time where Fore-aft acceleration > 2g	0.3 ms
Legform	Time where Tibia acceleration > 2g	0.4 ms
Upper legform	Time where Sum of forces > 100 N	0.5 ms

Supposing a linear behaviour of the acceleration within this delay, an error in the change of velocity

and in terms of deflection caused by this delay can be calculated as shown in the Table 2.

In the case of headform and legform tests, the velocity is fixed to 11.1m/s in the protocol. However, in the case of the upper legform tests, the parameters are dependent on the geometry of the vehicle.

This test configuration is performed at energy levels between 200 J and 700 J with a practical lower limit in the impactor mass behind the load cell (M_{LC}) of 6.95 kg, which limits the maximum speed in this configuration to 12.13 m/s. In this configuration, the worst case is considered to calculate the error.

Table 2: Summary of error parameters calculated.

Test	Delta V error
Headform	$0.5 \cdot (2g) \cdot (0.0003s) = 0.00294m/s$
Legform	$0.5 \cdot (2g) \cdot (0.0004s) = 0.00392m/s$
Upper legform	$0.5 \cdot (100/M_{LC} \text{ min}) \cdot (0.0005s) = 0.00359m/s$
Test	Deflection error
Headform	$11.10m/s \cdot 0.0003s = 0.00333m$
Legform	$11.10m/s \cdot 0.0004s = 0.00444m$
Upper legform	$12.13m/s \cdot 0.0005s = 0.00605m$

These change of velocity errors are rather below the impact velocity tolerance of the test (± 0.2 m/s). Furthermore, these errors are within the range the accuracy for the speed measurement devices and no extra error is added in these calculations.

Regarding deflection, the error obtained in the calculation process is of 3, 4 and 6 mm for the headforms, legform and upper legform respectively, which represent 3-4% with respect to the maximum deflection values found in the different test configurations.

It can be concluded that the velocity error is negligible while the deflection errors due to the t_0 definition is acceptably low for the scope of this methodologies .

Methodology applied for headform tests.

The pedestrian headform tests consist of a set of free flight impacts at 11.1 m/s (± 0.2) of a headform into the bonnet and windscreen area of the vehicle between WAD (Wrap Around Distance) 1000 and 2100 mm. (child and adult areas)

The pedestrian adult headform is a $4.8kg \pm 0.1$ rigid sphere of $165mm \pm 1$ diameter fitted with a vinyl skin. It impacts on the vehicle area determined by WADs between 1500 and 2100 mm, with an impact angle of $65^\circ (\pm 2^\circ)$ to the ground.

The pedestrian child headform is a smaller rigid sphere, $2.5 \text{ kg} \pm 0.05 \text{ kg}$ and $130 \text{ mm} \pm 0.1$ diameter also fitted with a vinyl skin. It impacts on a vehicle area determined by WADs between 1000 and 1500 mm, with an impact angle of $50^\circ (\pm 2^\circ)$ to the ground.

These two headforms are equipped with a tri-axial accelerometer in the centre of the sphere and the HIC is used as the rating criterion.

Further details on the headforms and the procedure are given in EEVC WG17 1998, EuroNCAP 2001, 2004.

The next table summarizes the test parameters measured in the test and calculated in the post-process to derive the force deflection functions from the headform tests.

Table 3: Tests parameters for headform tests.

Parameters	Value
Headform mass (M_H)	A (4.8 kg); C (2.5 kg)
Impact angle (α_I)	Measured.
Impact speed (V_0)	Measured.
Fore/aft acceleration (A_{FH})	Channel output.
Vertical acceleration (A_{VH})	Channel output.
Lateral acceleration (A_{LH})	Channel output.
<i>Normal angle at the impact point in headform coordinate system (α_H)</i>	<i>Calculated</i>
<i>Normal angle at the impact point with respect the impact angle (α_N)</i>	<i>Calculated.</i>
<i>Normal angle at the impact point with respect the ground level (α_{NG})</i>	<i>Calculated.</i>
<i>Normal Force at the impact (F_N)</i>	<i>Calculated</i>
<i>Normal velocity at the impact (V_N)</i>	<i>Calculated</i>
<i>Normal deflection (D_N)</i>	<i>Calculated</i>

Considering that the characteristic functions for a contact in multibody or facet surfaces need to be defined in terms of normal force vs. normal penetration (TNO, 2003), the normal at the impact

point is a key parameter to get the stiffness. Moreover, its importance is higher as the headform angles of impact with the car are not always perpendicular.

The headform protocol requires that the free flight headform direction prior to impact is to be contained in a vertical plane parallel to the midline of the car. However, in the rebound phase of the tests, the headform may be ejected from this plane due to many factors, for example the structure deformation or the surface curvature.

Moreover, as the impact is not performed perpendicular to the car surface, the high friction coefficients between the headform and the bonnet causes tangent forces that may induce rotation in the headform. The less perpendicular the impact is, the more important these effects become.

These two effects are not considered to be significant in the relevant window analysed in the tests (on average, the time to max acceleration is 10-15 ms) and, therefore rotations around both axis are neglected.

In the first moment of impact, the acceleration channels signs and values are such that the resultant acceleration coincides with the normal direction of impact. In this moment, the three angles of the acceleration components with respect to the headform reference coordinate system define the orientation of the normal at the impact point in the headform reference coordinate system.

If rotations are neglected during the relevant time window of the tests, it can be assumed that:

- These three angles will be constant during the relevant test window.
- As the headform c.o.g is contained in a vertical plane parallel to the midline of the car, the lateral acceleration contribution to the normal will be always equal to zero.
- The normal resultant acceleration A_{RN} will be the result of projecting, with their signs, the fore/aft and the vertical components of the acceleration.

Orientation of the normal direction at the impact point.

With the given assumptions, the normal direction at the impact point coincides with the direction of the normal resultant acceleration A_{RN} .

α_H is the angle of this normal resultant acceleration (A_{RN}) with respect the positive direction of A_{VH} , and therefore, of the normal direction at impact with respect to the headform coordinate system. This angle is obtained by calculating the inverse tangent of A_{VH} and A_{FH} , transformed to degrees. and it is defined as the normal angle at the impact point with respect the headform reference coordinate system (α_H).

To compare this angle with the one measured in the real car, a conversion to the laboratory coordinate system needs to be performed. To ease this conversion, α_H is expressed with respect to the impact angle direction by a 90° rotation, resulting in the α_N angle, that added to the impact angle (α_I) results in the normal direction angle at the impact point with respect to the ground level (α_{NG}).

This methodology has been verified geometrically measuring in the lab the normal to the impact point in several adult and child headform test locations and comparing it with the data obtained analytically.

Two cases are shown in Figure 2 and Figure 3 as examples: An adult headform test impacting on the windscreen and a child headform test impacting on the bonnet.

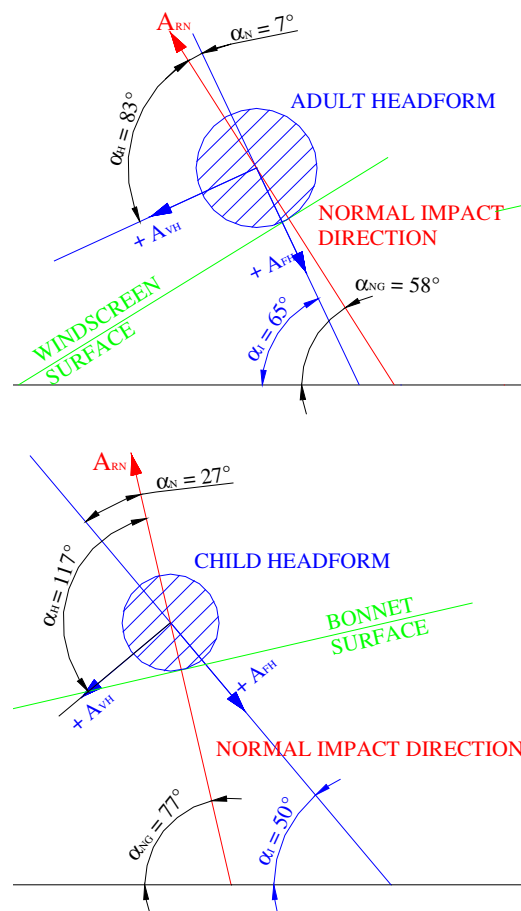


Figure 2: Summary of angles calculated for the example tests.

In the case of the adult headform test, the obtained normal angle at the impact point (α_N) with respect the impact direction, following the above calculations, has resulted to be -7° , which means that the normal angle at the impact point with respect the ground level (α_{NG}), considering an impact angle of 65° , turns out to be 58° .

In the child case, as the impact occurs in the bonnet, the calculated normal angle at the impact

point (α_N) with respect the fore-aft directions is 27° , which lead to a α_{NG} of 77° with an impact angle for the child headform of 50° .

On the other hand, the measures obtained in the laboratory for the car the same impact locations has led to normal angle at the impact point of 57° for the adult case and 79° for the child case (Table 4).

These results show that the method proposed to calculate the normal at the impact point (α_N) has an error within the tolerance interval that EuroNCAP permits for the impact angles in these tests protocols, therefore it is considered to be valid for the purpose of this methodology.

Table 4: Summary of angles calculated and measured compared to the tolerances in the EuroNCAP headform protocols.

	α_{NG} calc.	α_{NG} lab	Diff	Impact angle tolerance
Adult case	58°	57°	1°	$\pm 2^\circ$
Child case	77°	79°	2°	$\pm 2^\circ$

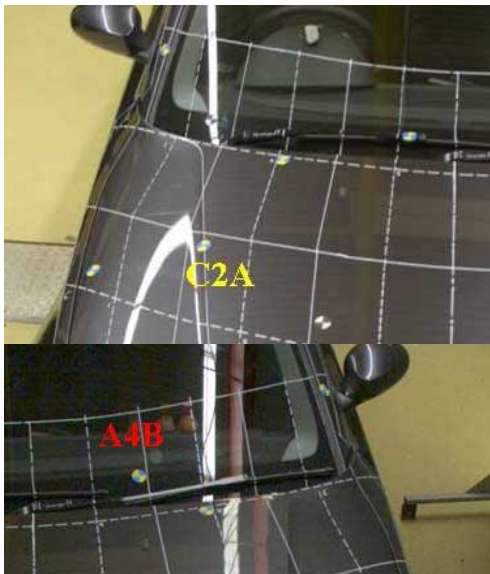


Figure 3: Impact point location of the adult headform and child headform tests example

Headform tests stiffness calculation.

With the assumption given regarding the lack of rotation, the next steps are followed to derive the stiffness.

- The test t_0 is determined when the fore-aft acceleration (A_{FH}) exceeds $2g$.
- In the ($t_0, t_0 + 1$ ms) interval, the normal angle at the impact point with respect the fore-aft direction (α_N) is obtained as it has been described earlier.

- The vertical and the fore-aft acceleration signals are projected with respect the normal of impact obtaining the resultant normal acceleration (A_{RN}) as the addition of both projections.
- Multiply the A_{RN} with the impactor mass, M_H to obtain the normal force in the impact F_N .
- Project the impact velocity (V_0) to the normal of impact to get the initial normal velocity (V_{0N}) at t_0 .
- Double integrate the A_{RN} to get deflection D_N using the V_{0N} as the initial velocity, making the zero of the displacement at t_0 .

Methodology applied in legform tests.

The pedestrian legform tests involve a set of, at least three tests, of a legform impacting horizontally in free flight with the bumper area of the car. The bottom of the legform impactor shall be at Ground Reference Level at the time of first contact with the bumper (tolerance ± 10 mm) and the impact velocity of the legform at this instant shall be 11.1 ± 0.2 m/s.

This test is only performed to cars when the lower bumper reference line is less than 500 mm above the ground reference level.

The legform impactor consists of two foam covered rigid segments, representing femur (upper leg) and tibia (lower leg), joined by a deformable, simulated knee joint. The overall length of the legform impactor shall be 926 ± 5 mm, having a required test mass of 13.4 ± 0.2 kg. A full description of the legform along with the EuroNCAP procedure is given in EEVC WG17 1998 and EuroNCAP 2001, 2004.

This legform is equipped with a uni-axial accelerometer in the non impacted part of the tibia and two potentiometers, one in the tibia and one in femur to account for shear and bending.

The parameters involved in the legform tests and the stiffness derivation are:

Table 5: Tests parameters for legform tests.

Parameters	Value
Legform mass (M)	13.4 kg (6.8 in femur and 4.8 kg in tibia)
Test Speed (V_0)	Measured.
Shear displacement (sh)	Channel output.
Bending angle (Bd)	Channel output.
Tibia acceleration (A_T)	Channel output.
Force in the impact (F_L)	Calculated

Velocity (V_L)	Calculated
Deflection (D_L)	Calculated

Legform tests stiffness calculation.

Considering the channels measured and the real kinematics of the bending, some channels are missing to undertake a fully realistic stiffness derivation.

In order to get some approximate values a simplification is done considering the whole legform as rigid, which is not true, but it may approximate well in cases where knee bending is low. With this assumption, the calculated force is likely to be an overestimate in most cases.

With the assumption of a rigid legform impactor, the following steps have been followed to derive the stiffness.

- Define the t_0 of the test.
- Multiply the tibia acceleration A_T with the impactor mass, M to obtain the force in the impact F_L .
- Double integrate the A_T to get displacement using the V_0 as the initial velocity and making the zero of the displacement in the t_0 . This displacement includes the car structure displacement together with the crush of the impactor (likely to be around 20 mm).

Methodology applied for upper legform tests.

The upper legform impactor is rigid, foam covered at the impact side and 350 ± 5 mm long.

Two load transducers are fitted to measure individually the forces applied at each end of the upper legform impactor, plus strain gauges measuring bending moments at the centre of the upper legform impactor and at positions 50 mm either side of the centre line.

The total mass of the front member and other components in front of the load transducer assemblies, together with those parts of the load transducer assemblies in front of the active elements, including the foam and skin, shall be 2.55 ± 0.15 kg.

The total mass of the upper impactor, as well as the impact angle and the impact velocity is dependent on the general shape of the front of the car. Further details on the impactor, the procedure and geometry dependencies are given in EEVC WG17 1998 and EuroNCAP 2001, 2004.

The upper legform tests parameters needed are the followings:

Table 6: Tests parameters for upper legform tests.

Parameters	Value
Upper Legform mass (M_{UL})	Geometry dependent
Impact angle (α_I)	Geometry dependent
Test Speed (V_0)	Geometry dependent
Force Top	Channel output.
Force Bottom	Channel output.
Sum of Forces (F_S)	Channel output.
Femur upper bending moment	Channel output.
Femur centre bending moment	Channel output.
Femur lower bending moment	Channel output.
Upper Legform mass behind the LC (M_{LC})	$M-2.55$ kg
Acceleration of the upper legform (A_{UL})	Calculated
Total Force (F_T)	Calculated
Velocity (V_{UL})	Calculated
Deflection (D_{UL})	Calculated

Upper legform tests stiffness calculation.

As the upper legform is a linear guided impact device measuring force, the following steps are needed to obtain the stiffness in these tests.

- Define t_0 of the test.
- Divide the sum of forces (F_S) with the upper legform mass behind the load transducer (M_{LC}) obtaining the acceleration of the whole device (A_{UL}).
- Multiply the calculated acceleration with the upper legform total mass (M_{UL}) to get total Force (F_T).
- Double integrate the A_{UL} to get displacement using the V_0 as the initial velocity and making the zero of the displacement in the very first moment of impact D_{UL} . Again, the displacement obtained through this procedure includes the displacement of the car structure together with the crush in the impactor (typically 40 mm).

PEDESTRIAN TESTS ANALYSIS.

Sample analysis.

EuroNCAP has made available for this analysis a total of 425 pedestrian sub-system tests, for a total of 26 vehicles, including super mini cars (SMC), small family cars (SFC), large family cars (LFC), multipurpose vehicles (MPV) and sport utility vehicles (SUV).

This sample represents hardly 10% of the whole set of vehicles tested by EuroNCAP but it is considered to be large enough for the scope of this work.

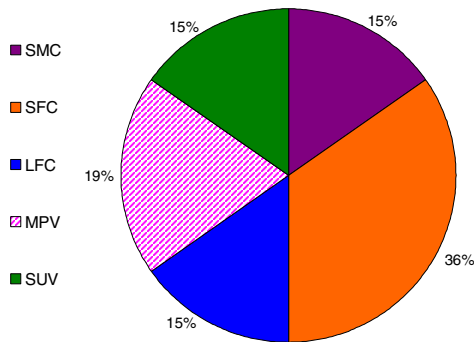


Figure 4: Vehicle type of the sample.

As defined in EuroNCAP pedestrian tests protocol (EuroNCAP 2004), a test is performed in the most dangerous point for a pedestrian to hit in each of the 18 areas in which a matrix divides each car front part. This matrix, defined individually for each car, consists of:

- Three zones for legform impact in the bumper and three zones for the upper legform impact in the bonnet leading edge.
- Twelve zones for the headform impact, six for the child headform at WAD between 1000 and 1500, and six for the adult headform at WAD between 1500 and 2100.

Table 7: Summary of tests considered in the study

Segment	Legform	Upper legform	Child head	Adult head	Total
SMC	14	15	25	15	69
SFC	24	32	63	34	153
LFC	9	12	22	13	56
MPV	14	16	39	11	80
SUV	8	9	26	24	67
TOTAL	69	84	175	97	425

The total number of tests analysed in this study is 425. The breakdown according test configurations and vehicle groups is found in Table 7.

Force-deflection curves derivation.

Following the methodologies defined the post-process of the EuroNCAP tests have been performed to get force-deflection curves for all the tests. Different trends were observed in each of the vehicle segment within the same configurations, not dependent on the vehicle groups.

Therefore a new variable needs to be incorporated capable to discriminate these tendencies. The EuroNCAP rating variable has been introduced in the analysis with such purpose.

As EuroNCAP rates each test individually to give a final rating to the car, the rating procedure followed by EuroNCAP (EuroNCAP 2004) has been applied in this point, with some remarks (* and **, see Table 8) to the whole set of tests.

Table 8: Rating procedure followed in the tests.

Test config	Red score	Green score	Yellow score
Headforms	HIC>1350	HIC<1000	Between red and green values
Upper legform*	Max bending >380Nm Total forces >6.0 kN	Max bending <300Nm Total forces <5.0kN	Between red and green values
*: As the total force is the parameter considered in the process to get to force-deflection, the rating procedure has only been based on results regarding total force criteria.			
Legform**	Max shear >7mm Max bending >20° Max tibia accel >200g	Max shear <6mm Max bending <15° Max tibia accel. <150g	Between red and green values
**: As the impactor has been considered rigid in the process to get to force-deflection, the rating procedure has only been based on results regarding the maximum tibia acceleration criteria.			

The next figure summarizes the distribution of the tests according to this rating procedure per each test configuration.

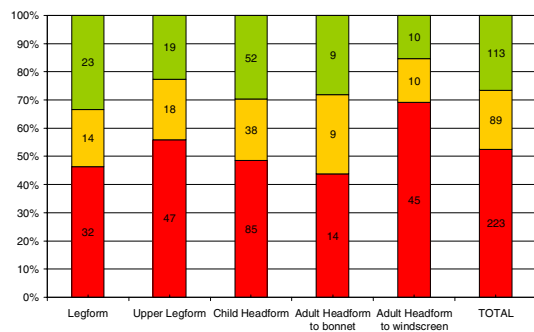


Figure 5: Distribution of test ratings along test configurations.

It can be seen that red curves represent in total over the 50% of all the tests, while green curves are near the 30%. Per test configuration, it seems that adult impacting on the windscreen area is the test configuration where red reaches its top value (almost the 70% of all the cases), while if it impacts in the bonnet area it reaches its minimum value (only the 45% of the cases).

Regarding the green curves, legform seems to be the test configuration where it reaches its maximum (33%) and the adult impacting on the windscreen where it reaches its minimum (15%).

Figure 6 to Figure 10 show the whole dataset once rated according to the criteria from Table 8.

Two trends in the legform tests are clearly highlighted and linked to the red or the green curves group. Figure 6 suggests, for all the segments, the existence of a high stiffness trend characterized by steep slopes that reaches high peak forces, (over 40 kN) in short deflections (0.04 to 0.06 m) and a low stiffness trend where the slopes are rather progressive, the peak forces are kept below 20 kN and deflection stands over 0.08 m or more.

It similarly happens in the upper legform tests. Figure 7 shows how the narrow bunch of curves in the start (below 0.03-0.04 m) starts to open up to red curves with peak force over 12 kN at 0.08 m of deflection and green curves with peak forces below 6 kN at 0.12 m of deflection.

Moreover, in these two configurations the yellow group fits in between the red and the green one, which is rather coherent with the process.

With respect to the bonnet middle area, it is seen that most curves reach its peak force near 0.02 m of deflection to start decreasing from then. Green curves slopes are rather soft to reach a maximum deflection over 0.06 m, while a trend for red curves exists where deflection is kept below 0.06 m in all cases and steeper unloading slopes are registered.

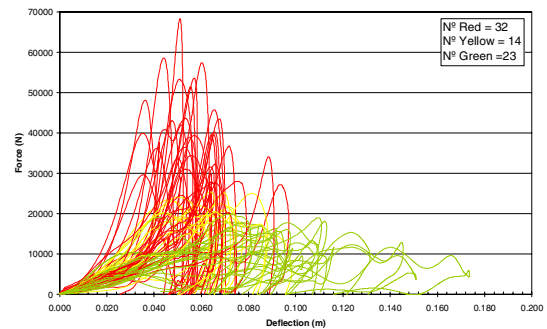


Figure 6: Force-deflection data for the bumper area.

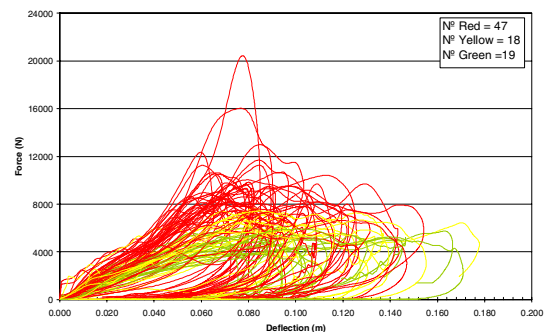


Figure 7: Force-deflection data for the bonnet front area.

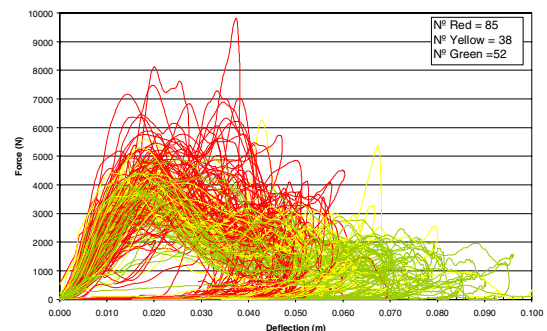


Figure 8: Force-deflection data for the bonnet middle area.

In the bonnet rear area, it can be seen red curves with soft loading slopes in the beginning and sudden steep slopes to get to the maximum and green curves where a plateau close to the maximum level is maintained throughout the deflection range. In terms of unloading slope, great difference appears according to the former ways of loading.

In the windscreen base impacts, it is generally observed an initial peak to describe the breaking of the glass during the impact (independent of the colour) and then, a softer slope to get a second maximum peak force, with the slope variation in this second loading, linked to the different ratings.

In general, in headform tests, the yellow curves fit below the red ones but they overlap significantly with the green curves.

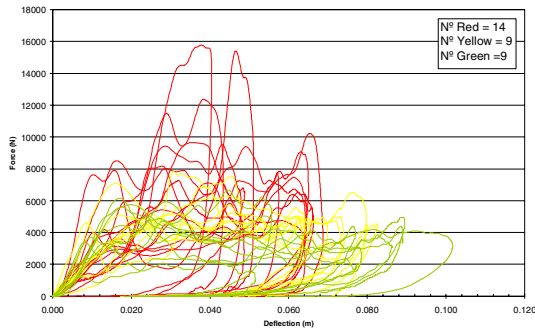


Figure 9: Force-deflection data for the bonnet rear area.

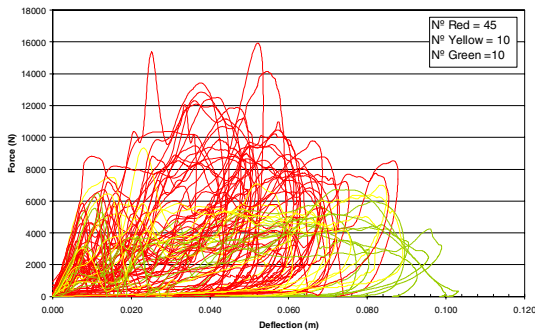


Figure 10: Force-deflection data for the windscreen base area.

PROPOSED STIFFNESS CORRIDORS.

The average parameters have been calculated for each of the 15 groups (red, yellow and red groups in each of the 5 test configurations defined) taken into account that:

- As the force deflection curves come from a cross plot between force-time and deflection-time, they result in curves with different sample rates in deflection in the same group.
- There are force deflection curves in the same group that reaches different maximum deflection levels.

To tackle the former, a re-sampling in deflection has been applied to all curves.

To address the latter, and not to penalize the average curves, only the curves with force level different from 0 in each deflection step are considered in the calculation of the averages instead of using the whole set of curves. Even with this approach, it can be observed in the averages the discontinuities caused by the end of the different curves. If the mean values were used instead, not only were these discontinuities higher but also, at high deflection levels, the mean curves will be considerably underestimating the actual curves.

Considering the great variation in force and deflection level of the peak value, the average force ± 1 standard deviation at each point in deflection is the method preferred (Hynd 2005) to derive the

contact characteristics corridors as it describes better the local behaviour of the curves.

However, due to that great variation, an overlapping between rating groups in some of test configuration appear, especially for the cases of the headform impactor.

This variation may induce some problems in the corridor interpretation if corridors are expected to univocally define red, green or yellow areas. However, considering how the corridors have been constructed, they aimed to represent the mean value of the sample with an indication of its variability through the standard deviation.

With these premises the average curves and corridors have been generated and are shown in Figure 12 to Figure 16. As seen in these figures, the calculated average curves, along with the upper and lower boundaries of the corridors, are reduced to a number of points that represents their real shape details in order to ease their handling as simulation inputs and dissemination possibilities. The tabular form of these curves is included in Appendix I.

The similarity of the simplified curves with the real curves has been ensured by restraining the difference in area below each curve to less than 1% difference in all cases, as shown in Figure 11.

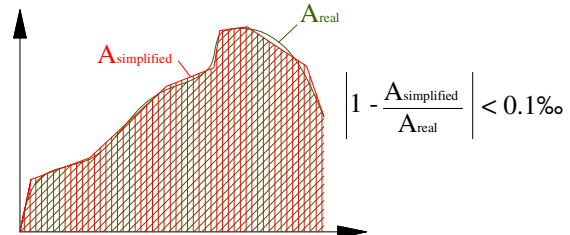


Figure 11: Area coverage between the simplified curve and the real curve.

It is relevant to observe that the rating does reflect three significantly different average trends for the legform and the upper legform tests, while this is not so clear in the case of headform tests, where trend differences are not so highlighted.

In Figure 12, legform red average curve reaches peak values over 25kN at deformations of 0.06m, while green average curve gets to peak values near 10kN at deformation of 0.08m and a plateau until deformations of 0.15m. In this case, the average yellow curve lies in between, with peak values below 20 kN and maximum deformations in 0.09m.

It can be seen in this figure that the corridor for the red group is broader than the green and yellow ones, especially in the areas of maximum forces, and considerably shorter in deflection. The higher deflection needed in green curves (over 0.1m, which may mean 0.08m in the vehicle) can give a hint on the deformation space needed in the bumper to achieve a “green score.”

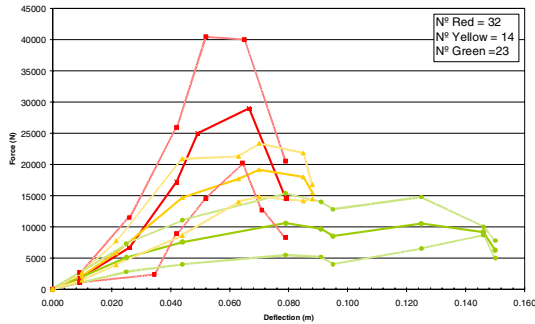


Figure 12: Simplified average force deflection curves and ± 1 standard deviation corridors for the bumper.

Regarding the upper legform, red average curves reach a peak value of 8.5kN at 0.08m of deformation, while green stands below 5.0kN with the same deformation levels. Again, the yellow average curves lie in between, with peak values of 6.0kN, although the first slope (deformation <0.06m) is the same as the green curve.

In the case of corridors, the red corridor width is again higher than for the yellow and green corridors, but the deflection ranges are rather similar. In any case, the overlap between the three corridors is clear, especially for the yellow and the green one, as it can be seen in the Figure 13.

It is interesting in this case that green curves maintains the force value close to 5 kN over 0.06m of deflection (which may mean 0.02-0.03 m deflection in the vehicle). This force value at these deflection ranges can be a valuable target for “green scores” in the bonnet front.

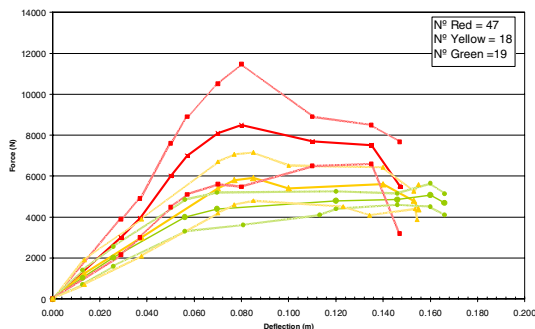


Figure 13: Simplified average force deflection curves and ± 1 standard deviation corridors for the bonnet front.

Regarding the child headform tests, the average red curve reach a peak of 4.0kN at 0.022m of deflection while the green one gets to 3.4kN at lower deflection (0.02m). Moreover, it can be seen in the Figure 14 that the average red curve maximum deflection is 0.06m, while for the green one, it goes up to 0.10m. The yellow curve stands in between red and green (peak value of 3.6kN and maximum deflection of 0.08m).

It is remarkable in this case that the initial slope (deformation <0.015m) is the same for the three average curves, however, when they reach the maximum, they decrease significantly when similar curves to the ones for the adult case may be expected. It seems that the high non-perpendicular impact angle of child tests causes this sudden decrease due to the slip of the impactor on the bonnet.

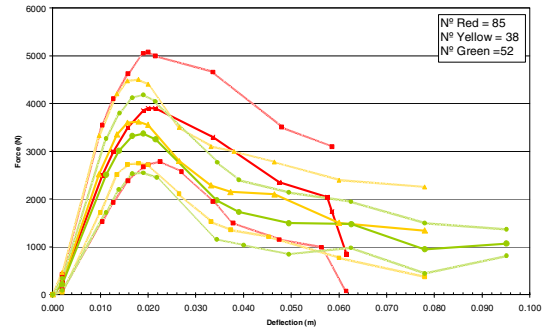


Figure 14: Simplified average force deflection curves and ± 1 standard deviation corridors for the bonnet middle.

In the case of the adult headform tests on the bonnet (Figure 15), red trend seems to deviate from the green-yellow one after 0.01m of deflection. Only then, the red curve continues increasing until values of 7.0kN, the green curve loads up to 4.3kN at deflection 0.018m and start decreasing from then and the yellow curve reaches its maximum also in 4.3kN but with an increasing slope until 0.05m of deflection.

In this case, green and yellow curves maintains the force value close to 4kN over 0.02 m of deflection. Again, these values can be good estimates for getting a “green” bonnet rear.

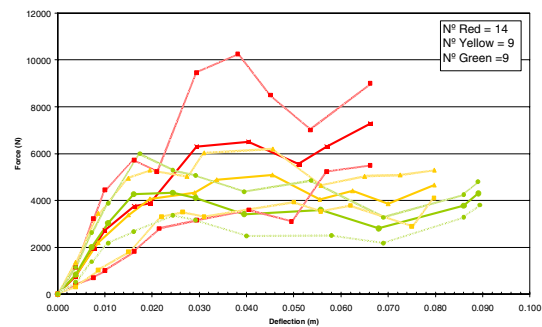


Figure 15: Simplified average force deflection curves and ± 1 standard deviation corridors for the bonnet rear.

At last, the adult headform tests on the windscreen in Figure 16 show the effect of glass breaking. The red average curve reflects it with a short plateau at deformation values of 0.01m and 2.5kN and then it continues increasing to 7.0kN at 0.06m.

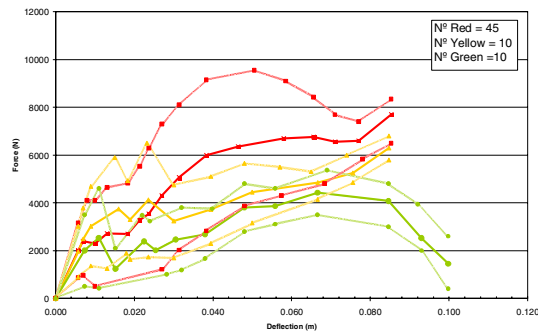


Figure 16: Simplified average force deflection curves and ± 1 standard deviation corridors for (in order) the windscreen base.

The green curve shows it with a first peak of 2.5kN at 0.01m and then, following an unloading phase, a moderate increasing phase until 4.5kN at 0.08m. Finally, the yellow curve, again mostly between the red and green curve, increase to values of 4.0kN at 0.02m, maintains similar values up to 0.03m, and then continues increasing up to 6.0kN at 0.08m.

In the case of headforms, the corridors overlap considerably, especially the green and yellow ones. Moreover, for the three configurations, the lower half red corridor is partially contained in the yellow or green corridors while the upper half red corridor stands differentiated.

For the case of unloading slopes, it is analysed as a range of variation (maximum-minimum) and is presented in Table 9.

In general, the slope ranges within each colour are rather wide (max/min is about 100 times), which indicates that the variability is very high for all configurations.

Table 9: Maximum, average and minimum unloading slopes for the different groups and impacted vehicles area.

Units: N/m	Bumper	Bonnet front	Bonnet middle	Bonnet rear	Wind screen base
Max	7.07 E8	1.70 E7	2.63 E7	1.38 E8	1.84 E7
Avge	9.61 E7	1.46 E6	2.05 E6	1.32 E7	2.85 E6
Min	1.58 E6	1.45 E5	4.031 E4	6.63 E4	1.60 E5
Max	1.35 E8	1.04 E7	8.82 E7	1.85 E6	6.00 E6
Avge	1.53 E7	1.66 E6	7.50 E6	8.47 E5	1.05 E6
Min	9.73 E5	9.00 E4	5.85 E4	1.40 E5	7.71 E4
Max	2.17 E7	2.08 E6	4.68 E6	1.51 E6	4.00 E6
Avge	3.29 E6	6.30 E5	4.92 E5	4.81 E5	8.79 E5
Min	2.51 E5	1.39 E5	2.85 E4	7.96 E4	2.01 E5

STIFFNESS CORRIDORS VALIDATION WITH MADYMO MODELS.

The main output of this work consists of a set of stiffness corridors for the different parts of the vehicle front to be used as input for simulation with pedestrian and vehicle interactions. To check that the corridors proposed behave accurately in simulation and they represent what it is expected, a validation has been performed in MADYMO.

To evaluate the force-deflection calculated corridors, different models have been constructed to reproduce the EuroNCAP pedestrian test configurations.

As in the case of upper legform and legform tests the vehicle geometry plays an important role, these cases have been kept out of this preliminary validation and only headform tests have been reproduced.

Two MADYMO models have been constructed to reproduce the adult and the child headform EuroNCAP pedestrian tests configurations on a real vehicle.

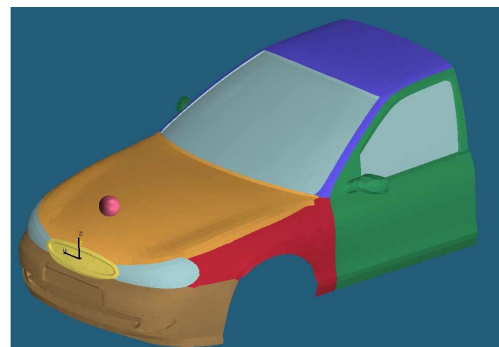


Figure 17: MADYMO models for the three EuroNCAP pedestrian configurations.

In both cases, the model consists of two systems:

- The MADYMO ellipsoid headform impactor, with the mass and geometry properties as well as the initial speed and direction from the EuroNCAP corresponding protocol.
- A real vehicle, with the contact characteristics given by the force-deflection simplified average curve calculated for the red, green or yellow cases in the bonnet middle, bonnet rear and windscreen area, with fixed friction coefficient (0.25 for the bonnet and 0.15 for the windscreen)

Comparison of results

In order to compare the simulation results with the experimental tests, the mean HIC value is obtained for the red, yellow and green test groups in each of the three configurations (adult-bonnet, adult-windscreen and child-bonnet). The average and the

standard deviation is including along with the results from the simulation in Table 10.

Table 10: Comparison of the HIC values.

		Child headform bonnet	Adult headform bonnet	Adult headform windscreen
Red	Expected	2324 (± 1014)	2440 (± 1306)	2388 (± 961)
	Obtained	2356	2444	2430
Yellow	Expected	1180 (± 108)	1169 (± 106)	1182 (± 140)
	Obtained	1273	1287	1255
Green	Expected	801 (± 114)	809 (± 109)	831 (± 115)
	Obtained	909	920	913

It can be seen that HIC output from the models in all cases is rather similar to the mean HIC value obtained from the tests.

It is remarkable that red behaviours are very close with their targets and very well distinguished from the other two rankings.

Regarding the yellow and green best fit, they are also considerably close to the target.

However, the output of these two models has been found to be dependant on the value in the hysteresis slope showing cases where green and yellow behaviour are exchanged, especially in the bonnet impacts. This behaviour is not surprising as the average curves in these two configurations show a significant overlap.

GUIDELINES TO APPLY THE STIFFNESS CORRIDORS TO THE CURRENT FLEET OF EUROPEAN VEHICLES.

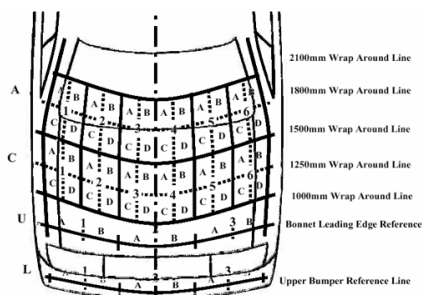


Figure 18: EuroNCAP test matrix definition.

Considering that EuroNCAP test selection is performed on an individual vehicle-based matrix (Figure 18), and this matrix is also the basis for the

ratings (Figure 19), it is coherent to use it as a template to apply the proposed characteristics.

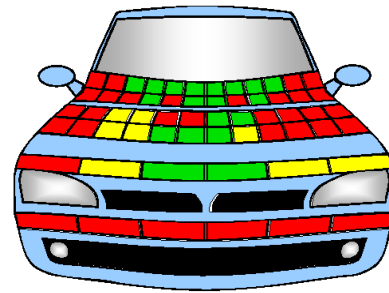


Figure 19: EuroNCAP typical pedestrian rating.

Moreover, as the result matrix for each car tested in EuroNCAP since September 2005 are available on the website, it can be used to apply the red, green and yellow curves obtained in this paper in the red, green and yellow rated areas on the car.

Four consideration are to be taken into account when applying these stiffnesses to the vehicle models:

- The force deflection curves derived do not separate the deflection of the vehicle and the one from the impactor. Therefore when the contact characteristic is defined in the model, this issue should be considered to define the stiffness correctly.
- The force deflection curves derived only cover deflections up to those seen in the EuroNCAP tests from which they were derived, so they may not be suitable for modelling higher severity impacts.
- The matrix areas on the A pillars are not tested in EuroNCAP and are given a red score directly. Red curves obtained in this study may underestimate the real stiffness of this part.
- The matrix areas on the middle of the windscreen are not tested in EuroNCAP and are given directly a green score. Green curves obtained in this study may not represent the real behaviour of this part and more dedicated studies on glazing impact should be used.

CONCLUSIONS.

The following conclusions can be drawn from the work herein presented.

1. Three methodologies have been developed and extensively applied to obtain force-deflection curves from the EuroNCAP pedestrian tests. These methodologies have proved to be accurate enough to obtain the contact characteristics from these tests.
2. The five sets of three stiffness corridors that have been generated in this work is an

important source of data for pedestrian simulation purposes that represents widely the European fleet stiffnesses ranges in the front part of the vehicle.

3. From these corridors, target values to get a “green” score can be derived based on the forces and deflection achieved in the tests. Deflections over 0.08m in the bumper and force levels in 4-5kN in the bonnet over 0.02m of deflection are valuable targets to get “green scores” in the different tests.
4. Newly tested cars may change the average green, yellow and red curves of the fleet herein obtained, however, since the evaluation has been done gathering red, yellow and green curves, their validity as estimates will be maintained while the EuroNCAP rating of the tests is maintained.
5. The stiffness maps for each individual vehicle segment define the way to implement the stiffness corridors into the current European fleet. Since 2005, EuroNCAP website publish this map for each tested vehicle.
6. These two sets of data are valuable not only to identify the gaps in the current European fleet regarding pedestrian protection, but also, and together with the feasibility limitations (Lawrence 2004), to focus future research efforts to further improve the pedestrian protection in Europe.

ACKNOWLEDGEMENTS.

This work has been developed within the APROSYS project (TIP3-CT-2004-506503 VI Framework Programme UE) Sub-project 3: Pedestrian and cyclist accidents.

The authors would like to thanks EuroNCAP for making available for APROSYS SP3 the pedestrian tests required to develop this task.

The authors would also like to thanks the Spanish Ministry of Science and Education, that partially founded this activity under the Complementary Action with reference number TRA2005-25911-E and the Community of Madrid, that contributed to this work through the SEGVAUTO programme (S- 0505/ DPI-0329).

REFERENCES.

- EEVC WG17 (1998). "Improved test methods to evaluate pedestrian protection for passenger cars." EEVC WG17 Report.
- EuroNCAP (2004). "EuroNCAP pedestrian testing protocols" Version 4.1 March 2004.
- EuroNCAP (2001). "EuroNCAP pedestrian testing protocols" Version 3. April 2001.
- Hynd D. (2005). "EEVC WG9 Biofidelity corridor calculation method." EEVC WG12 document.
- Lawrence G., Hardy B. J., Carroll J.A., Donaldson W.M.S., Visvikis C., Peel D.A. (2004) "A study on the feasibility of measures relating to the protection of pedestrians and other vulnerable road users" Project FIF.2003937 Final Report.
- Lestrelin D., Brun Cassan F., Fayon A., Tarriere C., Castan F. (1980) "PRAKIMOD: Mathematical Simulation of Accident Victims: Validation and Application to Car-Pedestrian Collisions". 8th ESV Conference 1980.
- MADYMO (2003) "MADYMO Reference manual" V 6.1 TNO Automotive, April 2003.
- Mizuno K., Kajzer J. (2000). "Head Injuries in Vehicle-Pedestrian Impact". SAE Paper N° 2000-01-0157.
- Van Hoof, J., R. de Lange, et al. (2003). "Improving pedestrian safety using numerical human models." Stapp Car Crash Journal 47: 401-436.
- Van Rooij L., Bhalla K., Meissner M., Ivarsson J., Crandall J., Longhitano D., Takahashi Y., Dokko Y., Kikuchi Y. (2003). "Pedestrian crash reconstruction using multi-body modelling with geometrically detailed, validated vehicle models and advanced pedestrian injury criteria." 18th ESV Conference 2003.
- Wismans J. and van Wijk J. (1982). "Mathematical Models for the Assessment of Pedestrian Protection Provided by a Car Contour." 9th ESV Conference 1982.
- Yao, J., Yang J., et al. (2005). "Reconstruction of head to bonnet top impact in child pedestrian to passenger car crash." IRCOBI 2005.

APPENDIX I: STIFFNESS SIMPLIFIED CORRIDORS.

The next tables present the different stiffness force-deflection corridors (deflection in m and force in N), in its simplified version, for each of the vehicle front parts and each of the three rating groups.

Table-AI- 1: Simplified force deflection data for the bumper area (from the legform tests).

BUMPER																	
AVERAGE						TOP						LOW					
Red		Yellow		Green		Red		Yellow		Green		Red		Yellow		Green	
0.0000	0	0.000	0	0.000	0	0.000	0	0.000	0	0.000	0	0.000	0	0.000	0	0.000	0
0.0092	1794	0.010	2183	0.025	5100	0.009	2685	0.010	2670	0.025	7300	0.009	1080	0.010	1500	0.025	2800
0.0260	6699	0.022	5844	0.044	7560	0.026	11500	0.022	7765	0.044	11090	0.035	2399	0.022	3950	0.044	4000
0.0420	17195	0.044	14700	0.079	10595	0.042	25900	0.044	20900	0.079	15400	0.042	8900	0.044	8650	0.079	5495
0.0492	25000	0.063	17700	0.091	9650	0.052	40450	0.063	21300	0.091	14000	0.052	14520	0.063	14026	0.091	5200
0.0665	29000	0.070	19150	0.095	8500	0.065	40000	0.070	23400	0.095	12800	0.064	20200	0.070	14850	0.095	4000
0.0790	14595	0.085	17995	0.125	10500	0.079	20500	0.085	21800	0.125	14800	0.071	12700	0.085	14150	0.125	6550
		0.088	15485	0.146	9160			0.088	16800	0.146	10000	0.079	8289	0.088	14450	0.146	8690
				0.150	6250					0.150	7800					0.150	4985

Table-AI- 2: Simplified force deflection data for the bonnet front area (from the upper legform tests)

BONNET FRONT																	
AVERAGE						TOP						LOW					
Red		Yellow		Green		Red		Yellow		Green		Red		Yellow		Green	
0.0000	0	0.0000	0	0.0000	0	0.0000	0	0.0000	0	0.0000	0	0.0000	0	0.0000	0	0.0000	0
0.0290	3000	0.0134	1250	0.0127	1030	0.0290	3900	0.0134	1900	0.0127	1400	0.0290	2150	0.0134	695	0.0127	700
0.0370	3946	0.0377	3000	0.0257	2015	0.0370	4900	0.0377	3900	0.0257	2550	0.0370	3000	0.0377	2100	0.0257	1600
0.0500	6000	0.0700	5400	0.0560	4000	0.0500	7600	0.0700	6700	0.0560	4850	0.0500	4475	0.0700	4190	0.0560	3300
0.0570	7000	0.0770	5800	0.0696	4400	0.0570	8900	0.0770	7065	0.0696	5200	0.0570	5100	0.0770	4600	0.0807	3615
0.0700	8100	0.0850	5910	0.1200	4800	0.0700	10500	0.0850	7150	0.1200	5250	0.0700	5600	0.0850	4800	0.1132	4100
0.0800	8500	0.1000	5400	0.1460	4850	0.0800	11470	0.1000	6511	0.1460	5150	0.0800	5480	0.1231	4500	0.1200	4400
0.1100	7700	0.1400	5600	0.1600	5075	0.1100	8900	0.1400	6425	0.1600	5645	0.1100	6495	0.1342	4080	0.1460	4600
0.1350	7500	0.1530	4800	0.1660	4690	0.1350	8495	0.1530	5250	0.1660	5142	0.1350	6590	0.1535	4400	0.1600	4500
0.1470	5510	0.1550	4380			0.1470	7675	0.1550	5590			0.1470	3197	0.1545	3875	0.1660	4100

Table-AI- 3: Simplified force deflection data for the bonnet middle area (from the child headform tests).

BONNET MIDDLE																	
AVERAGE						TOP						LOW					
Red		Yellow		Green		Red		Yellow		Green		Red		Yellow		Green	
0.0000	0	0.0000	0	0.0000	0	0.0000	0	0.0000	0	0.0000	0	0.0000	0	0.0000	0	0.0000	0
0.0020	250	0.0020	250	0.0020	215	0.0020	420	0.0020	465	0.0020	340	0.0020	99	0.0020	50	0.0020	90
0.0104	2500	0.0097	2520	0.0112	2510	0.0104	3550	0.0097	3325	0.0112	3270	0.0104	1530	0.0100	1715	0.0112	1720
0.0127	3000	0.0135	3350	0.0139	3010	0.0127	4100	0.0135	4199	0.0140	3800	0.0127	1930	0.0135	2515	0.0139	2200
0.0158	3500	0.0157	3600	0.0167	3323	0.0158	4625	0.0157	4475	0.0167	4120	0.0158	2380	0.0157	2725	0.0167	2535
0.0190	3850	0.0180	3620	0.0190	3370	0.0190	5050	0.0180	4500	0.0190	4180	0.0190	2675	0.0180	2750	0.0190	2550
0.0200	3900	0.0200	3550	0.0216	3250	0.0200	5075	0.0200	4400	0.0215	4045	0.0200	2720	0.0200	2720	0.0218	2450
0.0215	3900	0.0265	2795	0.0344	1975	0.0215	5000	0.0265	3500	0.0345	2770	0.0225	2785	0.0265	2110	0.0344	1155

0.0336	3300	0.0332	2285	0.0390	1730	0.0336	4660	0.0332	3100	0.0390	2400	0.0270	2575	0.0332	1525	0.0400	1034
0.0475	2355	0.0373	2150	0.0495	1495	0.0480	3505	0.0380	3000	0.0495	2140	0.0336	1950	0.0373	1355	0.0495	845
0.0575	2045	0.0465	2100	0.0626	1475	0.0585	3095	0.0465	2775	0.0625	1945	0.0378	1500	0.0453	1210	0.0625	980
0.0585	1740	0.0600	1500	0.0780	950			0.0600	2397	0.0780	1495	0.0475	1150	0.0600	770	0.0780	440
0.0615	853	0.0780	1341	0.0951	1068			0.0780	2250	0.0951	1364	0.0563	990	0.0780	369	0.0951	810
												0.0615	75				

Table-AI- 4: Simplified force deflection data for the bonnet rear area (from the adult headform tests).

BONNET REAR																	
AVERAGE						TOP						LOW					
Red	Yellow		Green		Red	Yellow		Green		Red	Yellow		Green				
0.0000	0	0.0000	0	0.0000	0	0.0000	0	0.0000	0	0.0000	0	0.0000	0	0.0000	0	0.0000	0
0.0038	765	0.0040	840	0.0038	825	0.0038	1140	0.0038	1350	0.0038	1140	0.0038	400	0.0038	310	0.0038	510
0.0076	1950	0.0086	2200	0.0072	2000	0.0076	3225	0.0086	3440	0.0072	2620	0.0076	700	0.0086	1020	0.0072	1380
0.0100	2723	0.0150	3375	0.0107	3030	0.0100	4450	0.0150	4950	0.0107	3880	0.0100	1000	0.0150	1800	0.0107	2180
0.0162	3750	0.0195	4070	0.0161	4265	0.0162	5725	0.0195	5290	0.0174	6000	0.0162	1820	0.0220	3300	0.0161	2665
0.0196	3875	0.0290	4334	0.0244	4330	0.0210	5235	0.0274	5020	0.0244	5285	0.0215	2800	0.0265	3500	0.0244	3365
0.0294	6300	0.0337	4880	0.0292	4110	0.0294	9450	0.0310	6020	0.0292	5060	0.0294	3150	0.0310	3300	0.0292	3155
0.0404	6500	0.0455	5080	0.0395	3410	0.0381	10250	0.0456	6200	0.0395	4370	0.0405	3600	0.0500	3925	0.0400	2485
0.0510	5550	0.0555	4050	0.0557	3600	0.0451	8500	0.0557	4630	0.0537	4850	0.0495	3100	0.0557	3530	0.0580	2500
0.0570	6300	0.0625	4400	0.0680	2800	0.0535	7005	0.0650	5030	0.0690	3271	0.0570	5225	0.0620	3780	0.0690	2180
0.0662	7283	0.0700	3865	0.0860	3774	0.0662	8999	0.0725	5080	0.0860	4250	0.0662	5500	0.0750	2890	0.0860	3280
		0.0798	4650	0.0891	4300			0.0798	5290	0.0890	4800			0.0797	4100	0.0894	3802

Table-AI- 5: Simplified force deflection data for the windscreen base area (from the adult headform tests)

WINDSCREEN BASE																	
AVERAGE						TOP						LOW					
Red	Yellow		Green		Red	Yellow		Green		Red	Yellow		Green				
0.0000	0	0.0000	0	0.0000	0	0.0000	0	0.0000	0	0.0000	0	0.0000	0	0.0000	0	0.0000	0
0.0057	2015	0.0057	1960	0.0074	2004	0.0057	3150	0.0057	3025	0.0074	3500	0.0057	870	0.0057	890	0.0074	500
0.0070	2388	0.0070	2485	0.0110	2525	0.0080	4100	0.0070	3785	0.0110	4600	0.0070	970	0.0090	1360	0.0110	425
0.0100	2295	0.0090	3027	0.0152	1235	0.0100	4100	0.0090	4685	0.0152	2100	0.0100	500	0.0131	1250	0.0282	1010
0.0131	2715	0.0160	3735	0.0225	2385	0.0131	4640	0.0151	5900	0.0220	3480	0.0270	1215	0.0180	1890	0.0320	1190
0.0183	2700	0.0190	3290	0.0254	2012	0.0183	4825	0.0183	4925	0.0240	3230	0.0314	2020	0.0190	1630	0.0380	1665
0.0214	3271	0.0236	4125	0.0305	2460	0.0214	5530	0.0232	6500	0.0320	3799	0.0383	2825	0.0236	1730	0.0480	2800
0.0237	3545	0.0300	3240	0.0380	2680	0.0237	6300	0.0300	4750	0.0398	3750	0.0480	3870	0.0300	1690	0.0558	3105
0.0270	4300	0.0395	3715	0.0480	3800	0.0270	7300	0.0395	5100	0.0480	4800	0.0574	4308	0.0395	2300	0.0665	3500
0.0314	5060	0.0500	4447	0.0558	3860	0.0314	8100	0.0480	5650	0.0558	4600	0.0684	4800	0.0500	3150	0.0846	2999
0.0383	5990	0.0666	4840	0.0666	4425	0.0383	9150	0.0570	5497	0.0690	5375	0.0780	5825	0.0666	4150	0.0930	2000
0.0464	6350	0.0756	5240	0.0846	4075	0.0505	9550	0.0650	5300	0.0846	4800	0.0853	6500	0.0756	4845	0.0998	399
0.0580	6700	0.0847	6300	0.0930	2520	0.0585	9100	0.0740	6000	0.0920	3941			0.0847	5800		
0.0656	6749			0.0998	1447	0.0656	8420	0.0847	6798	0.0998	2599						
0.0710	6550					0.0710	7690										
0.0770	6600					0.0770	7400										
0.0853	7699					0.0853	8351										

Technical solutions for enhancing the pedestrian protection

Christian Pinecki,
Richard Zeitouni.

PSA Peugeot Citroën
France
Paper number 07-0307

ABSTRACT

Since October 2005, the European regulation for pedestrian protection is applicable to new vehicles. Four impactors have been developed: leg, femur, child and adult heads for testing predefined areas on the front face of the vehicle.

This paper presents the technical strategy and the set of solutions which place PSA Peugeot Citroën as one of the best manufacturers for pedestrian protection with in particular Citroën C6, first and unique vehicle achieving 4 stars in EuroNCAP pedestrian protection assessment.

The scenario of head and leg protection is articulated around two requirements:

- keeping a space between the bonnet and the various hard elements of the engine, and behind the front bumper so that the impactors do not come into contact with rigid elements,
- softening the bonnet and the front bumper elements in order to generate a more progressive head and leg deceleration during the impact.

The level of constraint induced by these requirements penalizes heavily the style and the overhang of the vehicles. Massive development efforts have been invested in both fields of leg and head protection. The physical characteristics of the components and the design constraints have to be optimized under advanced computational analyses with finite elements model.

The protection of the leg requires the installation of two absorbers (upper and lower).

The head protection requires complex tuning of the stiffness of the bonnet and some components inside the engine compartment. For executive cars with long hood, like C6, it also implied the development of an active bonnet, triggered by fusible optic sensors, which is not only a technical challenge but also addresses outstanding issues in the field of quality and reliability.

The paper provides technical descriptions of the methods deployed by PSA Peugeot Citroën, associating numerical simulations and physical tests, for developing innovative solutions in the field of passive and active safety.

INTRODUCTION

Every year, approximately 8,000 pedestrians and cyclists are killed and 300,000 others injured in road accidents in Europe. The accidents are particularly frequent in urban zones. Even when cars are driving at relatively reduced speeds, very severe injuries can occur. Below a speed of approximately 40 km/h, it is nevertheless possible to considerably reduce the gravity of injury with modifications of the frontal parts of vehicles

Since 2005, a European directive (called "phase 1") requires the car manufacturers to treat their new vehicles for the protection of the pedestrians in case of impact. This directive is planned to be reviewed in the future to include more severe requirements. The current expected schedule is 2010 and the update is called "phase 2" (see [1]).

Moreover, the consumerist organisation Euro NCAP assess the pedestrian protection offered by a new through component test configurations which are identical to those proposed at present time for the phase 2 of the directive. The level of pedestrian protection is then ranked by attributing the vehicle a given number of stars (four at most).

The aim of this paper is to present various technical solutions used by PSA Peugeot Citroën to improve the performance of its vehicles in terms of pedestrian protection.

TEST PROTOCOLS

The assessment of pedestrian protection offered by a vehicle is made through three different and independent component test procedures corresponding to different body segment:

- the first one is related to the assessment of the protection of the leg. The test is called "legform to bumper test"
- the second one is related to the upper leg. The test is called "upper legform to bonnet leading edge"
- the last one is related to the head, adult head impact and child head impact. The tests are called

“Adult and Child headforms to bonnet and windscreen test”

Four specific body form impactors are used in these tests. They are propelled against the front part of the vehicle (from the bumper up to the windscreen depending on the type of test) and they are equipped with several sensors in order to measure biomechanical criteria that are used to assess the risk of injuries (see Figure 1).

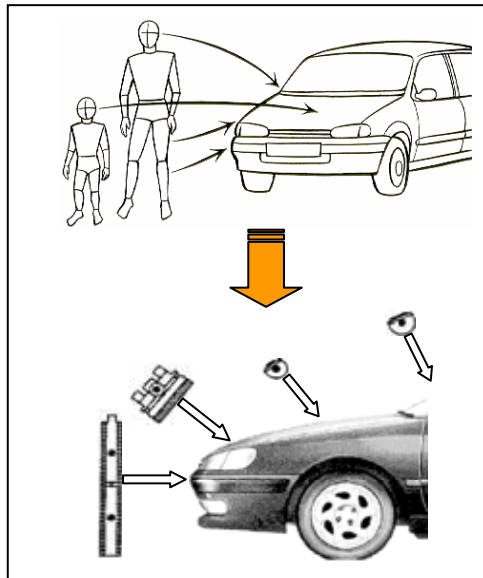


Figure 1. Pedestrian test made of 4 body form impactors propelled against the car front-end.

It is important to underline that accident data analyses show that upper leg injuries are almost non-existent during an impact of a pedestrian against a car. For this reason, the European Directive Phase 1 does not impose any limit on the biomechanical criteria for upper leg impact. It only requires the test to be carried out for monitoring purposes.

This paper presents some technical solutions developed by PSA Peugeot Citroën for the legform and the headform tests. Therefore, the current chapter is dedicated the presentation of these 2 impactors and the performance levels asked in Phase 1 and Euro NCAP requirements.

Then, in the next chapters, we will present the technical solutions (theory + actual solutions implemented in our cars) for each type of impact.

Leg to bumper tests: Legform impactor

The legform impactor represents the leg of an adult. It is made out of two stiff elements corresponding to the tibia and the femur, which are connected by a articulation representing the knee joint. The different parts are covered with foam

representing muscular tissues of the leg (see Figure 2).



Figure 2. Legform pedestrian test.

The test procedure consists in propelling the legform against the bumper, in free motion at 40 km/h. Direction of impact should be in the horizontal plane and parallel to the longitudinal vertical plane of the vehicle.

Three biomechanical criteria are recorded:

- the tibia deceleration (measured by an accelerometer on the tibia - non impacted side),
- the knee bending angle (measured by a potentiometer - on the top of the tibia),
- the knee shear displacement (measured by a potentiometer - on the bottom of the femur).

The biomechanical thresholds required by regulation are different than those required by Euro NCAP as shown in Table 1.

Table 1. Biomechanical thresholds for leg to bumper tests required by regulation and by Euro NCAP.

Protocols	European Directive “Phase 1”	EuroNCAP (high performance limits)
Tibia deceleration (g)	200	150
Knee bending angle (°)	21	15
Knee shear displacement (mm)	6	6

It is important to notice that the requirements imposed by Euro NCAP for its high performance level covers those of the European Directive Phase1. Indeed, the test protocol is identical and the biomechanical criteria in Euro NCAP are the most severe.

Adult and child headforms to bonnet and windscreen tests: Headform impactors

The different head impactors are all built in a identical way by an aluminium spherical part covered with a rubber skin (see Figure 3).

The test procedure consists in propelling the head impactor, in free motion, according to a specific angle. The mass and the size of impactors, as well as the speed and the angle vary according to protocols as shown in Table 2.

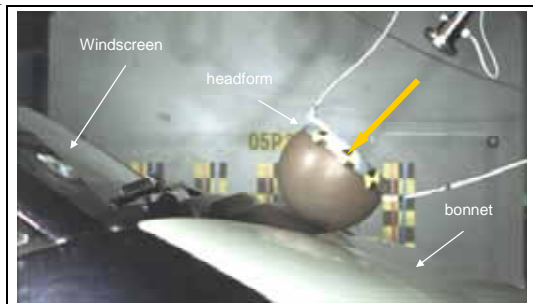


Figure 3. Headform pedestrian test.

Table 2. Headforms characteristics as required by regulation and by Euro NCAP.

Protocols	European Directive "Phase 1"		Euro NCAP	
	child	adult	child	adult
Type of headform	child	adult	child	adult
Mass (kg)	3,5	4,8	2,5	4,8
Radius (mm)	82,5	82,5	65	82,5
Speed (km/h)	35	35	40	40
Angle (°)	50	35	50	65

A single biomechanical criterion is measured to assess the level of protection: the HIC which is calculated from the head acceleration.

$$HIC = \max \left[\frac{1}{t_2 - t_1} \int_{t_1}^{t_2} a \, dt \right]^{2.5} (t_2 - t_1) \quad (1).$$

with: $(t_2 - t_1) \leq 15ms$

The biomechanical limits not to be exceeded during the headform tests vary with the protocols as shown in Table 3.

Table 3. Biomechanical thresholds for head impact tests required by regulation and by Euro NCAP.

Protocols	European Directive "Phase 1"		EuroNCAP (high performance limits)	
	child	adult	child	adult
Type of headform	child	adult	child	adult
Impact zone	B	W	B or W	B or W
HIC requirement	<1000 on 2/3 of the test area + <2000 on the area left	NA	< 1000	

B = bonnet W = windscreen

It is important to keep in mind that protocols are so different (in terms of mass, radius, and head impact speed), that the requirements fixed by the European Directive Phase 1 are not covered by the EuroNCAP ones and vice versa. Therefore, a vehicle fulfilling the Directive requirements is not sure to get a good score at the Euro NCAP rating, and conversely a vehicle with a good score in Euro NCAP pedestrian rating has no certainty fulfil the Phase 1 criteria.

SCENARIO FOR PROTECTING THE LEG

Protection of the leg requires the implementation of two absorbers behind the bumper:

- the first one located at the lower level of the tibia,
- the second one located at the level of the knee.

An example is shown in figure 4 which present the position of the two absorbers on the Citroën C4 Picasso.

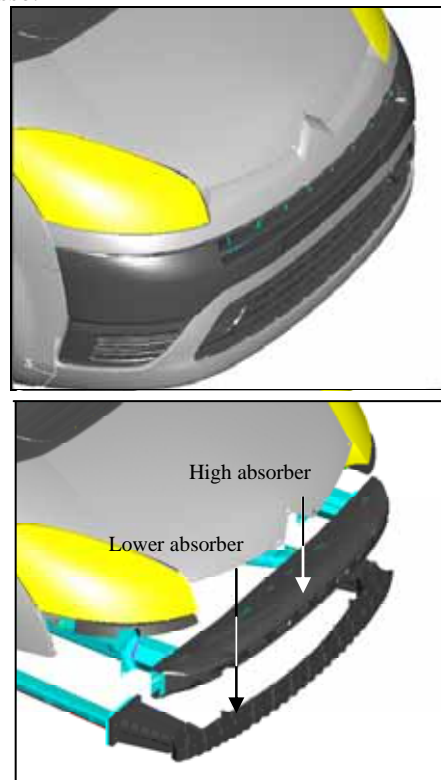


Figure 4. Citroën C4 Picasso – Position of the two absorbers designed to protect the leg of a pedestrian.

For this car model, impact energy is 825 J. A large part of this energy will be absorbed by the front face of the vehicle according to the following distribution:

- lower absorber: 20 %
- upper absorber: 40 %
- bumper: 40 %

Although dissipating a large part of the energy of the impact, the stiffness adaptation of the bumper for leg, is limited by its conception which is often limited by strong constraints of style and quality. Therefore, the tuning to match as much as possible the requirements is made on the lower and upper absorbers.

Description and role of the lower absorber

The lower absorber is made of a plastic or metal beam. Its role is to limit the bending of the knee during the impact thanks to its stiffness. He is hung either on the structure of the vehicle or directly moulded with the spoiler (see Figure 5 and Figure 6).

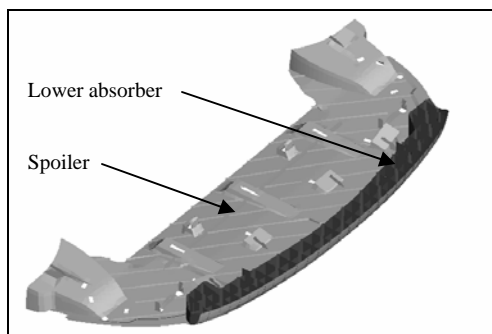


Figure 5. Lower absorber and its attachment on Citroën C4 Picasso.

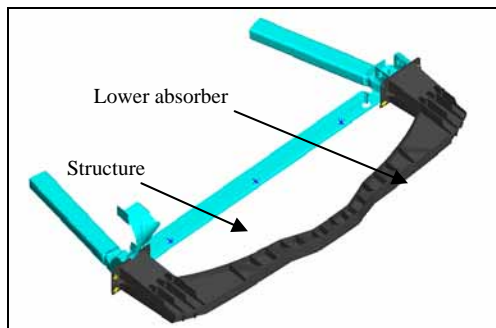


Figure 6. Lower absorber and its attachment on Citroën C4.

Note: Citroën C4 and Citroën C4 Picasso scored the full score (6 points out of 6) in the legform tests, in their Euro NCAP rating.

The upper absorber

The upper absorber is located on the level of the knee, and is hung on the rigid structure of the vehicle. It is constituted by a plastic skin whose stiffness is designed to be crushed gradually, thus to create a progressive deceleration for the leg during the impact.

Figure 7 presents the cross-section of the upper absorber on Citroën C4.

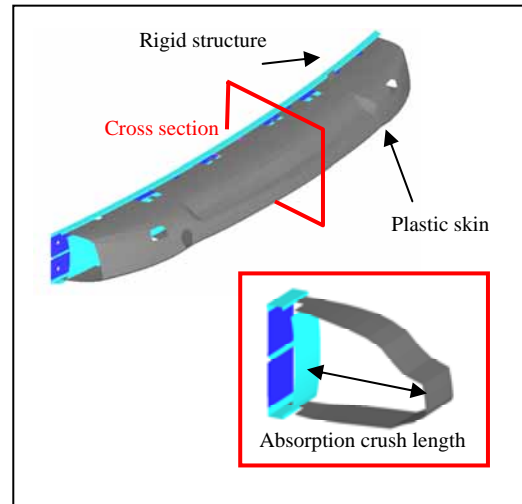


Figure 7. Cross section of the upper absorber on Citroën C4.

The kinematics of the impact

Figure 8 gives details of the Kinematics of impact on the Citroën C4.

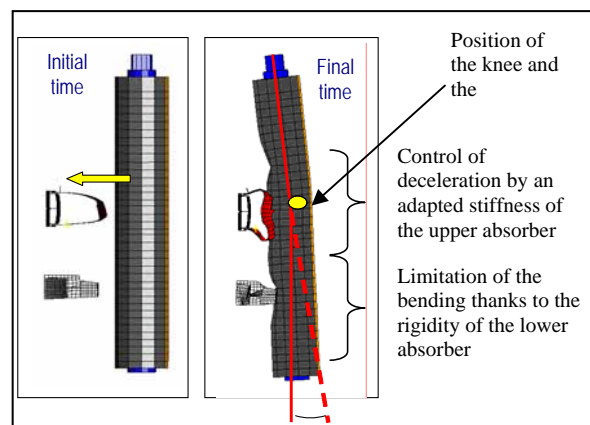


Figure 8. Kinematics of impact on Citroën C4 (cross section).

Figure 9 presents the deceleration curve measured on this impact.

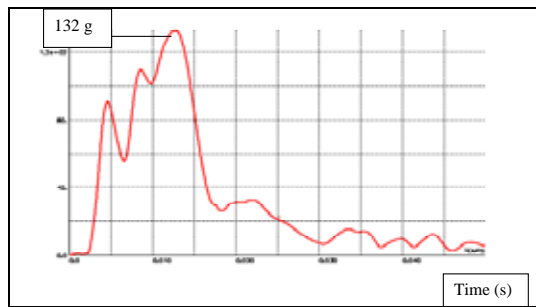


Figure 9. Deceleration curve on the legform for Citroën C4.

A too short length of absorption, and/or a too important flexibility of the upper absorber would cause a secondary peak of deceleration on the legform which could exceed the thresholds defined by the protocols. Furthermore, the addition of this upper absorber under the bumper increases the overhang of the vehicle and penalizes strongly the style. So the optimization of this length of absorption is of high importance.

Difficulties

During the impact of the legform on the front-end of the car, it is necessary that no rigid element interact and disturb the kinematics of impact. Otherwise, a too important peak of deceleration could be generated. According to the style of the vehicles, headlight can be sometimes found in the absorption length devoted to the leg. For this reason, sometimes, headlight should also be controlled for legform impactor test. This is the case for the Citroën C4 headlight, as shown in Figure 10.

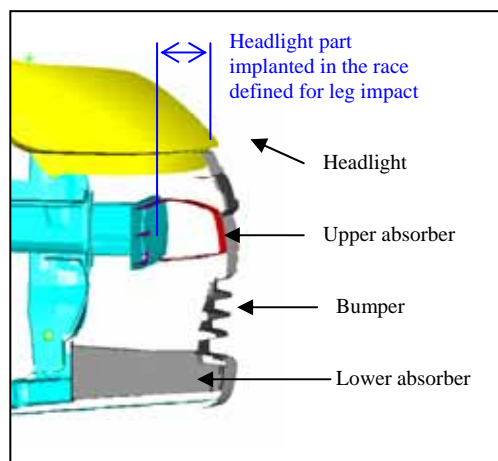


Figure 10. Positioning of headlight compared to the absorbers on the Citroën C4 (cross-section).

One of the solutions used, when the stiffness has to be controlled, is the use of replaceable fixing

brackets (see Figure 11). These special brackets will allow the headlight to move backward during the impact with the legform. The breaking efforts are then tuned so that to be consistent with the crush vs stiffness laws specified for the absorbers.

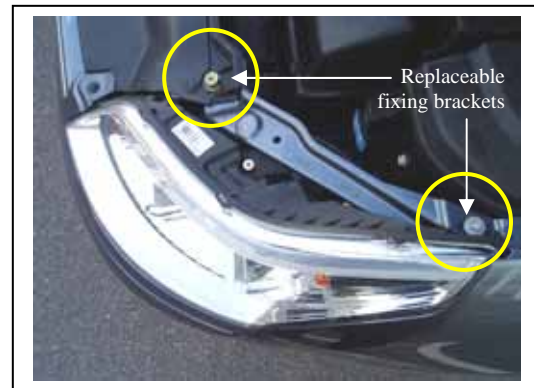


Figure 11. Replaceable fixing brackets of the Citroën C4 headlights.

Moreover, in order to give enough space for the headlights to move backward, it could also be needed to equip the wings with the same type of replaceable fixing brackets. This is also the case for the Citroën C4 as it is presented in Figure 12.

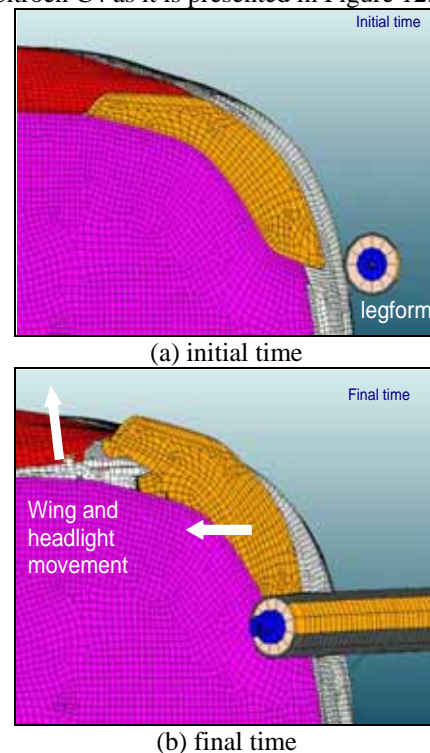


Figure 12. Kinematics of headlight and wing on the Citroën C4 (Top view) - (a) initial time, (b) final time.

Note: this type of kinematics is also used as a technical solution for the “reparability” impact (damageability test performed at 16 km/h) during which the minimum of parts must be changed, to limit the cost of repairs.

SCENARIO FOR PROTECTING THE HEAD

The head protection is driven by two requirements. On the one hand it is necessary to preserve a space under the bonnet so that the impactors do not come into contact with rigid elements such as the engine. On the other hand, it is also vital to soften the constitutive elements of the bonnet in order to control the head deceleration in a progressive way during the impact.

Figure 13 present the kinematics of impact of the headform test on the Citroën C4 Picasso. And Figure 14 presents the deceleration curve measured on this headform impact on the Citroën C4 Picasso.

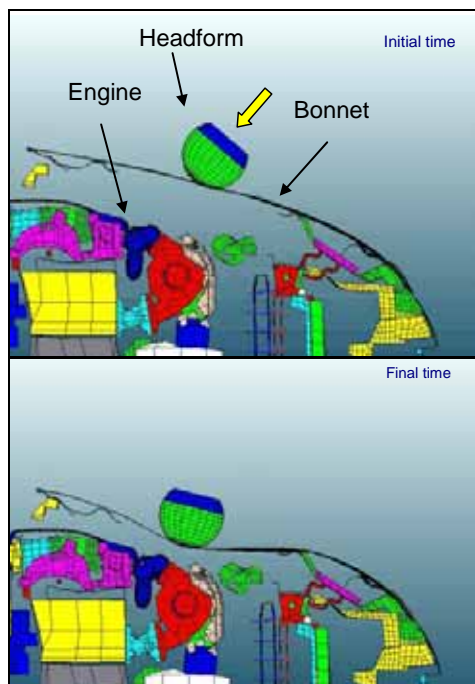


Figure 13. Kinematics of impact on the Citroën C4 Picasso (cross-section).

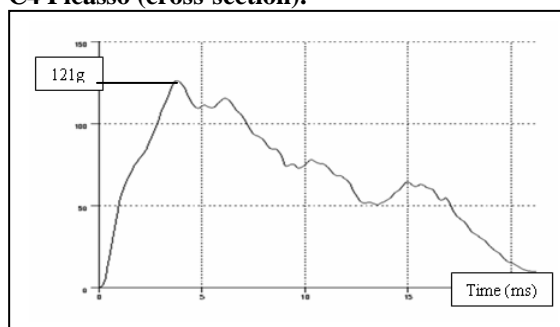


Figure 14. Deceleration curve measured on this headform impact on the Citroën C4 Picasso.

Therefore, all the elements likely to be impacted by the headform must have an adapted stiffness and usually may need to be softened (bonnet, scuttle, headlight...).

For this reason, the free space under the bonnet must be sufficient in order not to avoid a hard contact that will result in an important peak of deceleration that may increase the HIC value. This will have a consequence on the compaction of the engine.

Difficulties

Collapsible bonnet arrester

During the impact of the head on the bonnet, the bonnet arresters which ensure its correct positioning during the whole life of the vehicle, should not behave like hard points. One of the solutions is to use collapsible arresters which retract under a specific load.

The principle of function of a collapsible arrester is presented in Figure 15. The Citroën C4 Picasso example is shown in Figure 16.

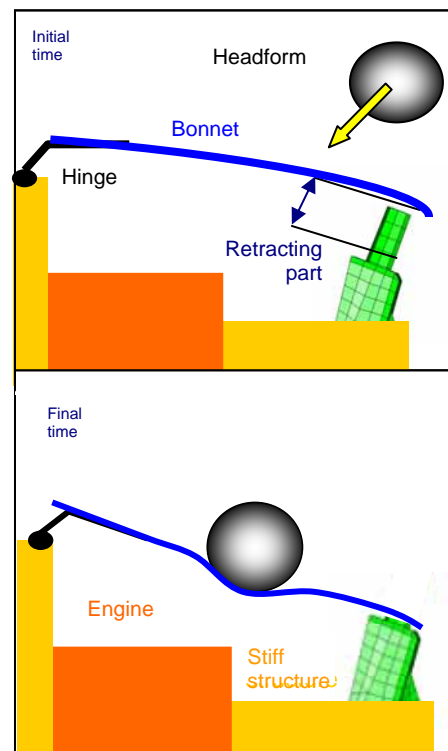


Figure 15. Principle of function of a collapsible arrester.

In its kinematics of impact, the head will first deform the bonnet. This one will then deflect and therefore press on the arresters which will be able to collapse. Therefore, the head will not be prevented to go downwards.



Figure 16. Bonnet arresters on the Citroën C4 Picasso

Active bonnet

When space under bonnet is insufficient, for instance with large engines, an active bonnet can be another solution to prevent the head from impacting hard points. This active bonnet will deploy as soon as an impact with a pedestrian is detected and then, the space under bonnet will be artificially increased.

The Citroën C6 is one of the first car model to be equipped with such a technology.

The sensors, located under the bumper, identify the type of obstacle according to stiffness and force parameters. When a pedestrian impact is detected, the springs positioned near the windscreen will lift the bonnet of 65 mm in less than 15 ms .So that the pedestrian's head is kept clear from the hard parts of the engine.

The principle of function of the C6 active bonnet is shown in Figures 17 and 18.

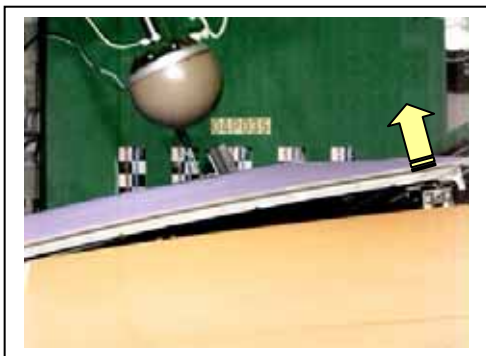


Figure 17. Example of the active bonnet of the Citroën C6.

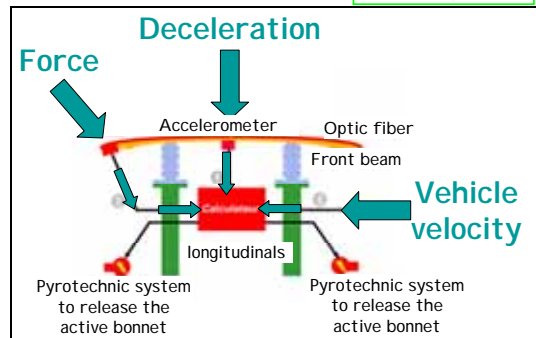
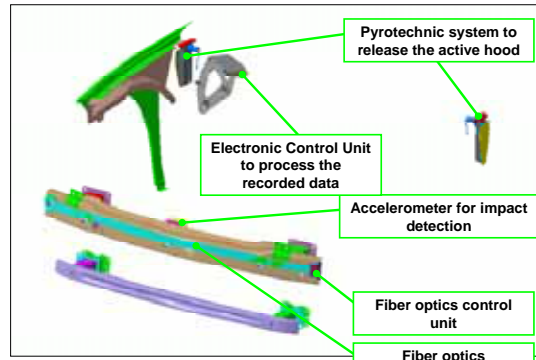
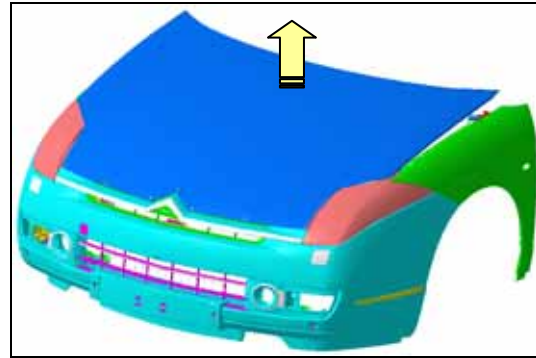


Figure 18. Principles of detection of a pedestrian impact for the Citroën C6 active bonnet.

Note: Citroën C6 and Citroën C4 Picasso respectively scored 9,64 and 8 points out of 12 on the child headform tests in their EuroNCAP rating.

METHODOLOGY FOR DESIGNING THE FRONT-END COMPONENTS

During the development phases of a vehicle, in order to limit the tests on expensive full prototypes, the various parts of the front-end are firstly designed thanks to C.A.D (virtual testing). Then during the manufacturing of the first components, their stiffness is validated thanks to component tests. In these tests, the components are fixed on a rigid frame and crushed using a rigid guided impactor which represent the leg or the head impactor.

With this methodology, the crush vs stiffness laws of each component of the front-end are validated for the pedestrian protection even before the first test on a complete prototype.

Some component tests are presented in Figure 19 to 22.

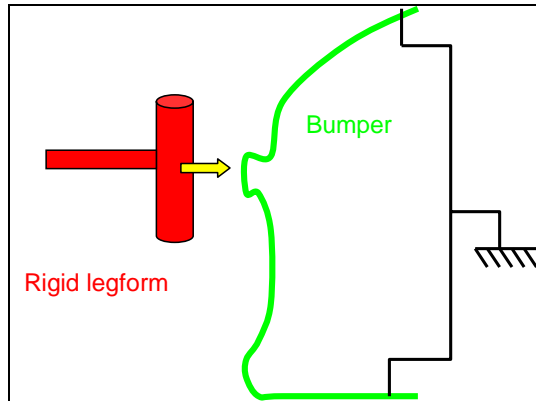


Figure 19. Principles of the component test carried out on the Peugeot 207 bumper

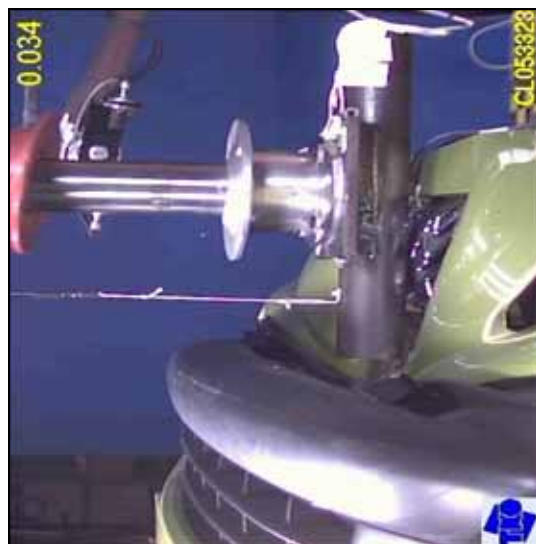


Figure 20. Example of a component test carried out on the Peugeot 207 bumper.

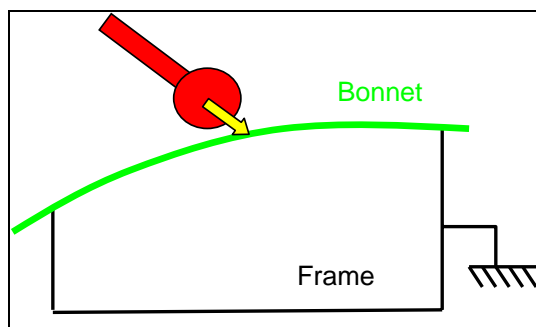


Figure 21. Principles of the component test carried out on the Peugeot 207 bonnet.



Figure 22. Example of a component test carried out on the Peugeot 207 bonnet.

DISCUSSION AND CONCLUSION

These solutions result from technical researches carried out by PSA Peugeot Citroën and convey the will of its Direction to improve the pedestrian protection and to anticipate the European Directives. They allowed PSA Peugeot Citroën to take place among the best car manufacturers in term of pedestrian protection.

Nevertheless, the text of the European Directive foresees an increase in the required performance for 2010 for the new vehicle types. This is called "Phase 2" and its requirements come from the EEVC WG17 proposal of procedure, which is currently used by Euro NCAP.

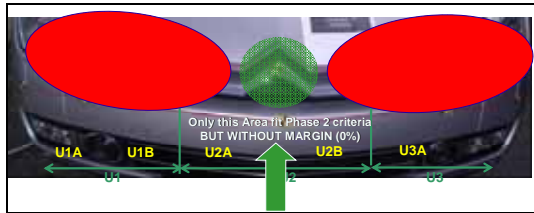
Currently, only one vehicle achieved a 4 stars pedestrian protection rating: it is the Citroën C6. But, it is important to highlight that despite this excellent score, Citroën C6 could not fulfil all the requirements defined in the EEVC WG17 proposal. Indeed, some points in the head and upper leg zones still exceed the EEVC WG17 threshold limits. This clearly shows that even with an improved and innovative technical solution, the EEVC WG17 requirements are too stringent.

Figure 23 and Figure 24 present the Citroën C6 overall results on the bonnet and on the bonnet leading edge.



Red Areas could not be "approved" regarding the EEVC WG17 requirements (HIC level too high)

Figure 23. HIC results on the Citroën C6 headform tests with respect to the EEVC WG17 / Phase 2 requirements.



Red Areas could not be "approved" regarding the EEVC WG17 requirements

Figure 24. Upper leg results on the Citroën C6 with respect to the EEVC WG17 / Phase 2 requirements.

Moreover, these technical constraints for the pedestrian protection are most of the time in contradiction with other important car requirements such as: visibility for the driver or mass reduction

Actually, pedestrian protection requirements tend to increase the bonnet height which is in contradiction with visibility requirements for the driver.

Furthermore, pedestrian protection requirements tend to increase the mass of the vehicle by adding extra components such as the upper and lower absorbers. These requirements also tend to decrease the overall volume of the engine in order to prevent the head to impact the stiff parts of the car front-end. This is in total contradiction with the Euro 5 standard requirements that force the engine to be wider and larger because of added components for antipollution control.

So to improve even more pedestrian safety, it would be necessary to investigate solutions linked to road infrastructures or linked to primary safety. For example, one proposal is to encourage the car manufacturer to equip their vehicles with a brake assist system.

REFERENCES

[1] EEVC WG17 Report – improved test methods to evaluate pedestrian protection afforded by passenger cars.

PEDESTRIAN HEAD IMPACT - WHAT DETERMINES THE LIKELIHOOD AND WRAP AROUND DISTANCE?

B. Johan Ivarsson

Jeff R. Crandall

University of Virginia

Christine Burke

Greg Stadter

Jurek Grabowski

Samir Fakhry

Honda INOVA Fairfax Hospital CIREN Center

United States

Rikard Fredriksson

Autoliv Research

Sweden

Matthias Nentwich

Autoliv GmbH

Germany

Paper Number 07-0373

ABSTRACT

The current study evaluates the influence of impact speed, pedestrian stature, and vehicle geometry on the likelihood and location of head-vehicle contact in a frontal pedestrian crash. Information on 408 pedestrian crashes in which the striking vehicle was either a car, pick-up truck, or an SUV was obtained from the Pedestrian Crash Data Study (PCDS), German In-Depth Accident Study (GIDAS), and Crash Injury Research and Engineering Network (CIREN) databases. Logistic regression was used to evaluate the importance of factors that determine the likelihood of head contact and sliding up the hood prior to head contact. Multiple linear regression was used to study the relative influence of impact speed, pedestrian stature, bumper height, hood height, and hood length on the wrap around distance (WAD) to head contact and to evaluate whether it is possible to predict this distance from these five parameters. As expected, the likelihood of head-vehicle contact increased with increasing impact speed and pedestrian to hood height ratio. The likelihood of sliding up the hood prior to head contact increased with increasing impact speed and was significantly higher in cases for which the pedestrian stature to hood height ratio was greater than two than in cases in which it was less than two. Of the variables considered, stature was the single most important predictor of WAD to head contact explaining 24% of the variation alone. Other significant predictors included the impact speed, whether the pedestrian was taller than twice the hood height, and hood length, which, together with pedestrian stature, explained a total of 40% of the variation. The low explanatory effect of this model suggests that

additional factors, such as the presence or absence of pre-impact braking and pedestrian stance and orientation, also affect the WAD to head contact.

INTRODUCTION

Injuries to pedestrians involved in pedestrian versus motor vehicle crashes are a significant contributor to death and disability in all motorized societies. The World Bank has estimated that 41-75% of worldwide road traffic fatalities are pedestrians (World Bank, 2006). Several epidemiological studies on various populations of pedestrian victims have indicated that, together with the lower extremities, the head is the most frequently injured body region (Chidester and Isenberg, 2001; Mizuno, 2003; Ballesteros et al., 2004; Ivarsson et al., 2005). Considering only serious to fatal injuries (AIS 3+), the head ranks higher in injury frequency than any other body region (Lane et al., 1994; Harruff et al., 1998; Otte, 1999; Crandall et al., 2002; Ivarsson et al., 2005; Ono et al., 2005). Although head injury can occur as a result of the pedestrian's secondary impact with the ground, head contact with various vehicle components has been reported to be the primary source for moderate to fatal head injuries (Ashton, 1975; Ashton et al., 1978; Mizuno, 2003; Kendall et al., 2006). Mizuno (2003) summarized the findings of a total of 1605 pedestrian cases that occurred in Australia, Germany, Japan, and the US and reported that 80% of the recorded AIS 2+ head injuries were due to contact with vehicle components including, but not limited to, the hood, windshield, and windshield frame. The widespread area of head contact locations on the vehicle shown by Mizuno (2003) has also been documented in other epidemiological studies. Chidester and Isenberg

(2001) analyzed the 420 frontal pedestrian crashes included in the Pedestrian Crash Data Study (PCDS) and reported that the wrap around distance (WAD) to head contact in the 228 cases for which there was evidence of head contact on the vehicle ranged from less than 60 cm to over 250 cm. Otte (1994) analyzed 372 frontal pedestrian crashes involving adult pedestrians ranging in height from 150 to 190 cm and found that the “throwing up distance” (the horizontal distance from the front end of the vehicle to the point of head contact) in the cases for which there was evidence of head contact on the vehicle ranged from approximately 40 to 210 cm.

The widespread distribution of potential head contact locations on the vehicle has led to the proposal of several different safety concepts for reducing the frequency and severity of pedestrian head injury. Windscreen airbags have been proposed for preventing the head from contacting the stiff windscreen shuttle and A-pillars (Crandall et al., 2002), whereas examples of safety concepts that provide increased deceleration space in the event of head contact with the hood include pyrotechnic devices that rapidly raise the hood (Fredriksson et al., 2001) and flexible and collapsible hood hinges (Kirkeling et al., 2005). Other indirect efforts taken towards reducing the overall aggressiveness of the vehicle towards the pedestrian head include the pedestrian test protocol that is part of the New Car Assessment Program (NCAP) in Europe (EuroNCAP), Japan (JNCAP), and Australia (ANCAP) and the legislative directives for pedestrian protection that recently have gone into effect in Europe (2003/102/EC) and Japan (TRIAS63-2004). Both NCAP and the legislative directives evaluate the aggressiveness of the vehicle towards the pedestrian head by measuring the impact response of adult and/or child sized headforms that are propelled into different spots within specified zones on the vehicle in which pedestrian head contact is deemed likely to occur. In NCAP, the child and adult head impact zones comprise the area of the vehicle front structure that falls within the geometric traces of the 1000-1500 mm (JNCAP: 1000-1700 mm) and 1500-2100 mm (JNCAP: 1700-2100 mm) WAD, respectively, whereas the current phase of the legislative directives limits the test zone to the hood top.

While the safety concepts and evaluation procedures described above should lead to an overall reduction of the frequency and severity of pedestrian head injury, it may be possible to achieve an even higher protective efficiency if vehicles could be designed to minimize the likelihood of pedestrian head contact, minimize the head contact velocity, and force the head to contact the vehicle in regions that offer extensive deceleration space. Several previous

investigators have reported that the likelihood and speed of head contact as well as the amount of slide up the hood prior to head contact (WAD to head contact minus pedestrian stature) are dependent on the impact velocity and the height of the pedestrian relative to geometrical vehicle parameters such as bumper height, hood height, and hood length (Ashton, 1975, 1980; Ashton et al., 1978; Niederer and Schlumpf, 1984; Otte, 1994; Roudsari et al., 2005).

The current study aims to evaluate the influence of impact speed, pedestrian stature, and vehicle geometry on the likelihood and location of head contact on the vehicle in a frontal pedestrian crash based on information from three detailed registries of real world pedestrian crashes. More precisely, we aim to evaluate how impact speed and pedestrian stature relative to bumper height, hood height, and hood length affect the likelihood of head contact on the vehicle and the likelihood of pedestrian slide up the hood prior to head contact (WAD to head contact > pedestrian stature). In addition, we aim to quantify the relative influence of impact speed, pedestrian stature, bumper height, hood height, and hood length on the WAD to head contact and evaluate whether it is possible to predict the WAD to head contact in a frontal pedestrian crash from these five variables.

METHODOLOGY

Data Sources

Data came from three real world pedestrian crash databases. The PCDS trauma registry is a compilation of detailed information on a total of 552 pedestrian crashes that occurred during the period from 1994 through 1998 in six metropolitan areas in the US (Chidester and Isenberg, 2001). A “pedestrian” was defined as any person located in a traffic-way, on a sidewalk or path contiguous with a traffic-way, or on private property. The striking vehicle had to be forward moving and of model year 1990-1996. Crashes in which a person was lying or sitting while struck were not included. The pedestrian impact had to be the only impact and the first point of contact had to be forward of the top of the A-pillar. The PCDS data are not weighted since the study was designed to be clinical rather than providing a national sample of all US pedestrian crashes.

The second data source was the German In-Depth Accident Study (GIDAS). This database consists of detailed information on several thousand traffic crashes that occurred in the areas of Hanover and Dresden in Germany. The current study only

used data from the pedestrian crashes included in GIDAS.

The third data source was the CIREN (Crash Injury Research and Engineering Network) pedestrian database from the Honda INOVA Fairfax Hospital CIREN center in Fairfax, Virginia (Longhitano et al., 2005). This database currently includes in-depth information on approximately 50 recent pedestrian crashes that occurred in the Washington, DC metropolitan region. The model year of the striking vehicles ranged from 1986 to 2004. The database consists of the National Automotive Sampling System Crashworthiness Data System (NASS-CDS) set of 650 data elements plus an additional 250 medical and injury data elements including complete injury documentation by means of Abbreviated Injury Scale, 1990 Revision (AIS-90) coding.

Filtering of the Data Sources

The three data sources were filtered to include only the cases fulfilling the following criteria:

- Frontal crash (pedestrian struck by the front of the vehicle),
- Striking vehicle a passenger car, sport utility vehicle (SUV), or pick-up truck
- Pedestrian in an upright position while struck,
- Information provided on:
 - Estimated impact speed,
 - Pedestrian stature,
 - Whether head contact on the vehicle occurred,
 - Bumper height (vertical height above ground of the top surface of the frontal bumper)
 - Hood height (vertical height above ground of the leading edge of the hood),
 - Hood length (flat plane distance from the leading edge of the hood to the trailing edge at the windshield),
- Pedestrian stature/hood height ≥ 1.40 (to avoid the potential inclusion of cases in which head contact occurred as a result of direct impact by the front of the vehicle rather than secondary to the pedestrian wrapping around the vehicle front).

The filtering procedure left 258 cases from PCDS and 32 from CIREN for analysis. GIDAS does not include any information on the height and length of the hood of the vehicle. However, from information provided in the library of vehicle models included in the Expert AutoStat® software (4N6XPRT Systems, La Mesa, CA, USA), these measurements were identified for 118 of the GIDAS cases that fulfilled all the other inclusion criteria. Thus, a total of 408 cases fulfilling all the inclusion criteria were available for analysis.

Analysis

Logistic regression was used to derive functions for the likelihood of head-vehicle contact and WAD to head contact > pedestrian stature. The independent variables were impact speed, pedestrian stature to bumper height ratio (PS/BH), pedestrian stature to hood height ratio (PS/HH), and pedestrian stature to hood length ratio (PS/HL). The logistic regression models were developed according to the approach outlined by Hosmer and Lemeshow (1989), which briefly includes the following eight steps:

- Screening of the individual importance of the potential predictors by means of univariate analyses.
- Multivariate analysis including variables of known biological importance plus any additional variables that demonstrated p-values less than 0.25 in the univariate analyses.
- Identify variables that do not significantly contribute to the multivariate model using likelihood ratio tests.
- Quartile grouping analysis to make sure that the logit for any of the variables identified as insignificant is not a symmetric or u-shaped function (any of these functional forms could explain why a linear fit has a zero slope).
- Fit a new model excluding all variables that have been found to be either biologically or statistically unimportant.
- Box-Tidwell transformation and subsequent quartile grouping analysis of the included variables that have been modeled as continuous to obtain their correct scale in the logit.
- Assessment of the importance of possible interaction terms using likelihood ratio tests.
- Fit a new model that, in addition to the main effects that already have been found to be important, also includes the statistically significant interaction terms that make sense from a biological perspective.

Three goodness-of-fit tests (Pearson, Deviance, and Hosmer and Lemeshow) were used to evaluate the null hypothesis of adequate model fit. In addition, the predictive ability of the models was evaluated using two measures of association (Kruskal's Gamma and Somers' D) based on percent concordance and discordance. A pair of observations with different outcomes ("event" and "no event") is concordant if the model predicts a higher likelihood of event occurrence for the event case than for the non-event case. A pair of observations is discordant if the event case has a lower model-predicted likelihood than the

non-event case. Kruskal's Gamma is defined by the number of concordant and discordant pairs in the dataset, so it is a measure of the model's ability to discriminate event from non-event cases:

$$\gamma = \frac{N_{\text{concordant}} - N_{\text{discordant}}}{N_{\text{concordant}} + N_{\text{discordant}}} \quad (1)$$

where $N_{\text{concordant}}$ is the number of concordant pairs and $N_{\text{discordant}}$ is the number of discordant pairs in the dataset. A Kruskal's Gamma value of zero indicates that the model has no predictive ability, whereas a value of one indicates perfect prediction. Somers' D (SD) is Kruskal's Gamma modified to penalize for any tied pairs of observations in the dataset:

$$SD = \frac{N_{\text{concordant}} - N_{\text{discordant}}}{N_{\text{concordant}} + N_{\text{discordant}} + N_{\text{tied}}} \quad (2)$$

Best subsets multiple linear regression was used to determine the relative importance of impact speed, pedestrian stature, bumper height, hood height, and hood length on the WAD to head contact and to evaluate whether it is possible to predict the WAD to head contact in a frontal pedestrian crash from these five variables. In addition to the "main effect" variables, all possible interaction terms were included as potential predictors in the analysis. All logistic and linear regression analyses were conducted using the statistical software package MINITAB (Minitab, Inc., State College, PA, USA, version 14).

RESULTS

The Likelihood of Head-Vehicle Contact

Of the 408 cases available for analysis, 210 showed evidence of head contact on the vehicle. Table 1 shows mean \pm SD and range of the potential predictors by outcome and for all cases combined as well as the individual p-values from the univariate analyses. As shown, both impact speed and PS/HH were significant variables while PS/BH demonstrated a p-value above 0.25 and therefore was excluded. Further analysis confirmed that PS/HL had no association with the occurrence of head contact and it was therefore excluded as well. Box-Tidwell transformations and subsequent quartile analyses of impact speed and PS/HH suggested that PS/HH should be modeled as continuous and linear and impact speed as continuous but logarithmic in the logit. Table 2 shows estimated coefficients, log-likelihood, goodness-of-fit, and measures of association for three models based on log(impact

speed) only (model 1), log(impact speed) and PS/HH (model 2), and log(impact speed), PS/HH, and the interaction between these two variables (model 3). According to the goodness-of-fit measures, all three models appear to provide adequate fit of the data. However, while the measures of association indicate that model 2 and 3 are equally good in discriminating between events and non-events, the likelihood ratio test comparing these two models indicate that model 3 fits the data better ($p = 0.029$) and consequently, that the individual effect of impact speed on the likelihood of head contact should not be evaluated without accounting for PS/HH and vice versa. Henceforth, model 3 is used to study the effects of impact speed and PS/HH on the likelihood of head contact on the vehicle.

Figure 1 shows the likelihood of head-vehicle contact as a function of impact speed for the 10, 25, 50, 75, and 90 percentiles of PS/HH. For the purpose of comparison, the corresponding curve determined from the univariate model 1 is shown as well. As shown, the likelihood of head-vehicle contact increases rapidly with impact speed up to approximately 50 km/h after which the rate of increase levels off. Also shown in Figure 1 is that for any impact speed exceeding approximately 15 km/h, an increase of the pedestrian stature or a reduction of the hood height is associated with an increasing risk of head-vehicle contact. This finding is further illustrated in Figure 2 which shows the likelihood of head-vehicle contact as a function of PS/HH for the 10, 25, 50, 75, and 90 percentiles of impact speed. For impact speed below 15 km/h, the model suggests a slightly decreasing risk of vehicle-head contact with increasing PS/HH (Figures 1 and 2). This is most likely not the case in the real world but instead a reflection of that the likelihood of head-vehicle contact is insensitive to PS/HH for low impact speeds.

Figure 3 provides a comparison of the individual effects of impact speed reduction and hood height increase on the odds of head-vehicle contact for the particular reference case of a pedestrian of height 177.3 cm (50-percentile male height) struck at 40 km/h by a vehicle with a hood height of 70 cm (50-percentile hood height of the 349 passenger cars included in the analysis). As an example of how to interpret the data in the figure, it shows that a reduction of the impact speed by 9 km/h (from 40 to 31 km/h) or an increase of the hood height by 17.5 cm (from 70 to 87.5 cm) would both reduce the odds of head-vehicle contact by 50%. It is important to emphasize that Figure 3 is only valid for the particular reference case used here.

Table 1.
Head-vehicle contact characteristics by outcome and for all cases combined along with the individual p-values from the univariate analyses

Independent variable	No head-vehicle contact (N = 198) mean ± SD (range)	Head-vehicle contact (N = 210) mean ± SD (range)	Total (N = 408) mean ± SD (range)	p-value
Impact speed (km/h)	20.04 ± 13.10 (2-74)	42.03 ± 19.66 (8-118)	31.36 ± 20.06 (2-118)	<10 ⁻⁹
Pedestrian stature/ bumper height	3.13 ± 0.46 (1.90-4.94)	3.17 ± 0.45 (1.88-4.56)	3.15 ± 0.45 (1.88-4.94)	0.297
Pedestrian stature/ hood height	2.25 ± 0.38 (1.42-3.40)	2.35 ± 0.40 (1.42-3.54)	2.30 ± 0.40 (1.42-3.54)	0.010
Pedestrian stature/ hood length	1.53 ± 0.22 (0.87-2.10)	1.56 ± 0.23 (0.94-2.14)	1.54 ± 0.22 (0.87-2.14)	0.188

Table 2.
Estimated coefficients, log-likelihood, goodness-of-fit, and measures of association for three logistic regression models predicting the likelihood of head-vehicle contact. P-values in brackets denote the significance levels of individual variables in the models

Model	Variables				Log-likelihood	Goodness-of-fit	Measures of association
	Constant	Log(impact speed) (km/h)	PS/HH	Log(impact speed)×(PS/HH) (km/h)			
1	-7.444 (p<0.0005)	5.311 (p<0.001)			-202.363	P = 0.986 D = 0.992 HL = 0.346	γ = 0.68 SD = 0.67
2	-9.220 (p<0.0005)	5.317 (p<0.001)	0.772 (p = 0.014)		-199.254	P = 0.604 D = 0.512 HL = 0.478	γ = 0.69 SD = 0.69
3	1.026 (p=0.826)	-1.911 (p=0.557)	-3.749 (p=0.072)	3.193 (p=0.029)	-196.877	P = 0.899 D = 0.565 HL = 0.373	γ = 0.69 SD = 0.69

Abbreviations: PS/HH = Pedestrian stature/hood height, P = Pearson, D = Deviance, HL = Hosmer and Lemeshow, γ = Kruskal's Gamma, SD = Somers' D.

Figure 4 shows the likelihood of head-vehicle contact at an impact speed of 40 km/h as a function of the hood height for pedestrian statures corresponding to the 50-percentile adult male, 5-percentile adult female, 95-percentile adult male, and 50-percentile 6-year-old child. The curves are only shown for the hood height intervals for which the model is valid ($1.42 \leq \text{PS/HH} \leq 3.54$), which explains why the risk of head contact for the 6-year-old child is not shown for hood heights exceeding 81 cm. As shown, there is a substantial difference in the likelihood of head-vehicle contact between the different anthropometries. Comparing for instance the 50-percentile adult male and the 6-year-old child struck by a vehicle with a hood height of 60 cm, the 50-percentile adult male is approximately four times as likely to sustain head contact on the vehicle.

The Likelihood of WAD to Head Contact > Pedestrian Stature

Of the 210 cases for which there was evidence of head contact on the vehicle, eleven did not include any information on the WAD to head contact and therefore had to be excluded. Of the remaining 199 cases available for analysis, 42 had a WAD to head contact that was less or equal to the stature of the pedestrian, whereas the remaining 157 cases had a WAD to head contact that was greater than the pedestrian stature. Table 3 shows mean ± SD and range of the potential predictors by outcome and for all cases combined as well as the individual p-values from the univariate analyses. As shown, impact speed, PS/BH, and PS/HH were all significant predictors of WAD to head contact > pedestrian stature while PS/HL demonstrated a p-value above 0.25 and therefore was excluded.

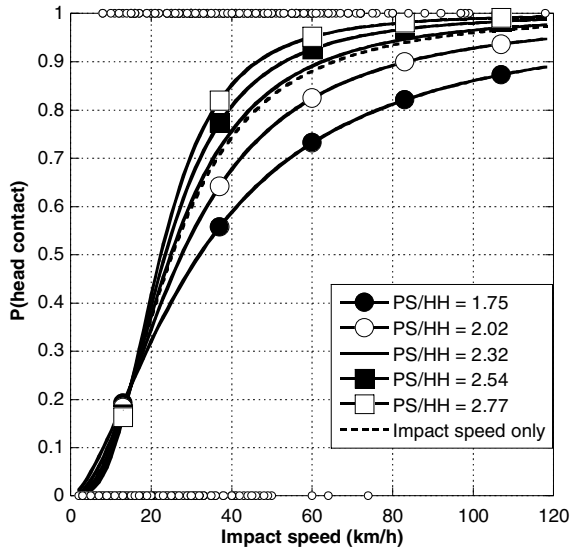


Figure 1. Likelihood of head-vehicle contact as a function of impact speed for the 10 (PS/HH = 1.75), 25 (PS/HH = 2.02), 50 (PS/HH = 2.32), 75 (PS/HH = 2.54), and 90 (PS/HH = 2.77) percentiles of PS/HH. Also shown is the corresponding risk function predicted by the univariate model HC1.

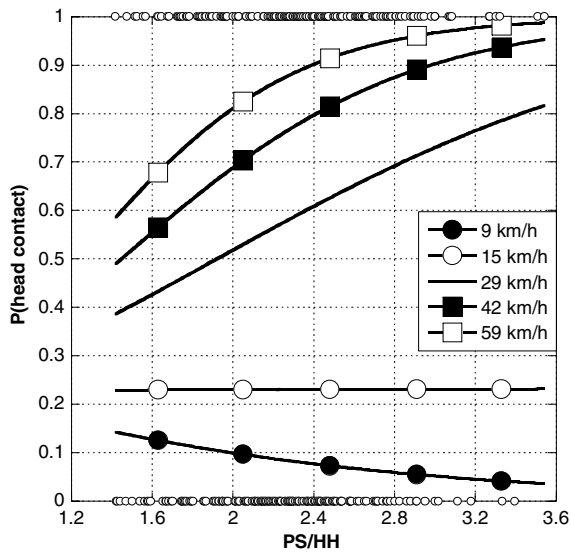


Figure 2. Likelihood of head-vehicle contact as a function of PS/HH for the 10 (impact speed = 9 km/h), 25 (impact speed = 15 km/h), 50 (impact speed = 29 km/h), 75 (impact speed = 42 km/h), and 90 (impact speed = 59 km/h) percentiles of impact speed.

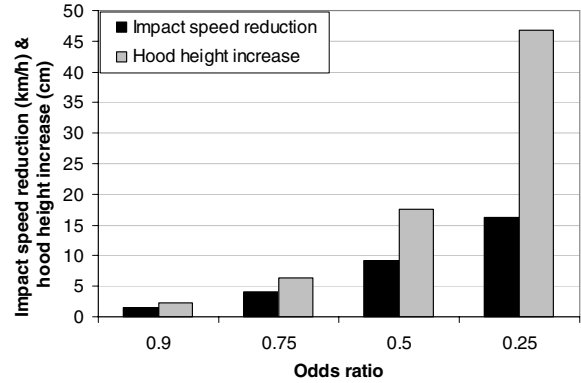


Figure 3. Individual effects of impact speed reduction and hood height increase on the odds of head-vehicle contact for the reference case of a pedestrian of height 177.3 cm struck at 40 km/h by a vehicle with a hood height of 70 cm.

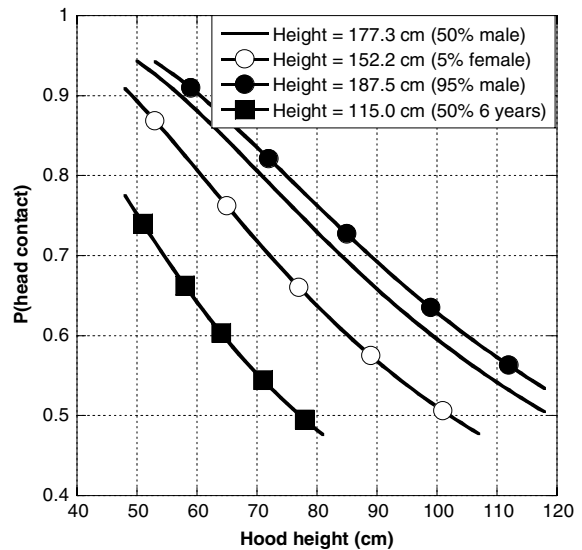


Figure 4. Likelihood of head-vehicle contact at an impact speed of 40 km/h as a function of hood height for pedestrian statures corresponding to the 50-percentile adult male, 5-percentile adult female, 95-percentile adult male, and 50-percentile 6-year-old child.

Subsequent analysis of the multivariate model with impact speed, PS/BH, and PS/HH as independents revealed that PS/BH did not add any explanatory effect (a model with impact speed and PS/HH as the only two dependents performed equally well) and was therefore excluded. Box-Tidwell transformations and subsequent quartile analyses of impact speed and PS/HH suggested that PS/HH should be modeled as a binary variable, PS/HH_bin, taking the value 0 for PS/HH < 2 and 1 for PS/HH ≥ 2, whereas the dependence on impact speed appeared to be best described by a logarithmic relationship. Table 4

shows estimated coefficients, log-likelihood, goodness-of-fit, and measures of association for three models based on log(impact speed) only (model 4), log(impact speed) and PS/HH_bin (model 5), and log(impact speed), PS/HH_bin, and the interaction between these two variables (model 6). According to the goodness-of-fit measures, both model 5 and 6 provide adequate fit of the data. However, while the measures of association indicate that they are equally good in discriminating between events and non-

events, the likelihood ratio test comparing these two models indicate that model 6 fits the data better ($p = 0.007$) and consequently, that the individual effect of impact speed on the likelihood of WAD to head contact > pedestrian stature should not be evaluated without accounting for PS/HH_bin and vice versa. Henceforth, model 6 is used to study the effects of impact speed and the ratio of pedestrian stature to hood height on the likelihood of WAD to head contact > pedestrian stature.

Table 3.
WAD to head contact versus pedestrian stature by outcome and for all cases combined along with the individual p-values from the univariate analyses

Independent variable	WAD to head contact \leq pedestrian stature (N = 42) mean \pm SD (range)	WAD to head contact > pedestrian stature (N = 157) mean \pm SD (range)	Total (N = 199) mean \pm SD (range)	p-value
Impact speed (km/h)	30.07 \pm 19.33 (8-99)	45.12 \pm 18.65 (8-118)	41.94 \pm 19.73 (8-118)	<10 ⁻⁵
Pedestrian stature/ bumper height	2.94 \pm 0.51 (1.88-3.82)	3.22 \pm 0.40 (1.96-4.56)	3.16 \pm 0.44 (1.88-4.56)	<0.001
Pedestrian stature/ hood height	2.15 \pm 0.48 (1.47-3.54)	2.40 \pm 0.36 (1.42-3.32)	2.35 \pm 0.40 (1.42-3.54)	<0.001
Pedestrian stature/ hood length	1.55 \pm 0.23 (1.01-2.00)	1.56 \pm 0.23 (0.94-2.14)	1.56 \pm 0.23 (0.94-2.14)	0.78

Table 4.
Estimated coefficients, log-likelihood, goodness-of-fit, and measures of association for three logistic regression models predicting the likelihood of WAD to head contact > pedestrian stature. P-values in brackets denote the significance levels of individual variables in the models

Model	Variables				Log-likelihood	Goodness-of-fit	Measures of association
	Constant	log(impact speed) (km/h)	PS/HH_bin	log(impact speed) \times (PS/HH)_bin (km/h)			
4	-5.41306 (p<0.001)	4.43038 (p<0.001)			-88.274	P = 0.010 D = 0.754 HL = 0.129	$\gamma = 0.55$ SD = 0.54
5	-6.96059 (p<0.001)	4.51352 (p<0.001)	1.92757 (p<0.001)		-78.638	P = 0.648 D = 0.636 HL = 0.133	$\gamma = 0.70$ SD = 0.69
6	-2.79316 (p=0.138)	1.81872 (p=0.131)	-5.74775 (p=0.042)	5.11781 (p=0.007)	-74.990	P = 0.946 D = 0.803 HL = 0.701	$\gamma = 0.70$ SD = 0.69

Abbreviations: P = Pearson, D = Deviance, HL = Hosmer & Lemeshow, γ = Kruskal's Gamma, SD = Somers' D.

Figure 5 shows the likelihood of WAD to head contact > pedestrian stature as a function of impact speed for pedestrians shorter (PS/HH < 2) and equal or taller (PS/HH \geq 2) than twice the hood height of the striking vehicle. As shown, the likelihood WAD to head contact > pedestrian stature increases with impact speed. Also shown in Figure 5 is that for any impact speed exceeding approximately 13 km/h, pedestrians equal to or taller than twice the height of the hood are more likely to slide up the hood prior to

head contact than pedestrians shorter than twice the hood height. For impact speed below 13 km/h, the model suggests the exact opposite, i.e. that the likelihood of WAD to head contact > pedestrian stature is greater for pedestrians shorter than taller than twice the hood height. This is most likely not the case in the real world but instead a reflection of that the likelihood of .that the likelihood of WAD to head contact > pedestrian stature is insensitive to PS/HH for low impact speeds.

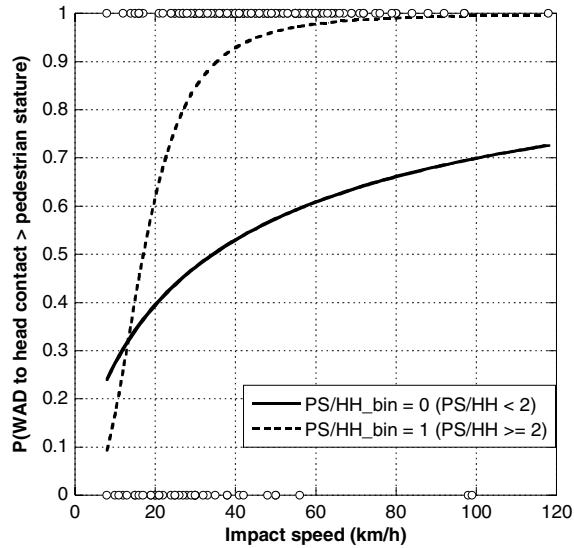


Figure 5. Likelihood of WAD to head contact > pedestrian stature as a function of impact speed for pedestrians shorter (PS/HH < 2) and equal or taller (PS/HH ≥ 2.00) than twice the hood height of the striking vehicle.

WAD to Head Contact

Preliminary analyses demonstrated that the influence of impact speed on the WAD to head contact was better described by a logarithmic than a linear relationship. Consequently, the logarithm of impact speed instead of impact speed was included as a potential predictor in the multiple regression analyses. Based on the results from the logistic regression analysis of the likelihood of WAD to head contact > pedestrian stature, the binary version of PS/HH (PS/HH_bin) which takes the value 0 for PS/HH < 2 and the value 1 for PS/HH ≥ 2, was added as a potential predictor. Thus, a total of 21 potential predictors (six “main effects” and fifteen interactions) were included in the analyses.

Table 5 lists the estimated coefficients, R^2 or multiple correlation coefficient (the fraction of variance in the dependent variable collectively explained by all of the independent variables), and R^2 -adjusted (the multiple correlation coefficient adjusted for the number of predictors included in the model) for the best models (highest R^2 -adjusted) including one, two, three, four, five, and six, predictors. The last column in Table 5 shows the p-value obtained from F-tests of the difference in R^2 -adjusted between the two best models with k and $k + 1$ predictors. Not surprisingly, pedestrian stature is the single most important predictor explaining 24% of the variance in WAD to head contact. Additional variables of significant importance include impact speed, the binary version of PS/HH, and the hood

length that, together with pedestrian stature, explain 40% of the variance in WAD to head contact. As shown in Table 5, the only additional variable that seem to have an explanatory effect on the WAD to head contact is the interaction between pedestrian stature and hood length ($p = 0.072$). However, inclusion of this term results in a net increase of R^2 -adjusted of only one percentage unit.

DISCUSSION

The current study used information on impact speed, pedestrian stature, bumper height, hood height, and hood length, whether head-vehicle contact occurred, and WAD to head contact from three detailed registries of real world pedestrian crashes to:

- develop logistic regression models predicting the likelihood of pedestrian head contact on the vehicle and likelihood of WAD to head contact > pedestrian stature,
- determine the relative importance of impact speed, pedestrian stature, bumper height, hood height, and hood length on the WAD to head contact, and
- evaluate whether it is possible to predict the WAD to head contact from impact speed, pedestrian stature, bumper height, hood height, and hood length.

The study was limited to cases in which the striking vehicle was a passenger car, SUV, or pick-up truck. Other vehicle types, like mini-vans and large vans, generally lack the relatively horizontal hood that characterize passenger cars, SUVs, and pick-up trucks and therefore cause slightly different pedestrian response kinematics. Also excluded were the thirteen cases in which the pedestrian stature to hood height ratio did not exceed 1.40. This was to avoid the potential inclusion of cases in which head contact occurred as a result of direct impact by the front of the vehicle rather than secondary to the pedestrian wrapping around the vehicle front. In agreement with the findings of Ashton (1975, 1980, 1997) and Ashton et al. (1978), the results indicated that the likelihood of head-vehicle contact increases with impact speed as well as with PS/HH. These two variables are, however, not independent of each other with the PS/HH having a stronger influence on the likelihood of head-vehicle contact when the impact speed is high than low. It is important to emphasize that although an increased hood height reduces the likelihood of head-vehicle contact for pedestrians taller than 1.4 times the hood height, it may increase the injury risk and injury severity for other body regions such as the torso and also increase the risk of head injury for the pediatric pedestrian population.

Table 5.

Estimated coefficients, multiple correlation coefficients R^2 , and adjusted multiple correlation coefficients R^2 -adjusted for the best linear regression models of WAD to head contact including one, two, three, four, five, and six predictors. The last column shows the p-value for the difference in R^2 -adjusted between the two best models with k and k + 1 predictors. Values in brackets denote the p-values of individual variables in the models

No. of predictors	Predictors							R^2	R^2 -adj	p-value
	Const	PS (m)	Log(IS) (km/h)	PS/HH_bin	HL (m)	PS*HL (m ²)	Log(IS)*HL (m×km/h)			
1	-10.51 (0.686)	1.24 (<0.001)						0.244	0.240	N/A
2	-72.38 (0.008)	1.14 (<0.001)	49.4 (<0.001)					0.335	0.328	<10 ⁻⁶
3	-55.1 (0.038)	0.925 (<0.001)	48.4 (<0.001)	25.0 (<0.001)				0.389	0.380	<10 ⁻⁴
4	-100.9 (0.001)	0.914 (<0.001)	45.1 (<0.001)	25.4 (<0.001)	0.488 (0.009)			0.411	0.399	0.014
5	409.5 (0.098)	-2.11 (0.148)	44.0 (<0.001)	24.6 (<0.001)	-4.25 (0.063)	0.028 (0.038)		0.424	0.409	0.072
6	596.9 (0.027)	-1.69 (0.251)	-119.2 (0.205)	24.7 (<0.001)	-5.96 (0.017)	0.024 (0.078)	1.51 (0.082)	0.433	0.414	0.202

Abbreviations: Const = Constant, PS = Pedestrian stature, IS = Impact speed, PS/HH_bin = Binary version of pedestrian stature to hood height ratio, HL = Hood length, R^2 -adj = R^2 -adjusted.

Neither PS/BH nor PS/HL had any influence on the likelihood of head contact. The absence of influence of PS/BH may be a consequence of that any initial effect on the pedestrian response kinematics from bumper contact is “washed out” by the subsequent interaction with the leading edge of the hood. The interdependence of PS/HL is not as easily explained. Intuitively, one would expect a reduction of the hood length to increase the likelihood of head contact since the wrap around distance to the windshield decreases. However, based on the results from the current study, this does not appear to be the case.

The likelihood of WAD to head contact > pedestrian stature also demonstrated strong positive correlation with the impact speed but showed a binary dependence of PS/HH with pedestrians taller than twice the hood height being more likely to slide up the hood prior to head contact than those shorter than twice the hood height. Similar to the case of the likelihood of head-vehicle contact, impact speed and PS/HH are not independent of each other with PS/HH having a greater effect on the likelihood of WAD to head contact > pedestrian stature at high than low impact speeds. The underlying reason for the increased likelihood of WAD to head contact > pedestrian stature for pedestrians taller than shorter than twice the hood height is most likely due to the increased effective mass above the leading edge of the hood, which encourages sliding up the hood. The most likely explanation to the lack of an effect of

PS/BH is probably the same as in the case of likelihood of head contact, namely that any initial effect on the pedestrian response kinematics from bumper contact is “washed out” by the subsequent interaction with the leading edge of the hood. According to Otte (1994), the windshield acts like a barrier limiting the distance that the pedestrian slides up the hood prior to head contact. Consequently, PS/HL should influence the WAD to head contact but not whether sliding prior to head contact occurs. This was confirmed in the current study for which the likelihood of WAD to head contact > pedestrian stature showed no association with PS/HL ($p = 0.78$).

The results from the WAD to head contact analysis demonstrated that pedestrian stature alone explained 24% of the variance in WAD to head contact. A total explanatory effect of 40% could be achieved by also accounting for the logarithm of impact speed ($p < 10^{-6}$), whether the pedestrian is taller than twice the hood height ($p < 10^{-4}$), and the hood length ($p = 0.014$). None of the other variables or interactions considered as potential predictors in the current study offered any additional explanatory effect. Consequently, we can conclude that it is not possible to predict the WAD to head contact in a frontal pedestrian crash from pedestrian stature, estimated impact speed, bumper height, hood height, and hood length.

While approximately 60% of the variation in WAD to head contact appears to be due to factors not considered in the analysis, it is important to

emphasize that these factors most likely affect the likelihood of head-vehicle contact and WAD to head contact > pedestrian stature as well. These factors include but are not limited to:

- Whether or not pre-impact braking occurred – Braking causes pitching of the vehicle front end towards the ground and consequently, a reduction of the height of the bumper and hood above ground compared to the non-decelerated state. The current study used the original bumper and hood heights regardless of whether pre-impact braking occurred.
- Front end stiffness – The stiffness of the vehicle front end affects the frictional force between the pedestrian and vehicle during initial contact which, in turn, influences subsequent response kinematics including the WAD to head contact (Ashton, 1980, Okamoto et al., 2003).
- Pedestrian stance and orientation - Results from computer simulations of pedestrian crashes indicate that the stance and orientation of the pedestrian relative to the vehicle at impact influence the subsequent response kinematics (Meissner et al., 2004; Kendall et al., 2006).
- Vehicle front end shape - Passenger cars of recent design have a relatively rounded front end without the distinct edge that demarcates the grille from the hood in older designs. The majority of vehicles included in the current study were of model years 1990 or newer but a few vehicles from the GIDAS database dated as far back as 1983.
- Bumper lead – According to Ashton (1983), bumper lead (the distance by which the bumper is further forward than the leading edge of the hood) has an influence on the relative importance of the bumper and hood leading edge as sources of injury. Consequently, bumper lead may also affect pedestrian response kinematics.

Finally, it needs to be pointed out that despite that the registries used in the current study are believed to be among the most accurate and comprehensive real world pedestrian crash databases currently available, the uncertainty associated with some of the parameters including the impact speed, whether head contact on the vehicle occurred, and head contact location on the vehicle, most likely influenced the results as well.

DISCLAIMER

Work was performed for the Crash Injury Research and Engineering Network (CIREN) Project at Inova Fairfax Hospital Center in cooperation with the United States Department of Transportation/National Highway Safety Administration (USDOT/NHTSA). Funding has been provided

by Honda R&D Co. Ltd. under Cooperative Agreement Number DTNH22-03-H-08625. Views expressed are those of the authors and do not represent the views of any of the sponsors or NHTSA.

REFERENCES

Ashton, S. J. 1975. "The Cause and Nature of Head Injuries Sustained by Pedestrians." In Proceedings of the 1975 International IRCOBI Conference on the Biomechanics of Impact, pp. 101-113.

Ashton, S. J., Pedder, J. B., Mackay, G. M. 1978. "Pedestrian Head Injuries." In the 22nd Annual Proceedings of the American Association of Automotive Medicine, pp. 237-244.

Ashton, S. J. 1980. "A Preliminary Assessment of the Potential for Pedestrian Injury Reduction through Vehicle Design. In Proceedings of the 24th Stapp Car Crash Conference, pp 609-635. SAE Technical Paper 801315.

Ashton, S. J. 1983. "Benefits From Changes in Vehicle Exterior Design – Field Accident and Experimental Work in Europe." SAE Technical Paper 830626.

Ashton, S. J. 1997. "The Influence of Vehicle Design on Pedestrian Injury." In Proceedings of the International Symposium on Real World Crash Injury Research, Leicestershire, UK.

Ballesteros, M. F., Dischinger, P. C., Langenberg, P. 2004. "Pedestrian Injuries and Vehicle Type in Maryland, 1995-1999." Accident Analysis & Prevention 36(1), pp. 73-81.

Chidester, A. B., Isenberg, R. A. 2001. "Final Report – the Pedestrian Crash Data Study." In Proceedings of the 17th International Technical Conference on the Enhanced Safety of Vehicles.

Crandall, J. R., Bhalla, K. S., Madeley, N. J. 2002. "Designing Road Vehicles for Pedestrian Protection." British Medical Journal 324, pp. 1145-1148.

Fredriksson, R., Håland, Y., Yang, J. 2001. "Evaluation of a New Pedestrian Head Injury Protection System with a Sensor in the Bumper and Lifting of the Bonnet's Rear Part." In Proceedings of the 17th International Technical Conference on the Enhanced Safety of Vehicles. Paper 131.

- Harruff, R. C., Avery, A., Alter-Pandya, A. S. 1998. "Analysis of Circumstances and Injuries in 217 Pedestrian Traffic Fatalities." *Accident Analysis and Prevention* 30(1), pp. 11-20.
- Hosmer, D. W. and Lemeshow, S. 1989. "Applied Logistic Regression." John Wiley & Sons, Inc. ISBN 0-471-61553-6.
- Ivarsson, B. J., Henary, B., Crandall, J. R., Longhitano, D. 2005. "Significance of Adult Pedestrian Torso Injury." In the 49th Annual Proceedings of the Association for the Advancement of Automotive Medicine.
- Kendall, R., Meissner, M., Crandall, J. 2006. "The Causes of Head Injury in Vehicle-Pedestrian Impacts: Comparing the Relative Danger of Vehicle and Road Surface." SAE Technical Paper 2006-01-0462.
- Kirkeling, C., Schäfer, J., Thompson, G. 2005. "Structural Hood and Hinge Concepts for Pedestrian Protection." In Proceedings of the 19th International Technical Conference on the Enhanced Safety of Vehicles.
- Lane, P. I., McClafferty, K. J., Nowak, E. S. 1994. "Pedestrians in Real World Collisions." *The Journal of Trauma* 36(2), pp. 231-236.
- Longhitano, D., Burke, C., Bean, J., Watts, D., Fakhry, S., Meissner, M., Ivarsson, J., Sherwood, C., Crandall, J., Takahashi, Y., Katodani, Y., Hitchcock, R., Kinoshita, Y. 2005. "Application of the CIREN Methodology to the Study of Pedestrian Crash Injuries." In Proceedings of the 19th International Technical Conference on the Enhanced Safety of Vehicles, Paper 05-0404.
- Meissner, M., van Rooij, L., Bhalla, K., Crandall, J., Longhitano, D., Takahashi, Y., Dokko, Y., Kikuchi, Y. 2004. "A Multi-Body Computational Study of the Kinematic and Injury Response of a Pedestrian with Variable Stance upon Impact with a Vehicle." SAE Technical Paper 2004-01-1607.
- Mizuno, Y. 2003. "Summary of IHRA Pedestrian Safety WG Activities (2003) – Proposed Test Methods to Evaluate Pedestrian Protection Afforded by Passenger Cars." In Proceedings of the 18th International Technical Conference on the Enhanced Safety of Vehicles.
- Niederer, P. F., Schlumpf, M. R. 1984. "Influence of Vehicle Front Geometry on Impacted Pedestrian Kinematics." In Proceedings of the 28th Stapp Car Crash Conference, pp 135-147. SAE Technical Paper 841663.
- Okamoto, Y., Sugimoto, T., Enomoto, K. 2003. "Pedestrian Head Impact Conditions Depending on the Vehicle Front Shape and Its Construction – Full Model Simulation." *Traffic Injury Prevention* 4, pp. 74-82.
- Ono, Y., Komiyama, Y., Yamazaki, K. 2005. "Introduction of Pedestrian Head Protection Performance Test In J-NCAP." In Proceedings of the 19th International Technical Conference on the Enhanced Safety of Vehicles.
- Otte, D. 1994. "Influence of the Fronthood Length for the Safety of Pedestrians in Car Accidents and Demands to the Safety of Small Vehicles." In Proceedings of the 38th Stapp Car Crash Conference, pp 391-401. SAE Technical Paper 942232.
- Otte, D. 1999. "Severity and Mechanism of Head Impacts in Car to Pedestrian Accidents. In Proceedings of the 1999 International IRCOBI Conference on the Biomechanics of Impact, pp. 329-341.
- Roudsari, B. S., Mock, C. N., Kaufmann, R. 2005. "An Evaluation of the Association Between Vehicle Type and the Source and Severity of Pedestrian Injuries." *Traffic Injury Prevention* 6(2), pp. 185-192.
- World Bank 2006. "Road Safety." <http://web.worldbank.org/WBSITE/EXTERNAL/TOPICS/EXTHEALTHNUTRITIONANDPOPULATION/EXTPHAAG/0,,contentMDK:20780317~menuPK:64229809~pagePK:64229817~piPK:64229743~theSitePK:672263,00.html>. (accessed January 15, 2007).

PEDESTRIAN-VEHICLE ACCIDENT: ANALYSIS OF 4 FULL SCALE TESTS WITH PMHS

Catherine Masson, Thierry Serre

Laboratory of Applied Biomechanics. French National Institute for Transport and Safety Research-Faculty of Medicine of Marseille, Marseille, France

Dominique Cesari

Scientific Direction. French National Institute for Transport and Safety Research. Bron, France

Paper 07-0428

ABSTRACT

In industrialized nations, more than 25% of road traffic fatalities concern pedestrians. In some large urban areas, pedestrians account for as much as 40 to 50 percent of traffic casualties. To investigate pedestrian impact requirements for regulation in Europe, four full-scale pedestrian impact experiments were performed on embalmed PMHS. Two impacts were conducted in a standard condition with the PMHS laterally at the center line of the vehicle with the struck-side limb positioned anteriorly. The 2 other tests were a reconstruction of two real accidents and the PMHS were hit by the vehicle front laterally from $\frac{3}{4}$ right. Each PMHS was instrumented to measure the acceleration at points along the lower limb, the pelvis, the head. Pedestrian height being an important factor in the type of injuries sustained, the vehicle profile in relation to pedestrian height was recorded. After each test, a necropsy of each PMHS revealed the injuries to the tested PMHS. The distribution of vehicle contact areas and throw distance were noted. Because the head and lower limbs are the most commonly injured body parts for adult pedestrians, with head injury being the main cause of fatality, the analysis was focussed on these two body parts. The kinematics response of the pedestrian surrogates head was measured using precisely located targets. In particular, head velocity and head impact angle on the windscreen have at the instant of the impact been evaluated. The results provide complementary data for future pedestrian test methods and biofidelity assessment of a pedestrian dummy.

INTRODUCTION

Pedestrian crashes constitute the most frequent cause of traffic-related fatalities worldwide. On Europe roads, around 6 000 pedestrians are killed every year [3]. This translates in a death rate for the EU for 2002 of 15.7 killed pedestrians per 1 Million inhabitants. In Australia this figure is 12.3, in the USA 16.4 and in Japan 21.8. In developing nations, the number of killed vulnerable road users is even

higher. The high number of pedestrian accidents justifies more safety efforts worldwide.

Full scale experimental studies were performed to represent condition of pedestrian accident. If impact configurations are complex and varied, nevertheless it can be seen that lateral impacts make up for 74% of pedestrian collision (Henary B, 2003). Chidester and Isenburg (2001) reports that 356 (68%) of the pedestrians struck were oriented with their side to the striking vehicle, with 89 (17%) facing the vehicle and 53 (10%) facing away.

Head (31.4%) and legs (32.6%) each accounted for about one-third of the AIS 2-6 pedestrian injuries (Mizuno, 2003). But pedestrian injuries depend on a lot of parameters as the subject anthropometry, the initial position of the pedestrian, the front-end vehicle geometry which influences its kinematics (Meissner, 2004).

Many tests have been performed to study the behaviour of the pedestrian positioned laterally at the vehicle center line in a mid-stance gait position ("standard position"). Kerrigan et al (2005) studied mainly the kinematics of the pedestrian lower limb during impact and the kinematics of the head just before impact on the windscreen. The purpose of Kam's study was to document the development of a full-scale pedestrian impact test plan for dummies and PMHS. These tests were designed to accurately reproduce the kinematics and some of the injuries experienced by pedestrians struck laterally.

The primary objective of the current study was to examine the pedestrian behaviour according real accidents conditions. Four full-scale pedestrian impact experiments were performed on embalmed PMHS. Two initial positions of the pedestrian were studied. The first concerns the "standard position", the pedestrian were struck laterally. The second is based on real accidents reconstructions, with a $\frac{3}{4}$ frontal right pedestrian struck.

MATERIAL AND METHODS

PMHS preparation and characteristics

All PMHS were obtained and treated in accordance with the ethical guidelines approved by the Timone Faculty of Medicine in Marseille, and all PMHS testing and handling procedures were approved by the Ethical committee of the Faculty of Medicine too. The subjects were embalmed and preserved at 3°C in Winckler's preparation which is made of many standard embalming ingredients: phenol, alcohol, formalin, glycerin, sodium and magnesium sulfate, potassium nitrate. Based on Crandall study, this fluid distorts only a few of the properties of hard tissues and the results for Winkler fluid appeared to approximate most closely those of the fresh tissue (Crandall, 1994). It allows to keep supple the sampling and to preserve for several months the soft tissues elasticity. Prior to testing, anthropometrical measurements were made and X-Rays radiographs of the body were taken to verify the osseous integrity. Mean anthropometric characteristics of PMHS used in this study are given in Table 1.

Table 1.
Cadaver Physical data

	Test01	Test02	Test03	Test04
Gender	M	M	M	M
Age	88	74	85	80
Height (cm)	175	185	161	175
Weight (kg)	67	86	44	62

Full scale methodology

Prior to the vehicle striking him, the PMHS was maintaining in initial position by a neck harness. This harness was attached to a tension load cell which determined the timing of surrogate release. It was switched off 10 milliseconds before the impact so the subject was submitted to the gravity during the 10 ms before the impact. This allowed for the subject to be nearly freestanding at the initial bumper contact and to take into account the friction shoe-ground as it is in reality. After positioning of the subject was complete, the car was propelled by a horizontal catapult toward the pedestrian and was decelerated 10ms after the impact.

Positioning

Two aspects of pre-crash stance were considered for this study. Two impacts were conducted with the PMHS in standard position. The 2 other tests were a reconstruction of two real accidents.

Standard position

Body orientation: Pedestrian is impacted on its right side. A lateral impact was chosen as standard position because this position is representative of real world accidents as a majority of pedestrians are struck laterally by a vehicle.

Leg positioning: both feet are in contact with the ground and support the body's weight equally. The width between both feet was chosen to have a stable stance.

Position in real accidents

Body orientation: the PMHS were hit by the vehicle front laterally from $\frac{3}{4}$ right, at the center line of the vehicle

Leg positioning: both limbs are in contact with the ground. The struck leg was back along the centerline of the vehicle.

Test Matrix

Four full-scale pedestrian impact tests were performed. The vehicle used for the standard tests are a small one (Test01) and a big one (Test02).

Table 2.
Test matrix

				
Subject position	standard	standard	Real position	Real position
Speed	39.2km/h	39.7km/h	29.7km/h	37.2km/h
Vehicle	Small sedan	Big sedan	Small sedan	Big sedan

Instrumentation and measurement

The instrumentation was mounted on the posterior side of the subject to avoid damages in the instrumentation during impact. The PMHS was instrumented with accelerometers fixed on the lower limb and the head. Four high-speed video cameras operating at 1000 frames per second were placed in order to record the kinematics during the impact event. After the test, the car deformations, the Wrap Around Distance (WAD) to head strike was measured. The WAD corresponds to the distance between the head impact and the floor along the front end of the car. An in-depth necropsy was performed. Trajectory and velocity data for the head were calculated from films.

RESULTS

Accelerations of the tibia and head

Head and proximal part of the tibia accelerations were recorded. Due to the variability in subject anthropometry, the PMHS responses were normalised to the standard characteristics of the 50th percentile male weighing 75kg (Eppinger, 1984). The scaling variable λ and the scaled test parameters with subscript s were expressed in terms of the initial parameters with subscript i in following equations.

$$\text{Scaling variable } \lambda = (75 / M_i)^{1/3} \quad (1)$$

$$\text{Velocity } V_s = V_i \quad (2)$$

$$\text{Acceleration } A_s = A_i / \lambda \quad (3)$$

$$\text{Time } T_s = \lambda \times T_i \quad (4)$$

Acceleration-time histories are presented in Figures 1-4 for each test. The time of initial contact between the vehicle bumper and the PMHS's lower extremity was defined to be $t=0$.

Head impact occurred earlier in the standard tests (around 120ms after leg impact) than in real reconstruction (around 174ms after leg impact). We noted higher acceleration levels in real reconstruction (103g-112g) than in standard tests (67g-90g) although impact velocity was lower, especially for the test03. Moreover, if head impact peaks are very short in the case of real accident, the head acceleration at the head impact is clearly longer.

Figures 1-4 (a) show the tibia acceleration during the first 25ms because the study focussed on the knee and leg injuries associated to the front bumper impact. Tibia acceleration showed a first initial peak with peak values between 89g (test03) and 245g (test02-test04), these two tests having been performed with the big sedans at a almost identical impact velocity. In test02, a second peak is recorded in the tibia acceleration around 3ms after the first one, with a peak value of 766g. After 15ms, in three tests (test01, test02, and test04) the tibia is accelerated again until a significant peak value. The analysis of these peaks will be proposed in the discussion according to necropsy results given the injuries sustained in each test.

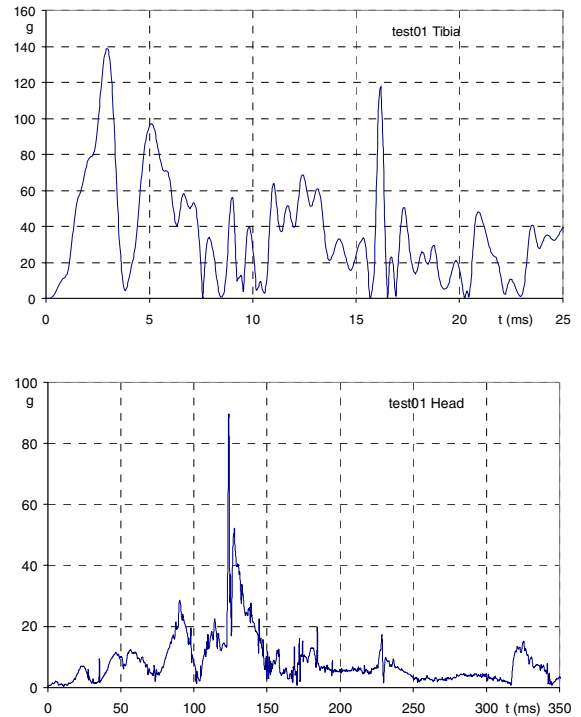


Figure 1. Test01: tibia acceleration (a) and head acceleration (b).

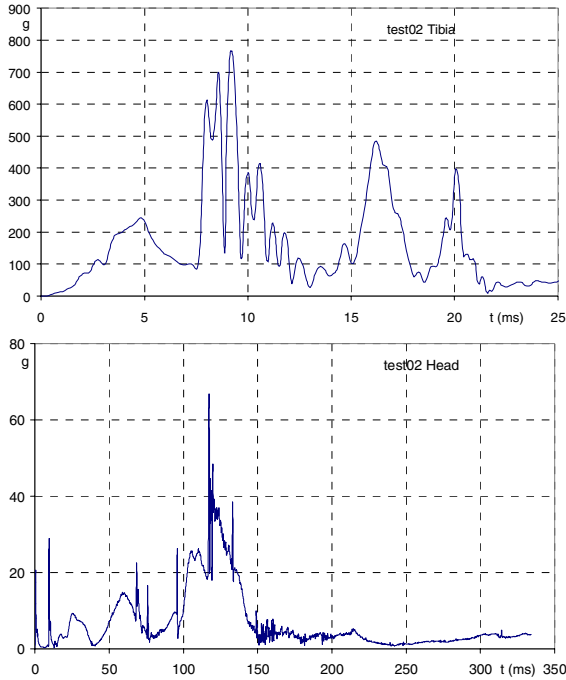


Figure 2. Test02: tibia acceleration (a) and head acceleration (b)

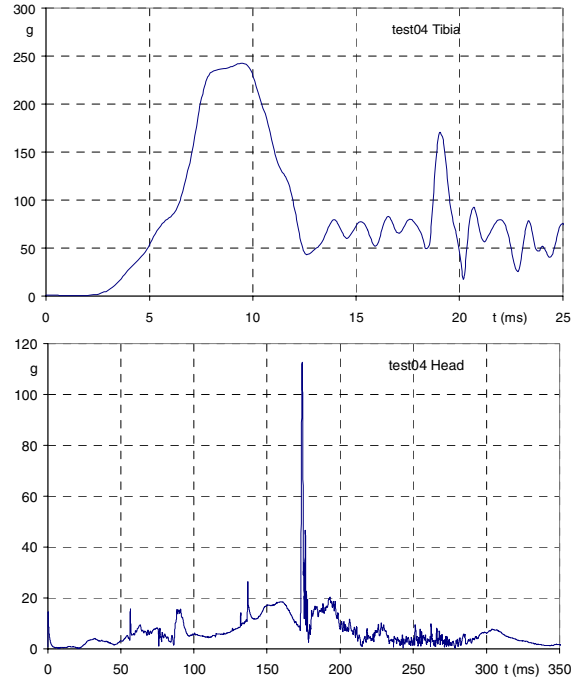


Figure 4. Test04: tibia acceleration (a) and head acceleration (b)

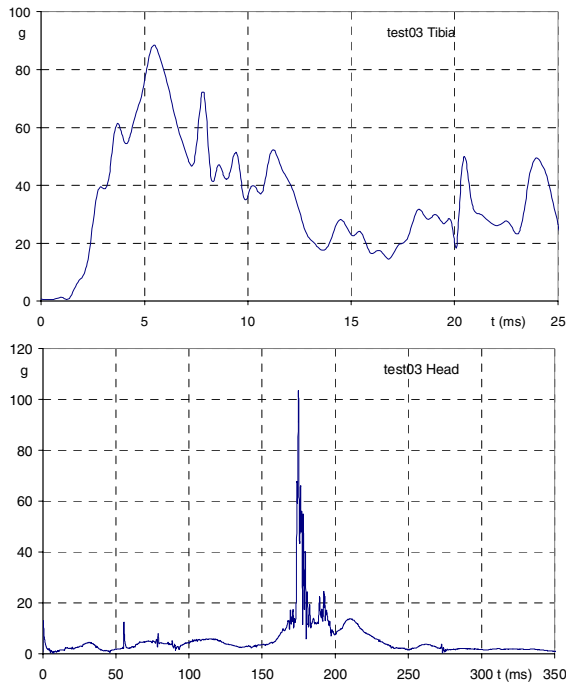


Figure 3. Test03: tibia acceleration (a) and head acceleration (b).

Kinematics

An important parameter is the specific pedestrian kinematics. The cinematic response of the pedestrian PMHS was evaluated using photo targets mounted on the head, on the proximal and distal parts of the femur, and on the proximal and distal parts of the tibia. The motion of each photo target was measured by recording the location of each photo target from high speed video images. The frame coordinate system, defined by the view of the high speed imager, is fixed with respect to the laboratory. A vehicle coordinate system was defined too.

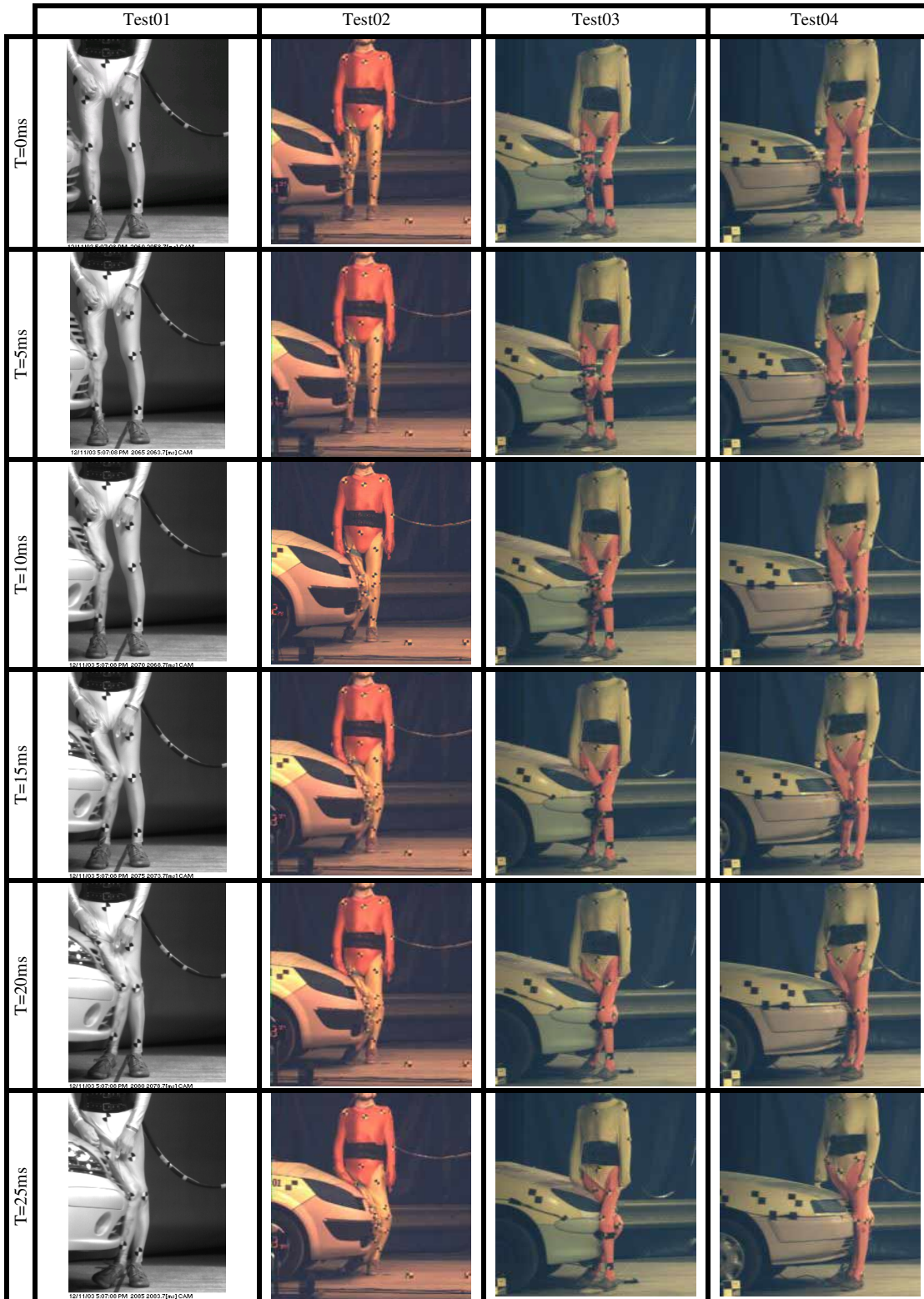


Figure 5. High speed video images for the lower limb.



Figure 6. High speed video images for the head.

Figure 5 shows the kinematics of the first impacted lower limb during the first 25ms. The first contact occurred between the bumper and the leg, followed by the pelvis or thigh-to-bonnet edge contact.

In the full scale tests in standard position, the right lower limb impacted then the left lower limb. This second impact occurred at 30ms in the test01, and at 15ms in the test02. In the full scale tests in real situation, because of a more frontal initial position, the bumper impacted the second lower limb directly after 24ms in the test03 and after 26ms in the test04.

Figure 6 shows the kinematics of the head. In each test a visual examination of the video data allowed to determine the time of head strike. The head impact

velocity, in the vehicle coordinate system, and head impact angle were measured and are given table 3. There is a significant difference in the shape of the head trajectory with head impact angles between 33° and 50°. Head impact velocities differed too, and for an equivalent car impact speed in the same PMHS initial posture, they could be lower (test01) or higher (test04) than the impact vehicle velocity.

Table 3.
Impact velocity and angle of the head

	Test01	Test02	Test03	Test04
Head impact velocity	37km/h	58km/h	30km/h	46km/h
Head impact angle	33°	50°	42°	42°

Necropsy

After testing, radiographs were taken and pre- and post-radiographs of the both lower limbs were analysed and compared. The post test necropsy results are presented in table 4. Only one fracture of the tibial diaphysis was observed. Ligament damages were observed in 3 tests in which the anterior cruciate ligament of the first impacted leg, the right one, was always injured. The PMHS used in the test01 sustained a lot of lower limb injuries, in particular bone damage were noted in the second impacted lower limb.

Table 4.
Necropsy results

	Test 01	Test 02	Test 03	Test 04
Right knee				
<i>Knee ligaments</i>				
MCL	×			×
LCL				
ACL	×	×		×
PCL	×			
<i>Articular capsule</i>	×			
<i>Fracture of the femur</i>				
internal condyle	×		×	
external condyle				
<i>Fracture of meniscus</i>				
<i>Fracture of the tibia</i>				
plateau	×			
diaphysis		×		
spine				
malleolus			×	
<i>Fracture of the fibula</i>				
diaphysis		×	×	
malleolus				
Left knee				
<i>Knee ligaments</i>				
MCL				
LCL	×	×		
ACL				×
PCL				
<i>Articular capsule</i>	×			
<i>Fracture of the femur</i>				
internal condyle	×		×	
external condyle	×			
<i>Fracture of meniscus</i>	×			
<i>Fracture of the tibia</i>				
plateau	×	×		×
diaphysis				
spine	×			
<i>Fracture of the fibula</i>				
diaphysis				
malleolus				×

DISCUSSION-CONCLUSION

Four full scale tests were performed with PMHS. In two tests, the pedestrian had an initial lateral position (standard position) and in the next two tests, the pedestrian was impacted by the vehicle front laterally from $\frac{3}{4}$ right with a significant lower car impact velocity in one case (test03). These different initial configurations induced different consequences on the lower limb accelerations, head impact velocities and head impact angles.

The results have showed a higher tibia initial acceleration in two tests (test02 and test04). For both tests, the vehicle used was a big car and the impact speed around 39km/h. An identical impact velocity was chosen in test01 but the full scale test was performed with a small sedan. This suggests that shape and model of the car has an effect on the tibia acceleration more significant than car velocity only. Because of the small number of tests, this suggestion has to be confirmed

In the pedestrian leg impact requirement, the acceleration measured at the upper end of the tibia shall not exceed 200 g. (DIRECTIVE 2003/102/EC) to avoid contact bone fractures. In this present study, only one tibial diaphysis fracture was listed, but the maximal acceleration was around 760g. Peak acceleration around 200g induced no bone fracture. But the impact locations of the lower leg depend directly on the posture and the height of the pedestrian. An improved understanding of the relation between bumper height and knee-joint injuries is need.

Ligament injuries were noted in 3 tests, two tests being in standard position. With a lateral pure impact as test01, the knee was bent laterally without bone fracture; leading to medial collateral ligament injury Nevertheless in this kind of initial posture, the lateral position of the left lower limb in the tests induced injuries of collateral ligaments on the left knee while the $\frac{3}{4}$ right latero-frontal position of the PMHS in the tests in real configuration induced cruciate ligament injuries. The second tibia acceleration peaks, recorded 15ms after the impact seem to be due these ligament injuries.

The kinematics response of the head was analysed in the four tests. The head impact velocity and the head angle were calculated in the vehicle system to be compared to EEVC tests. Generally, between the time of initial impact and head impact, the pedestrian is accelerated up to the velocity of the vehicle. The ratio

of the head velocity to the car travel speed is 0.66 for the test01, 1.1 for the test02, 0.67 for the test03, and 1.12 for the test04. These results are in agreement with the ratios reported by Pritz. for big cars and Cavallero et al (1983) for small cars;

The head impact angle differed in the 4 analysed cars. The different pedestrian heights do not explain the variation in the measurement of the impact angle. An identical impact angle was found for two tests (test03, test04) while the pedestrian height was 161 cm (test03) and 175cm (test04). Moreover, the car velocity was higher in test04.

The pedestrian head impact requirement, proposed by the EEVC, with an impact angle and a head impact speed not depending on the car geometry do not reproduce correctly real conditions of pedestrian accident. It appears that new requirement have to be develop more especially for the head protection.

ACKNOWLEDGEMENT

This work is included in the framework of the APPA project (Amélioration de la Protection du Piéton lors de collision par des Automobiles).

REFERENCES

Akiyama A., Okamoto M., Rangarajan N. 2001 "Development and application of the new pedestrian dummy". Paper 463, 17th Conference on the Enhanced Safety of Vehicles, Amsterdam, The Netherlands.

Cavallero C, Cesari D, Ramet M., Billault P., Fariisse J., Seriat-Gautier B., Bonnoit J. 1983. "Improvement of pedestrian safety: influence of shape of passenger Car-Front structures upon pedestrian impact injury & assessment", SAE pp225-237

Chidester A, Isenberg R. 2001. Final Report – The Pedestrian Crash Data Study. National Highway Traffic Safety Administration. United States of America. Paper Number 248.)

DIRECTIVE 2003/102/EC OF THE EUROPEAN PARLIAMENT AND OF THE COUNCIL of 17 November 2003 relating to the protection of pedestrians and other vulnerable road users before and in the event of a collision with a motor vehicle and amending Council Directive 70/156/EEC

Henry B, Crandall J, Bhalla K, Mock C, Roudsari B. 2003. "Child and Adult Pedestrian Impact: The Influence of Vehicle Type on Injury Severity". 47th Annual Proceedings, Association for the Advancement of Automotive Medicine, 22-24

Kam CY, Kerrigan J, Meissner M, Drinkwater C, Murphy D, Bolton J, Arregui C, Kendall R, Ivarsson J, Crandall J, Deng B, Wang JT, Kerkeling C, Hahn W. 2005 "Design of a Full-Scale Impact System for Analysis of Vehicle Pedestrian Collisions." Paper 05-433

Kerrigan J., Murphy D., Drinkwater D., Kam C., Bose D., Jeff R. Crandall J. 2005. "Kinematic corridors for PMHS tested in full scale pedestrian impact tests. Paper Number ESV 05-0394

Meissner M, van Rooij L, Bhalla K, Crandall J, Longhitano D, Takahashi Y, Dokko Y, Kikuchi Y. 2004 "A Multi-Body Computational Study of the Kinematic and Injury Response of a Pedestrian with Variable Stance upon Impact with a Vehicle". SAE 2004 World Congress, SAE Paper #2004-01-1607

Pritz H. B. 1983 "Experimental investigation of pedestrian head impacts on hoods and fenders of production vehicles". SAE 67-76

PEDESTRIANS AND THEIR SURVIVABILITY AT DIFFERENT IMPACT SPEEDS

Richard Cuerden

David Richards

TRL Limited

United Kingdom

Julian Hill

Loughborough University

United Kingdom

Paper Number 07-0440

ABSTRACT

The UK's On The Spot (OTS) accident data collection project started in 2000 and continues to investigate 500 crashes per year. Investigations are undertaken minutes after the collision has occurred to gather all the perishable information. At the time of writing over 3,000 crashes involving all road users and all injury severities have been examined. The OTS database provides a unique insight into the prevailing factors that have been seen to cause crashes and the associated human injuries and vehicle and infrastructure damage that have been witnessed by the crash investigation teams.

The research objective of this paper is to outline the pre and post-crash circumstances of 108 pedestrian crashes. The nature of the events that led to the collision, including the respective travelling speeds, time and distance from the moment the impact was inevitable are described. The information provided can be used to begin to outline the potential effectiveness of future crash mitigation systems. Further, the impact speeds are correlated to the injuries the pedestrians suffered with respect to the impact partner. Lower limb and head injuries are highlighted to be the most frequently injured body regions. The risk of injury for pedestrians with respect to the cars' speed at the point of impact is outlined and comparison made with the literature.

The small sample size is a limitation to the work, which has not at this stage been proven to be representative of the UK pedestrian accident population. Further, the nature of real world crash investigation means that some of the calculated speed values have reasonably large ranges. However, the work does offer an up to date review of the risk and type of injury versus impact speed for modern vehicles. In addition, the study starts to describe the in-depth pre-crash circumstances witnessed in real life crashes.

INTRODUCTION

Significant numbers of pedestrians are injured or killed as a result of being struck by motor vehicles every year. The relative importance of pedestrians

with respect to all traffic casualties varies between different countries, but typically the most common crash scenario involves them being struck by the front of a passenger car. One major factor that influences pedestrian injury outcome during a collision is the vehicle speed at the point of impact. This study provides a comparative review of real world casualty injury severity for pedestrians who were struck by the front of a car with respect to the speed at impact.

BACKGROUND

Vehicle speed affects both the risk of an accident and the associated injury severity. It has been observed that a reduction of the speed limit on a road from 60 kph to 50 kph produced a 20 % drop in pedestrian accidents, and a 50 % drop in pedestrian fatalities [1]. Also, pedestrian accidents are known to occur at a wide variety of speeds [2], although the majority (about 85 %) are believed to be below 50 kph [3]. Pedestrians are usually hit from the side, and are 3 to 4 times more likely to be crossing the path of the vehicle than travelling in a parallel direction to it. Cases where the vehicle runs over the pedestrian (where the wheels travel over the pedestrian as they lie in the road) are rare, with estimates varying between 2 % and 10 % [4] of pedestrian casualties.

The body parts with the highest risk of injury (frequency x severity) for a pedestrian struck by a vehicle are the head, followed by the lower extremities, the thorax, and the pelvis [4]. For non-fatal injuries, the lower extremities have been seen as the most frequently injured. These injuries tended to be to the knee ligaments for impact speeds around 20-30 kph, and to be fractures for accidents around 40 kph [5].

The head is often subject to two impacts, the first with the car itself, and the second with the ground as the pedestrian is thrown from the car. In relation to the relative severity of these two impacts, the literature is divided. Some observe that the primary impact (with the car) is the most severe impact [4]. This is in line with papers suggesting that the injuries caused by secondary impact are fewer and

less serious than those caused by primary impact [6]. However, others claim that the secondary impact is often a source of injury comparable to the primary impact [3].

Euro NCAP undertakes pedestrian sub-system impactor tests that are designed to rate new car models on the protection they offer to pedestrians in a frontal impact. In order to produce repeatable and scientific measurements leg forms and head forms are used to represent the pedestrian's associated body regions. The leg and head forms are projected towards the vehicle at 40 kph. The leg forms impact with the bumper and the bonnet leading edge and the head forms strike the bonnet at a variety of locations. The impactors are instrumented and the resulting measurements are used to predict the risk of injury.

While speed is certainly a factor directly linked to the severity of injury during pedestrian-vehicle collisions, other factors also come into play, making a pure assessment of the effects of speed very difficult. For example one study has shown that a long bonnet on a car reduces the injury risk of pedestrians in collision with that car [4]. This difficulty is exacerbated by the varied nature of pedestrians, who will be of all ages, and have very different biomechanical tolerances [2]. As people age their biomechanical strength decreases leaving them more vulnerable to injury for a given loading condition.

For several reasons, including those noted above, it is impossible to predict solely from the speed of an accident what the injury outcome of a given pedestrian will be. Fatal accidents have occurred at very low speeds, under 20 kph and as low as 12 kph; and slight injuries have been seen at much higher speeds (above 40 kph) [2] [4]. However, it is possible to identify boundary speeds, where the proportion of accidents changes from being mainly slight accidents to mainly severe accidents, and where the proportion changes from mainly survivable accidents to mainly fatal accidents.

In 1979 these boundary speeds were observed by Ashton and Mackay as being 30 kph for the transition from mostly slight to mostly severe (AIS 2+), and between 50 and 60 kph for the transition from mostly survivable to mostly fatal [2]. Ashton and Mackay determined the impact speed distribution of cars involved in pedestrian accidents where the pedestrian was contacted by the front of the car. This data was taken from at-the-scene studies at the Accident Research Unit, University of Birmingham. They weighted the data so it matched the proportions of slight, serious and fatal casualties seen in the national UK data.

The causes of the pedestrian injuries were also discussed by Ashton and Mackay. The at-the-scene studies showed that contact with the vehicle was responsible for more life-threatening or fatal head injuries than contact with the ground, and also that the windscreen frame was more likely to give a serious head injury than contact with the windscreen glass or the bonnet. There were other trends in the type of injuries suffered: head injuries were the most frequent injury sustained by those having non-minor injuries, with leg injuries being the second most common. The likelihood of injury for all the body regions increased with injury severity.

Their work has been used in the "Think! Road Safety" campaign by the Department for Transport, and is also a good basis for comparison with the results of this report. With changes in medical technology, population demographics and vehicle design, the boundary speeds, causes and distribution of injuries may now have changed.

METHOD

OTS Methodology

The On-The-Spot (OTS) Accident Data Collection Study has been developed to overcome a number of limitations encountered in earlier and current research. Most accident studies (such as the UK Co-operative Crash Injury Study, CCIS) are entirely retrospective, in that investigations take place a matter of days after the accident and are therefore limited in scope to factors which are relatively permanent, such as vehicle deformation and occupant injuries. They do not, in general, record information relating to evidence existing at the crash site, such as post-impact locations of vehicles, weather and road surface conditions, nor do they consider events leading up to the accident, such as the driving conditions encountered as the protagonists approached the crash site and their behaviour. It is these factors which give an insight into why the accident happened. The police, who do attend the scenes of accidents while such "volatile" data are still available to be collected, tend to have other priorities, such as ensuring the injured receive help, clearing the scene to restore the flow of traffic and looking for indications that any of the parties involved has broken the law.

The philosophy of the OTS project was to put experienced accident researchers at the crash scene at the same time as the police and other emergency services. The Study is thus still retrospective, in that the accident has already happened, but the timing is such that it should be possible to gather information on the environmental and behavioural conditions prevailing just before the crash. This

provides valuable in-depth data on the causes as well as the consequences of crashes, and allows countermeasures to be developed in the fields of human behaviour and highway engineering as well as vehicle crashworthiness. This is potentially a major improvement on the data currently available from other studies. A study of this type had not been conducted in the UK for over 20 years, and comparison of the results of the current study with those of the previous one should provide interesting insights into the changes which have taken place over that period.

The Study involves two teams, from the Vehicle Safety Research Centre at Loughborough University (VSRC) and the Transport Research Laboratory Limited (TRL), working in close co-operation to produce a joint dataset. Work on the development of the Study design and procedures began in 1998. Protocols were developed to be consistent with recent international activities. These include the EC proposals for the development of a Pan-European Accident Database based on recommendations from the Standardisation of Accident and Injury Registration Systems (STAIRS) project.

Funding for the project came from the Road Safety Division at the Department for Transport and from the Highways Agency. Full data collection began in 2000 with a requirement to collect detailed information on 500 accidents per year. This was a large and complex activity, involving close collaboration between two geographically remote research teams operating from TRL in Berkshire and VSRC in Nottinghamshire. Both teams developed the project using common protocols and liaison techniques with the emergency services, hospitals, HM Coroners and local authorities and including routine technical links with the expertise available at the two institutes.

The Study has seen a very close working relationship between the research teams and their respective local police in Nottinghamshire and Thames Valley. This link was strengthened by the inclusion of a serving police officer on each team, which provided a secure, direct and reliable link with the local police command and control systems, thus ensuring immediate crash notifications. Response vehicles, fitted with blue lights and driven by seconded police officers, were used to transport each research team safely to the scene. In this way it was possible to cover a larger area than in previous studies. The response technique ensured that the combination of a relatively large area and increased traffic densities on modern roads allowed larger samples of crashes to be investigated than were attained in some earlier studies.

Given the attention to detail in establishing the necessary infrastructure, the well designed sampling plan and conformity to common investigation protocols, the DfT/HA OTS project provides an example of “best practice” in this field. As far as the authors are aware, no other country is systematically collecting on-scene data, to a pre-defined sampling plan and with such effective co-operation from all relevant public services contributing to the necessary input data.

It takes many years to establish useful databases and it is essential to have continuity to gain the best value from the database over the long term. The OTS project has two main strengths, compared with more conventional studies. The first is having access to volatile scene data including transient highway factors and climatic conditions, which are particularly important for determining accident circumstances, especially when investigating vulnerable road user accidents. The second is the ability to interview witnesses at the scene, thus gaining an insight into behavioural characteristics, and how these may have been influenced by the transient factors referred to above.

Terminology and Definitions of Key Variables

Impact Speed - The collision or impact severity is determined by the OTS investigation team. Wherever possible, physical scene evidence is used to derive estimates of the speed of the vehicle at the point of impact. These techniques include mathematical reconstructions based on the trace marks which vehicle tyres leave on the road surface due to heavy braking and evaluation of the pedestrians’ throw distance correlated to the probable impact speed.

Often there is very little physical evidence either on the road surface or vehicle that can be used to calculate an impact speed. Sometimes the only evidence of pedestrian impact with the vehicle are faint cleaning marks on the bumper or bonnet surface. In such cases it is still possible to estimate impact speeds, but the level of accuracy is clearly lower. The OTS team collates information from witnesses, crash participants and the characteristics of traffic flow along with other scene related information to validate and help inform any vehicle to pedestrian impact speed measures.

Police Injury Severity - The casualties’ injury severity is classified by Road Casualties Great Britain (RCGB) [7] and by OTS according to the UK government’s definitions of Fatal (Killed), Serious or Slight.

'Fatal' injury includes only those where death occurs in less than 30 days as a result of the accident. Fatal does not include death from natural causes or suicide.

Examples of 'Serious' injury are:

- Fracture of bone
- Internal injury
- Severe cuts
- Crushing
- Burns (excluding friction burns)
- Concussion
- Severe general shock requiring hospital treatment
- Detention in hospital as an in-patient, either immediately or later
- Injuries to casualties who die 30 or more days after the accident from injuries sustained in that accident

Examples of 'Slight' injuries are:

- Sprains, not necessarily requiring medical treatment
- Neck whiplash injury
- Bruises
- Slight cuts
- Slight shock requiring roadside attention

Abbreviated Injury Scale (AIS) - The OTS casualties' injuries and characteristics (gender, age, height, weight etc.) are obtained from police reports, questionnaires, hospital records or HM coroner reports depending on the casualties' injury severity. The injuries sustained are coded using 'The Abbreviated Injury Scale (AIS) 1990 Revision' (Association for the Advancement of Automotive Medicine, AAAM).

Each injury description is assigned a unique six digit numerical code in addition to the AIS severity score. The first digit summarises the body region; the second digit identifies the type of anatomical structure; the third and fourth digits identify the specific anatomical structure or, in the case of injuries to the external region, the specific nature of the injury; the fifth and sixth digits identify the level of injury within a specific body region or anatomical structure. Finally, the digit to the right of the decimal point is the AIS severity score. This study specifically uses the AIS code for the body region injured and the AIS severity score. The body regions injured are classified by:

- Head
- Face
- Neck
- Thorax
- Abdomen
- Spine (cervical, thoracic and lumbar)
- Upper Extremity

- Lower Extremity
- Unspecified

The AIS severity score is a consensus-derived anatomically-based system that classifies individual injuries by body region on a six point ordinal severity scale ranging from AIS 1 (minor) to AIS 6 (currently untreatable), shown in table 1.

Table 1.
Possible values of AIS

AIS Score	Description
1	Minor
2	Moderate
3	Serious
4	Severe
5	Critical
6	Maximum
9	Unknown

MAIS denotes the maximum AIS score of all injuries sustained by a particular occupant. It is a single number that attempts to describe the seriousness of the injuries suffered by that occupant.

HAIIS denotes the highest AIS score of all injuries to a given body region sustained by an occupant. It is a single number that attempts to describe the seriousness of the injuries to a given body region suffered by that occupant.

The AIS system therefore allows injuries to be coded by their type and severity in terms of threat to life. In OTS, the injuries are then correlated with the associated vehicle damage to try to determine the ultimate cause of each individual injury.

The research undertaken by Ashton and Mackay used an earlier version of the AIS dictionary (1976 Revision). In summary the two dictionaries can not be directly compared for specific injuries, but like the AIS 1990 Revision, this version had six injury scores per injury ranging from 1 to 6. There were however, far fewer injury descriptions and the overall evaluation was much simpler than that documented later in AIS 1990. The severities of some individual injuries have also changed between the two versions, with some now having a higher AIS severity score, but others a lower score. Therefore, direct comparisons between Ashton and Mackay are not necessarily 'like by like' for the different AIS scores for the body regions injured.

OTS Sample Selection

OTS crashes involving pedestrians were selected and further filtering applied to identify cases with all the pertinent data available. Each case was

reviewed in detail and where appropriate enhancements were made to the information available with respect to the injury severity, type and causation and the vehicle impact speed. The case reviews were undertaken by researchers working at the VSRC and TRL. The work was coordinated to ensure harmonisation between the two research centres and a common database was populated. All OTS crashes involving pedestrian casualties that were available in July 2006 were reviewed.

A separate database was created from the data for the use of this project, including all the details which would be required for a study of pedestrian casualties. This consisted of data on 175 pedestrians struck by vehicles, and for each pedestrian the best estimate of the impact speed was given. The impact speed was calculated using physical evidence if present, and other means of estimating the speed if the physical evidence was inconclusive. Of the 175 pedestrians, 41 % had an impact speed based on robust physical evidence, with the remaining 59 % having an impact speed estimated with other methods, sometimes including some physical evidence and on other occasions relying more on subjective opinion.

Physical evidence which was used to estimate impact speed includes the length of skid, and the distance the pedestrian was thrown after impact. Other methods used for estimating the impact speed include the speed limit of the road and the likely speed given the conditions, damage to parts of the car such as the windscreen, and the estimates of witnesses and the investigation team at the scene. Figure 1 shows a photograph of a car involved in a pedestrian impact. The impacts with the bonnet and windscreen can clearly be seen, and such evidence can be used to estimate the impact speed.



Figure 1. Car involved in a pedestrian impact.

Of these 175 pedestrians, only those involved in frontal impacts with cars were used. In addition, only those whose injury severity (both MAIS and

police injury classification, slight, serious or fatal) was known were included in the study. This reduced the sample to 108 pedestrians. Of these 108, 49 % had impact speed calculated using physical evidence, while the remaining 51 % of impact speeds were estimated using other methods. Figure 2 shows how the methods of determining the impact speed were distributed.

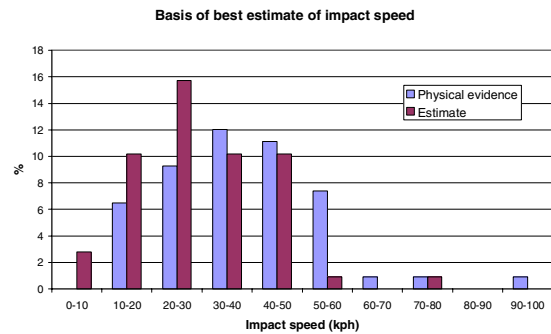


Figure 2. Basis of impact speed measurements for the 108 pedestrians.

RESULTS

Pre-Crash Characteristics

Braking Before Impact - The OTS pedestrian database recorded details of any braking believed to be performed by each car before it struck the pedestrian. Table 2 shows these details for the 108 pedestrian casualties in the sample.

Table 2. Braking before impact for the vehicles striking the 108 pedestrians

	Number of pedestrians			
	Fatal	Serious	Slight	Total
Braking	1	7	26	34
Unknown				
Locked Wheels	2	10	9	21
No Braking	2	8	11	21
Some Braking	2	11	19	32
Total	7	36	65	108

For about a third of the pedestrians it was not known whether the car attempted to brake before the impact. The effect of braking on the impact speed is shown in figure 3, which shows the cumulative impact speeds for the 108 pedestrians.

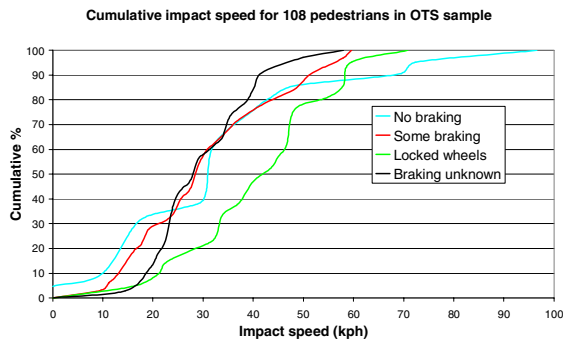


Figure 3. Variation of cumulative impact speed with braking.

Accidents where the car locked wheels before the accident tend to have larger impact speeds than accidents where there was some or no braking. But the cases with the highest impact speeds occur when there is no braking.

Causes and Contributory Factors - The OTS database records the likely causes of each accident in a number of different ways. The first method is to select a “precipitating factor” for each accident. The 108 pedestrians in the OTS sample were from 107 accidents, 99 of which had a “definite” precipitating factor. These precipitating factors are shown in table 3.

Table 3. Precipitating factors in pedestrian impacts

Precipitating factor	No. of cases	% of cases
Pedestrian entered carriageway without due care (driver not to blame)	78	72.9
Failed to avoid pedestrian (pedestrian not to blame)	10	9.3
Failed to stop	3	2.8
Pedestrian fell in road	3	2.8
Loss of control of vehicle	2	1.9
Failed to avoid object or vehicle on carriageway	1	0.9
Failure to signal or gave misleading signal	1	0.9
Other	1	0.9
No definite factor	8	7.5

This shows that in the vast majority of cases the precipitating factor was the pedestrian stepping into the carriageway without due care.

For each of the precipitating factors, one or more contributory factors can be given which are deemed to have contributed to the precipitating factor. The 11 most frequent contributory factors for the 107 pedestrian accidents are shown in table 4.

Failure to look is the most frequent contributory factor recorded here, although it does not distinguish between failure of the driver or pedestrian.

Table 4. Contributory factors to pedestrian impacts

Contributory factor	No. of cases	% of cases
Failed to look	23	21.5
Inattention	21	19.6
Carelessness, reckless or thoughtless	20	18.7
Cross from behind parked car	16	15.0
Ignored lights at crossing	10	9.3
Surroundings obscured by stationary or parked car	10	9.3
Failure to judge other persons path or speed	8	7.5
Impairment through alcohol	7	6.5
In a hurry	7	6.5
Person hit wore dark or inconspicuous clothing	3	2.8
Lack of judgement of own path	3	2.8

In 2005, another method of recording the contributory factors toward the accident was introduced in OTS (and the older cases were retrospectively coded to the new standard). This does not give the contributory factors towards the precipitating factor, but rather the contributory factors to the accident itself. The 8 most frequent contributory factors to the 107 pedestrian accidents in the OTS sample are detailed in table 5.

Table 5. Contributory factors (2005) in pedestrian impacts

Contributory factor	No. of cases	% of cases
Pedestrian: Failed to look properly	43	40.2
Pedestrian: Crossing road masked by stationary or parked vehicle	20	18.7
Pedestrian: Wrong use of pedestrian crossing facility	6	5.6
Injudicious Action: Exceeding speed limit	5	4.7
Injudicious Action: Disobeyed automatic traffic signal	4	3.7
Pedestrian: Failed to judge vehicle's path or speed	4	3.7
Pedestrian: Impaired by alcohol	4	3.7
Error or Reaction: Failed to look properly	3	2.8

Once again, the majority of the accidents are deemed to have been caused by the pedestrian.

Injury Causation

Risk of injury by impact speed – Ashton and Mackay produced risk curves which attempted to show the risk of injury to a pedestrian for a given impact speed. The following graphs compare the findings from the OTS sample of pedestrians to those in Ashton and Mackay.

Figure 4 shows the cumulative impact speed for the 108 pedestrians in the OTS sample. Figure 5 shows the cumulative impact speed for the pedestrians with non-minor (MAIS > 1) injuries, and Figure 6 shows the cumulative impact speed for the fatalities. The equivalent curves from Ashton and Mackay are also shown.

In the OTS data, pedestrians tend to be struck at higher speeds than those seen in the Ashton & Mackay paper. The 50th percentile for all the casualties is about 30 kph for the OTS pedestrians, compared to only 20-25 kph for the Ashton & Mackay dataset. It also appears that a greater proportion of non-minor injuries are caused at higher speeds for the OTS data. The 25th percentile impact speed for non-minor injuries in OTS is approximately 25 kph compared to about 30 kph for the Ashton and Mackay data, while the 75th percentile impact speed is approximately 7 kph faster for OTS.

Although there are very few fatalities in the OTS data (only 7), these follow a similar trend to the non-minor injuries. However it should be noted that while fewer non-minor injuries and fatalities are occurring at high speeds, more fatalities and non-minor injuries are occurring at lower speeds, even though overall the number of casualties injured at a given speed has reduced. This trend of injuries occurring over a wider speed range than shown by Ashton and Mackay is true for both non-minor and fatal injuries.

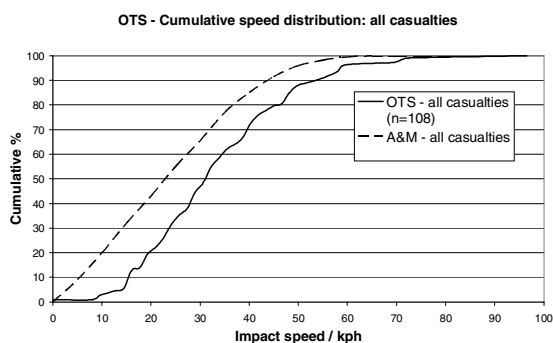


Figure 4. Cumulative impact speed for all pedestrian casualties.

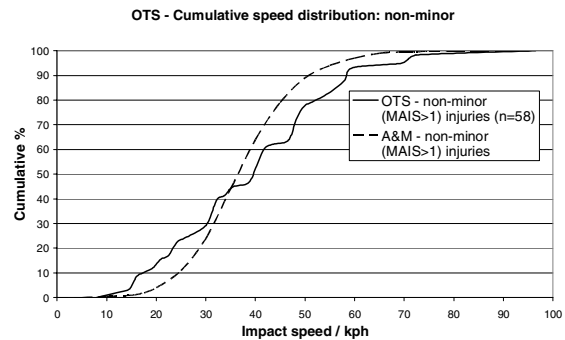


Figure 5. Cumulative impact speed for non-minor (MAIS > 1) casualties.

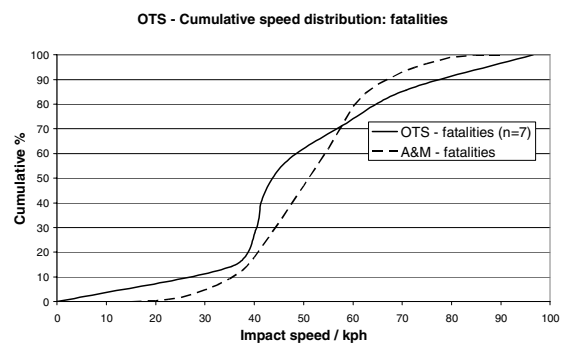


Figure 6. Cumulative impact speed for fatalities.

From the OTS data, figure 7 was produced which shows how the probability of suffering each severity of accident varies with impact speed. Note that the non-minor category no longer includes fatalities. This has been changed so that all injuries add up to 100 %.

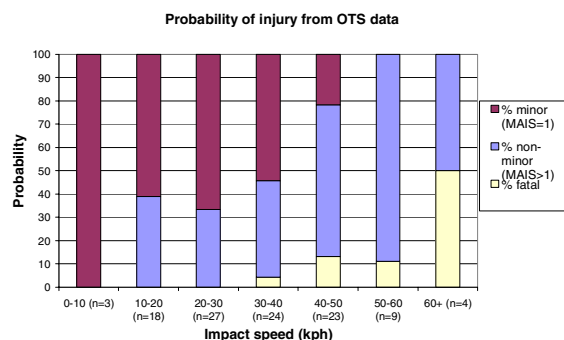


Figure 7. Probability of injury from OTS data, by MAIS.

As speed increases the probability of suffering a minor injury decreases, and the probability of suffering a serious injury or fatality increases. The number of cases at high speeds was very small, so the pedestrians with impact speeds above 60 kph have been combined. A second version of this figure is shown in figure 8 where the Police definitions of slight, serious and fatal are used to describe the casualties, rather than MAIS.

This can be compared with figure 9, which shows a reproduction of data in the Ashton & Mackay paper to produce a similar graph showing the probability of injury. Note that the Aston & Mackay paper does not give clear details of the number of casualties, so these have not been included. This figure was produced by estimating the area under the curves of a graph, and so is probably only accurate to about 10 %. But this is enough to compare the trend shown with that given by the OTS data.

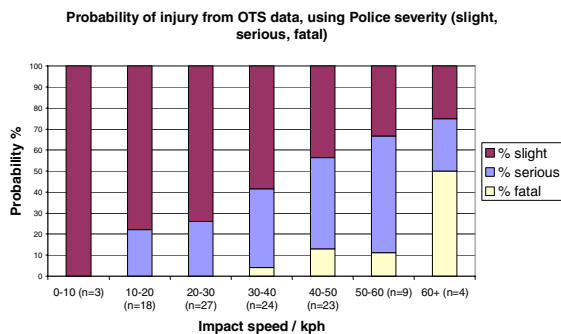


Figure 8. Probability of injury from OTS data, by Police severity.

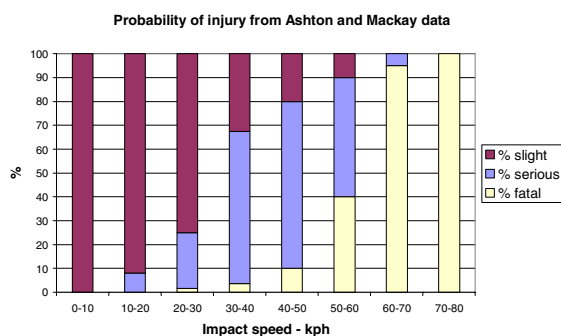


Figure 9. Probability of injury from Ashton and Mackay data, by Police severity.

Comparing these figures tells a similar story to the cumulative impact speed curves. At impacts below 30 kph, the incidence of serious injuries is the same or higher in the OTS data than in the Ashton & Mackay data. At speeds above this, pedestrians in the OTS data were less likely to suffer a serious or fatal injury than those in the Ashton & Mackay dataset.

Body Regions Injured - Figure 10 details the distribution of injuries suffered by all surviving pedestrians aged between 15-59. This age range is chosen to match that used by Ashton & Mackay to display the same data, and gives 43 pedestrians from the 108 in the OTS dataset. The injury distribution is demonstrated using the most severe injury suffered to a particular body region (HAIS), and is given as a percentage of the 43 pedestrians. For example, about 50 % of pedestrians had

injuries to the head, with the highest injury being an AIS 1 injury. About 20 % of pedestrians had injuries to the head the worst of which has an AIS greater than 1. So in total, over 70 % of the pedestrians suffered an injury to their head.

Most of the pedestrians hit by the front part of a car suffer injuries to the head, arms and legs. This agrees with the Ashton and Mackay data.

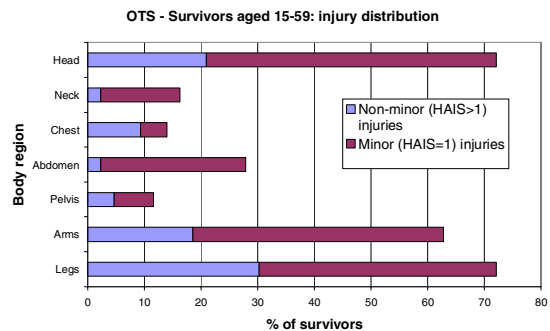


Figure 10. Injury distribution of OTS survivors aged 15-59.

Figure 11 shows the results for the 22 pedestrians with non-minor (MAIS > 1) injuries, who survived. The same data from the Ashton & Mackay paper is also included, which had 308 survivors suffering non-minor injuries.

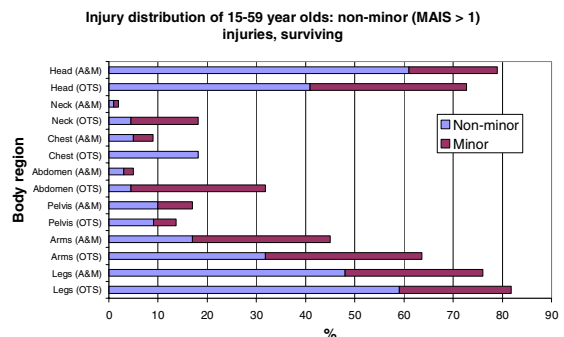


Figure 11. Injury distribution of non-minor (MAIS > 1) casualties from OTS and Ashton and Mackay.

For all body regions apart from the head and pelvis, a larger percentage of pedestrians in the OTS dataset suffered some kind of injury. In the arm, leg, and pelvis region the percentage suffering minor injuries is not very different between the two sets of data. There is a slight increase in minor head injuries to the OTS pedestrians, and a large increase in minor neck and abdomen injuries.

The OTS data shows large increases in non-minor injuries for the neck, chest, arm and leg regions, and a decrease in non-minor injuries to the head. The decrease in non-minor injuries to the head is possibly the most important change as far as

fatalities are concerned. Ashton & Mackay showed that over 90 % of pedestrians who were fatally wounded had a non-minor injury to their head.

There were only two fatalities present in the OTS data for the age range 15-59, so the details of those cases have not been included here.

Causes of Injury - Figure 12 shows the causes of the head injuries sustained by pedestrians in the OTS dataset. This is shown as the percentage of injuries of that severity (all, non-minor (AIS > 1), and causing death) for which the cause was known, rather than the percentage of pedestrians. Of the 108 pedestrians in the dataset, there were 144 head injuries of known origin.

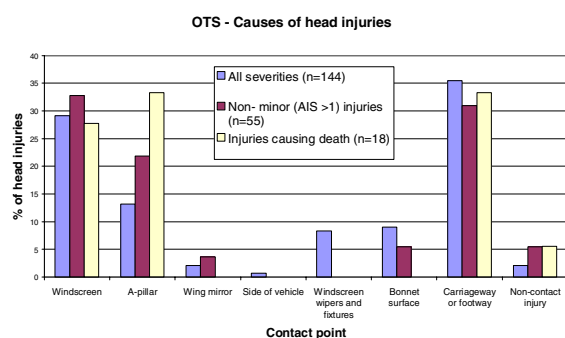


Figure 12. Causes of head injuries in OTS dataset.

The windscreen, A-pillar and contact with the ground cause the most head injuries, of all severities. Although contact with the vehicle does cause more injuries than contact with the ground (as stated by Ashton & Mackay), there is no single part of a car which causes as many injuries. While injuries caused by the A-pillar become increasingly important as the severity increases, contact with the windscreen and the ground causes more injuries of all severities.

Figure 13 shows the causes of the leg injuries suffered by pedestrians in the OTS sample.

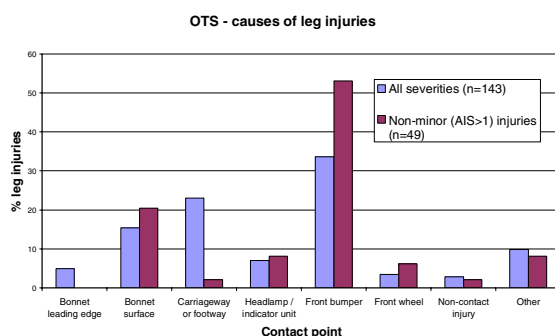


Figure 13. Causes of leg injuries in OTS dataset.

The front bumper is the most frequent cause of all leg injuries, and is by far the most important cause of non-minor leg injuries. Contact with the ground is the second most frequent cause of leg injuries, although the vast majority of these are minor, AIS 1 injuries. The bonnet surface is the second most important cause of non-minor leg injuries.

Figure 14 looks at leg injuries caused by contact with the front bumper (the most important cause of leg injuries), and shows how the injury severity depends on the impact speed.

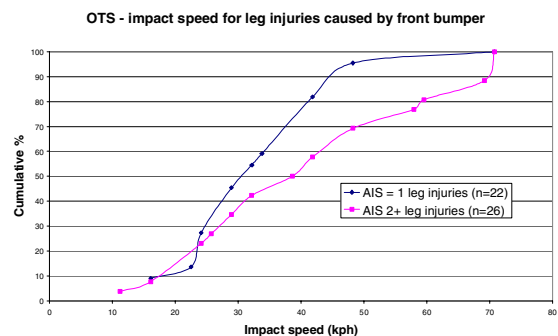


Figure 14. Cumulative impact speed of leg injuries caused by front bumper.

As would be expected, pedestrians struck at higher speeds receive more serious injuries. Above 30 mph (48 kph) all leg injuries caused by the front bumper are at least of severity AIS 2. A similar effect is seen between impact speed and head injury, which is shown in Figure 15.

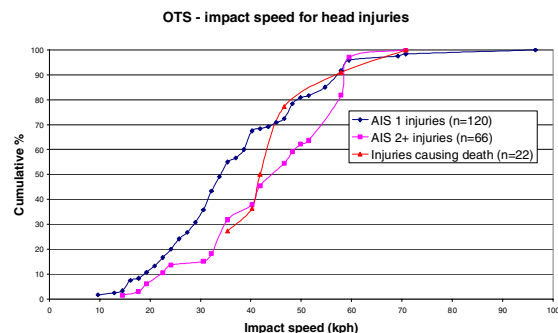


Figure 15. Cumulative impact speed for head injuries.

Non-minor head injuries occur at greater speeds than minor (AIS 1) head injuries. The 50th percentile is about 43 kph for AIS 2+ injuries, compared to about 34 kph for minor head injuries.

DISCUSSION

Pre-Crash Characteristics

Braking before the accident does seem to have an effect on the injury severity of the pedestrian. From

the 108 pedestrian impacts studied in detail, 41 % of those where there was “some braking” were killed or seriously injured, compared to 48 % of those where there was “no braking”. But of the pedestrians where the braking was recorded as “locked wheels”, 57 % were killed or seriously injured.

The impact speeds for pedestrians where the car locked wheels seem to be higher than those for other braking conditions, which explains why these pedestrians were more often killed or seriously injured. But this does not explain why cars whose wheels had locked have higher impacts than those where there was no braking. This is likely to be due to statistical variation in the relatively small sample.

The majority of the pedestrian impacts seemed to be caused by poor judgement on the part of the pedestrian, with the 3 most frequent contributory factors (as used in OTS from 2005) relating to mistakes by the pedestrian. Of the causes attributed to the driver of the car, exceeding the speed limit was considered a contributory factor in only 5 % of cases (compared to 40 % of cases where the pedestrian did not look properly).

Impact Speed

Large differences are seen when the cumulative impact speed curves from the OTS data are compared to the equivalent curves from Ashton & Mackay. Firstly, the difference between the speeds at which fatalities occur compared to the impact speeds for all casualties is much greater in the Ashton and Mackay data. Taking the 50th percentile, there is a difference of about 28 kph between the fatalities and all the casualties, compared to about 12 kph for OTS. The impact speeds for all the casualties are also lower in Ashton & Mackay than in OTS, by about 8 kph.

There are also differences in the shape of the curves. The OTS curves change more gradually than the Ashton & Mackay curves, and the curves cross above the 50% line. This means that the Ashton & Mackay casualties are spread over a smaller speed range, and peak at lower speeds than the OTS casualties.

These relationships between impact speed and injury severity are complicated. The largest difference is that, in general, the impact speeds for all the casualties being hit in the OTS dataset are higher than those shown by Ashton and Mackay. Making the assumption that all pedestrians who are struck by a car are injured in some way, there are a few possible explanations for this: either pedestrians are, on average, struck at higher speeds;

the datasets are biased to include more accidents at higher speeds; or the methods used to estimate the impact speeds tend to overestimate (or Ashton & Mackay under-estimated).

When the casualties are split by severity, it appears that the non-minor and fatalities in Ashton & Mackay were occurring at lower speeds, and over a smaller spread of speeds, than in the OTS data. The increase in speed required to inflict a non-minor injury would suggest that cars have become more pedestrian-friendly in some way since 1979, with higher impact speeds required to produce the same degree of injury. The increase in speed for a fatality agrees with this improvement in pedestrian friendliness, and could also suggest that pre-hospital and hospital trauma care has improved a pedestrian’s chance of surviving.

These changes are also present in the graphs which attempt to show the probability of suffering a slight, serious or fatal injury at different speeds. For example, from the Ashton & Mackay paper the chance of a pedestrian being killed between 60-70 kph is approximately 95 %, whereas the probability of a fatality at impact speeds greater than 60 kph is about 50 % in OTS. Unfortunately, at these higher speeds the sample sizes are very small in the OTS data, but impacts between 50-60 kph also produce a lower percentage of fatalities in OTS.

At speeds lower than this, the percentages of fatalities in the two sets of data are similar. At speeds between 20-60 kph there tend to be fewer serious casualties in OTS compared to Ashton and Mackay, although at speeds lower than this there are more serious injuries in OTS.

It is possible that the methods used to estimate the impact speeds could have an effect on the results, for example if they consistently overestimated the impact speed. For the OTS data, it has been shown that estimates based on physical evidence tend to give larger impact speeds than estimates made using other methods. This is probably due to the fact that there is less likely to be suitable physical evidence (such as pedestrian throw or skid marks) at impacts of lower speed, so other methods of estimation need to be used. There is no evidence that these other methods under/over estimate compared to the estimates based on physical evidence.

The increase to the impact speed observed in the boundary condition between serious and fatal injury outcome is a very interesting finding. This could be due to many interrelated factors. Not least, in the 30 years since Ashton and Mackay completed their innovative research the standard of pre-hospital and hospital medical care has

significantly improved with advances in technology and working practices. There have been significant road and vehicle design changes that have also occurred in this period. In addition, the exposure and associated pedestrian demographics have changed, resulting in different groups of people being more or less at risk of being struck by a car with respect to their age and even socio-economical status.

Injury Distribution

For all survivors the head, arms and legs are the body regions of pedestrians which most frequently suffer both minor (AIS = 1) and non-minor (AIS > 1) injuries. Unfortunately, because there are so few fatalities in the OTS dataset the difference in injury distribution between non-minor casualties and fatalities could not be investigated. The OTS data shows that increasing impact speed is related to increasing severity of both head and leg injuries. The most consistent difference between the data sets is that there are more head injuries in the Ashton & Mackay data for non-minor casualties and fatalities. This is one possible explanation for the greater percentage of fatalities in the Ashton & Mackay data, although the increase in head injuries is relatively small.

Apart from a small decrease in head injuries, the pedestrians who are hit by cars do not show any great reduction in injuries to separate body parts compared to those seen by Ashton & Mackay in 1979, even though it has been shown that higher speeds are required to produce the same injury severity. It is possible that this is related to the higher impact speeds compared to the 1979 data, where any possible improvement is being masked because pedestrians are being hit at higher speeds. To determine whether this is the case, the data would need to be split by both body region and speed, which unfortunately would leave the sample sizes too small to be meaningful.

Causes of injury

The two regions most frequently injured in a pedestrian impact are the legs and the head, and it is these regions where the causes have been investigated in more detail.

The majority of leg injuries are caused by the front bumper, as would be expected. This is shown in the OTS data, with 53 % of AIS 2+ leg injuries caused by the front bumper for the OTS pedestrians. Impact with the bonnet surface makes up another 20 % of the non-minor leg injuries.

Head injuries are the leading cause of fatalities to pedestrians, so determining the causes of these

injuries is very important if cars are to be further adapted to be pedestrian friendly. For the pedestrians in the OTS dataset, the most common causes were contact with the windscreen, the A-pillar and the carriageway/footway. Ashton and Mackay identified contact with the A-pillar as causing more serious injuries than contact with the windscreen or bonnet, and for OTS the proportion of injuries caused by the A-pillar increases as the injury severity increases.

Although more injuries are caused by contact with the car than with the road, contact with the ground causes more injuries than any single region of a car. The bonnet, which has been the focus of many attempts to improve the results of pedestrian crashes, has been shown here to be one of the least important causes of fatalities. This could mean that improvements in bonnet design have been successful, but now efforts should probably be concentrated elsewhere.

CONCLUSIONS

- The majority of pedestrian impacts are caused by the actions of the pedestrian.
- In 1979, Ashton and Mackay reported that the boundary car impact speed for the transition from mostly slight to mostly severe (AIS 2+) pedestrian casualties was approximately 30kph. The OTS dataset mirrors this finding.
- Further, Ashton and Mackay reported that the boundary car impact speed for the transition from mostly severe to mostly fatal pedestrian casualties was between 50 and 60kph, whereas the OTS dataset shows this change to occur above 60 kph. However, the number of fatal cases in the OTS database above 60kph is very small and this is an important factor to note when presenting the data.
- The OTS pedestrian impact speeds are more distributed than reported by Ashton and Mackay with proportionally more at the lower and higher speed ranges respectively.
- Head and leg injuries are the most frequent in the OTS dataset, which agrees with the findings of Ashton and Mackay.
- Most head injuries in the OTS dataset are caused by contact with the A-pillar, windscreen or the ground. Contact with the bonnet seems to be relatively unimportant. The most frequent cause of leg injuries is impact with the front bumper.

In terms of future work, the following points should be considered.

OTS is a continuing project. As more pedestrian accidents are investigated, the greater numbers will allow more robust conclusions to be drawn from the results, and may also allow other factors to be investigated. Estimates of impact speed will also become more representative and reliable.

While this project has concentrated on pedestrian collisions with the front of cars, the OTS project investigates accidents involving all types of vehicles. It would be a simple extension to this project to consider these vehicles, although there are far fewer associated pedestrian injuries. A further study could also investigate collisions with other vulnerable road users, such as pedal cyclists and motor cyclists.

The OTS project investigates a representative sample of all traffic crashes, involving all road users and injury outcomes. There would be some merit in enhancing a percentage of crash investigations with additional reconstruction effort beyond the current scope of the OTS project to provide analysis projects, such as this study, with comparative cases that could be used to validate the wider database findings. Examples could include utilising specialist crash reconstruction software techniques to give a more in-depth understanding of the crash kinematics for a sub-sample of cases.

ACKNOWLEDGEMENTS

The OTS project is funded by the Department for Transport and the Highways Agency. The On The Spot investigations are carried by teams at the Transport Research Laboratory (TRL) in Berkshire and the Vehicle Safety Research Centre (VSRC) Loughborough University. The project would not be possible without help and ongoing support from many individuals, especially including the Chief Constables of Nottinghamshire and Thames Valley Police Forces, and their officers. The views expressed in this paper belong to the authors and are not necessarily those of the DfT, HA, Nottinghamshire Police or Thames Valley Police.

REFERENCES

[1] Costano, A (1985). *General Problems concerning Car-Pedestrian collision*, Tenth International ESV conference, vol 2, p943-8.

[2] Ashton, S J; MacKay, G M (1979). *Some characteristics of the population who suffer trauma as pedestrians when hit by cars and some resulting implications*, Proceedings of the 4th IRCOBI conference 1979.

[3] Gavrilu, DM; Marchal, P; Meinecke, MM (2003). *Vulnerable Road User Scenario Analysis*, SAVE-U Project Deliverable 1-A.

[4] Appel, H; Sturtz, G; Gotzen, L (1975). *Influence of Impact speed and vehicle parameter on injuries of children and adults in pedestrian accidents*, IRCOBI 1975.

[5] Matsui, Y (2005). *Effects of Vehicle Bumper Height and impact Velocity on type of lower extremity injury in vehicle-pedestrian accidents*, Accident Analysis and Prevention, v37 n4 p633-40.

[6] Dietmar, O; Pohlemann, T (2001). *Analysis and Load Assessment of Secondary Impact to Adult Pedestrians after Car Collisions on Roads*, IRCOBI 2001.

[7] Road Casualties Great Britain: 2005, DfT National Statistics, see <http://www.dft.gov.uk>

[8] Cuerden, R; Lunt, H; Fails, A; Hill, J; On The Spot Crash Investigations In The UK: New Insights For Vehicle Safety Research. Paper No. 353, 18th ESV conference, Nagoya, 2003.

ACTIVE PEDESTRIAN HEAD PROTECTION AGAINST WINDSCREEN

Violaine Tinar
Nicolas Bourdet
Caroline Deck
Rémy Willinger

ULP-CNRS-7507
Biomechanical Systems Transport and Safety
Institut de Mécanique des Fluides et des Solides
2 rue Boussingault, 67000 STRASBOURG (FRANCE)

ABSTRACT

In road traffic accidents involving pedestrians or cyclists against cars, head injuries are one of the most common injury types and the main cause of fatalities. Recent in deep accident analysis demonstrates that the windscreen, pillars and bonnet are very often involved in case of severe pedestrian head injury. The present study proposes an active protection system for pedestrian or cyclist head impact against the windscreen (and in particular against the pillar) and bonnet area. In case of an automotive impact with a pedestrian, contact or non contact transducers record the impact and transfer the information to actuators which open the bonnet and eject a dampened flexible protective panel which covers the windscreen and pillars. This active protection system prevents the pedestrian's head to come into direct contact with the hard windscreen or pillar and provides a dampened surface on which the head hits, decreasing the risk of head trauma. The panel can eventually be released a few hundreds of milliseconds after head impact in order to provide visibility to the car driver. A second panel is added under the bonnet in order to decrease the risk of head injuries when the pedestrian head impacts the bonnet.

The present proposal suggests illustrating the efficiency of the proposed active and passive protection systems based on the simulation of the pedestrian kinematics and the numerical analysis of the head-protective system interaction at the time of impact. In a first step, the multibody simulation of the pedestrian kinematics showed that an activation of the protective panel within 100 ms and remaining until 250 ms after the impact is appropriate to avoid any direct head contact with the windscreen or the pillar. The multi layered flexible protective panel has then been optimised in terms of layer thickness, elastic-plastic and failure properties against both, HIC value and new biomechanical head injury criteria for adults. Simulations have also been done to evaluate the bonnet system in terms of HIC and biomechanical criteria.

INTRODUCTION

Accident statistics [1] show that more than 42.000 fatalities occur in traffic accidents in Europe per year. Among these accidents 15% are pedestrian and 10% are cyclist. 71% of the pedestrian accidents are non severe or mild, 27% are serious and 2% are fatal. In the case of pedestrian accidents the most frequent injuries concern the head (31%) and the legs (32%). 60% of all fatalities are caused by head injuries occurring when the pedestrian's head impacts the front of the vehicle (bonnet or windscreen) or the ground. As the fatal or severe head injuries are strongly correlated with car initial speed, these impacts concern most often the windscreen and pillar area.

The European Enhanced Vehicle Safety Committee (EEVC WG 10 and WG 17) has developed test procedures to assess the level of pedestrian protection for vehicle fronts. Based on the EEVC WG 17 report, legal requirements have been derived, such as European Directive 2003/102/EC [2]. In order to be conform to the legal requirements of the phase I (took effect in 2005) and phase II (will take effect in 2010) of the European Directive 2003/102/EC on pedestrian protection, passive and active protection systems must be developed. New conception solutions must be found for the bumper, the front end and especially for the bonnet and the windscreen to provide the ability of these parts to absorb kinetic energy without exceeding load limits for the pedestrian. Concerning the windscreen area, it is well known that the central area seldom causes severe injuries but, as soon as the head impact is close to the frame or against the pillar, the outcomes are quasi-systematically dramatic. A possible solution, proposed by Kuehn [3] consists in adding an airbag system under the bonnet. These airbags uplift the bonnet and cover the A-pillars and the lower windscreen frame. The bonnet is raised 40 ms after the impact of pedestrian's legs on the bumper. This system is illustrated in Figure 1 and allows an important decrease of the HIC (Head Injury Criteria) value for a velocity of 40 km/h. This solution has two main advantages: firstly, the airbags uplift the bonnet and increase thus the

deformation space under the bonnet (which enhances the kinetic energy absorption) and secondly, they protect the pedestrian against the A-pillars. However this system only protects the lower part of the A-pillars and does not take into account the upper part and the roof edge. Moreover, this protective design is known to be a quite expensive solution.



Figure 1. Passive protection system with airbags uplifting the bonnet (Kuehn, [3]).

Other solutions exist, but only for the bonnet improvement with regards to pedestrian head protection. As illustrated in Figure 2 the bonnet inner panel is traditionally designed as a rib structure supporting the bonnet outer panel.

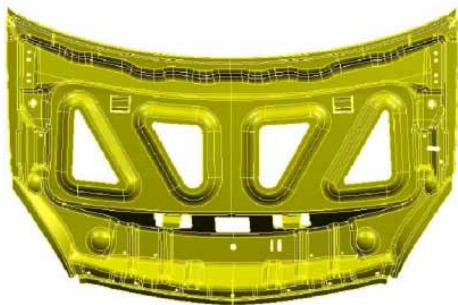


Figure 2. Traditionnal bonnet inner panel rib structure (Kerkeling, [4]).

The main problem with this type of structure is the presence of stiff points: at these points the HIC (or HPC) often exceeds the limit of 1000. With regards to pedestrian protection it would be preferable to have a uniform stiffness all over the bonnet. This is the reason why many automobile manufacturers have proposed new bonnet inner panels. One solution is to increase the number of ribs in the inner panel: this makes the stiffness more homogenous even though some stiff points remain. Another solution is to change the structure of the bonnet inner panel: multi-cones are drawn in the inner panel and glued to the outer panel. The main advantage of this solution is the ability to adjust the bonnet stiffness by several parameters: geometry of cones, cut-outs of cones and glue type. The Figure 3 illustrates these two bonnet inner panel structures

[4]. The both solutions yield much more homogeneous stiffness distribution.



Figure 3. New bonnet inner panel structures:

- **top: inner panel with more ribs**
- **bottom: multi-cones inner panel (Kerkeling, [4]).**

The improvement of the capability for kinetic energy absorption for the bonnet without exceeding load limits for the pedestrian requires appropriate bonnet stiffness as well as an adequate deformation space under the bonnet. To achieve these requirements a new solution consists in setting actuators under the bonnet so as to raise the bonnet after sensors have detected a collision with pedestrian legs [5]. This system is illustrated in Figure 4.

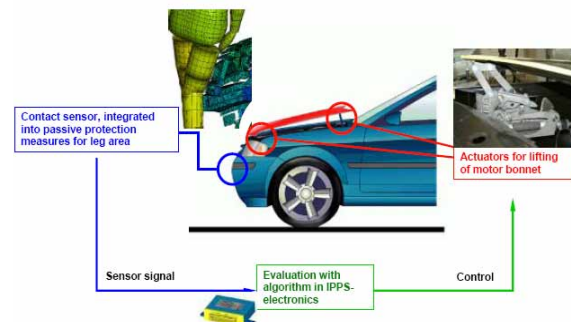


Figure 4. Passive protection system with sensors and actuators for lifting of motor bonnet (Scherf, [5]).

In the present study a solution that was designed to protect the pedestrian head against both the windscreen (with the A-pillars) and the bonnet is proposed. In the case of an automotive impact with

a pedestrian, contact or non-contact transducers record the impact at bumper level and transfer the information to actuators which open the bonnet and eject a dampened flexible protective panel which covers the windscreen and the pillars as shown in Figure 7. This active panel prevents the pedestrian's head to come into direct contact with the hard windscreen and provides a damping surface on which the head hits, diminishing the risk of head trauma. The plate can eventually be released a few hundreds of milliseconds after head impact in order to provide visibility to the car driver. During a vehicle-pedestrian accident the head does not always hit the windscreen: the impact point depends of several parameters, such as the vehicle speed or the pedestrian size. For this reason, a new bonnet structure with a protective panel under the upper panel of the bonnet has been designed.

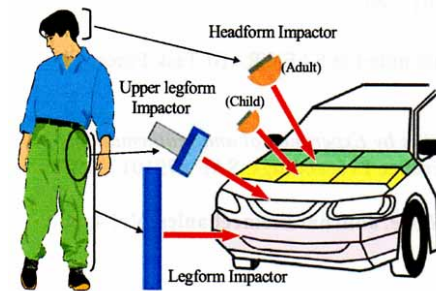
The timing of this new system has first been evaluated with multibody pedestrian kinematics simulation in order to define the appropriate time for ejecting the protective panel. This new active protection system has then been modelled with finite element software and evaluated in terms of HIC and maximum acceleration (according to European Directive 2003/102/EC). Finally the new design has been evaluated numerically by modelling the head impact with an anatomical head FEM model. This permitted it to express the performance of the solution against biomechanical based head injury criteria. The same procedure has been used to evaluate the bonnet solution: first, according to European Directive, simulations with a standard pedestrian head have been carried out and secondly an anatomical head has been used to evaluate the bonnet in terms of biomechanical criteria.

REQUIREMENTS

Directive 2003/102/EC

In the Directive 2003/102/EC [2] two head forms are considered: a child head with a mass of 2.5 kg and an adult head with a mass of 4.8 kg. The impact angles of the head forms are set to 50° measured from the ground reference line for the child head and to 65° for the adult head. Both head forms should impact the bonnet with a velocity of 40 km/h.

In terms of head criteria the Directive 2003/102/EC advocates an HIC (Head Injury Criteria) lower than 1000 for both child and adult head forms, and a maximal linear acceleration of the centre of gravity of the head form (γ_{max}) between 405 and 495g for a child head form and between 337.5 and 412.5g for an adult head form. All these requirements are illustrated in Figure 5.



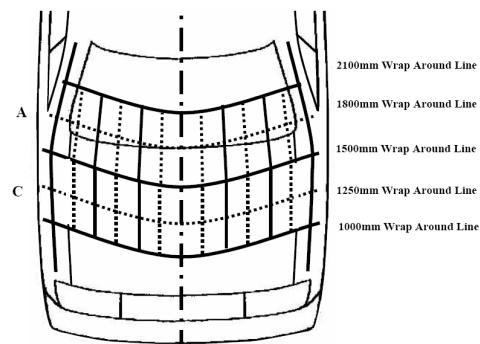
	Child head	Adult head
velocity	40 km/h	40 km/h
mass	2.5 kg	4.8 kg
HIC	1000	1000
γ_{max}	405 to 495g	337.5 to 412.5g

Figure 5. Directive 2003/102/EC requirements.

EuroNCAP

The impactor characteristics in EuroNCAP tests [3], in terms of mass and impact velocity, are the same as in Directive 2003/102/EC. Nevertheless the impact zones are more precisely defined in this protocol thanks to a splitting of the bonnet into 48 zones, as shown in Figure 6. This splitting enables the definition of two impact zones: one for the child head (C) and one for the adult head (A).

In term of injury criteria the one chosen is the HIC, the value of which must not exceed 1000.



	Child head	Adult head
velocity	40 km/h	40 km/h
mass	2.5 kg	4.8 kg
HIC	1000	1000

Figure 6. EuroNCAP Protocol requirements.

THE ACTIVE PROTECTION SYSTEM

Pedestrian Kinematics

The entire kinematics of the pedestrian was computed with a multibody approach (Madymo code) in order to fix the triggering of the system. Of particular importance was it to define the time range between bumper-leg contact and head – windscreen contact. Therefore a side impact between a pedestrian and a car has been carried out

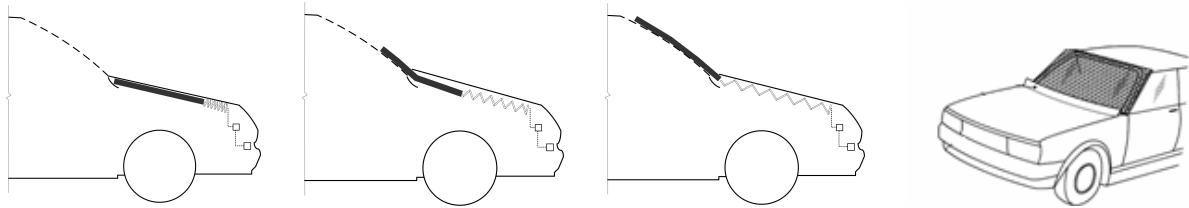


Figure 7. Illustration of the active pedestrian head protection system.

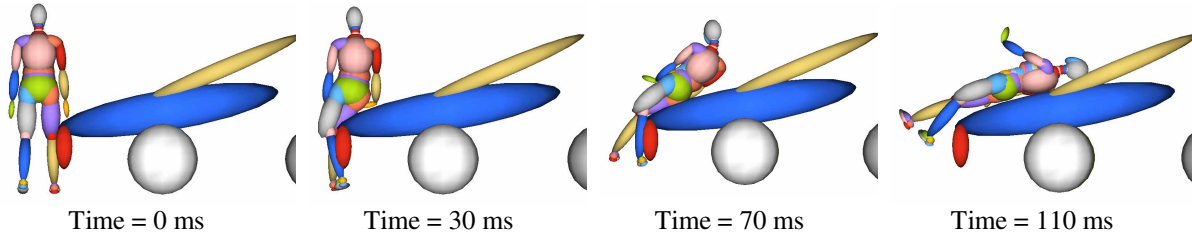


Figure 8. Illustration of pedestrian kinematics when hit by a car for protective panel activation triggering purpose.



Figure 9. Illustration of the active pedestrian head protection system. The arrow in the picture points the active panel and its positioning over the windscreen pillar and roof rail.

with the initial velocity of the car set to 11.28 m.s^{-1} . The multi-body simulations show that an activation of the protective panel within 100 ms after the impact for approximately 150 ms is appropriate to avoid any direct head contact with the windscreen or the pillars as illustrated in Figure 8. It has been shown that this time range is efficient for typical vehicle speed, i.e. 11 m.s^{-1} .

The relevance of the proposed protective system has then been evaluated numerically with a windscreen model or panel model and two different head models, a standard pedestrian head and an anatomical head.

Head Modelling

Two head finite element models have been used for the head impact simulations: a standard pedestrian head model and an anatomical head FEM model for which injury criteria have been defined in earlier studies.

The pedestrian head model is the standard ISO model represented in Figure 10, which consists of three parts, i.e. an aluminium sphere, an aluminium plate and a rubber skin. Each of the three parts is modelled with an elastic law in conformity with values reported in Table 1. The head model is made of 3020 eight-node brick elements.

The anatomical head model is the ULP finite element head model [6]. This model, which is described more in details in the literature, includes the face, the dura matter (falx and tentorium), the subarachnoidal space, the brain and the cerebellum as shown on the Figure 11.

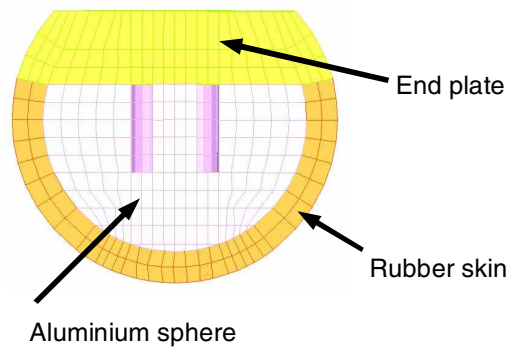


Figure 10. Standard ISO pedestrian head model.

Table 1. Mechanical properties of the different parts of the pedestrian head finite element model.

	$\rho \text{ (kg.m}^{-3}\text{)}$	$E \text{ (MPa)}$	ν
Aluminium sphere	2800	200000	0.29
Rubber skin	1950	7	0.4
End plate	2800	200000	0.29

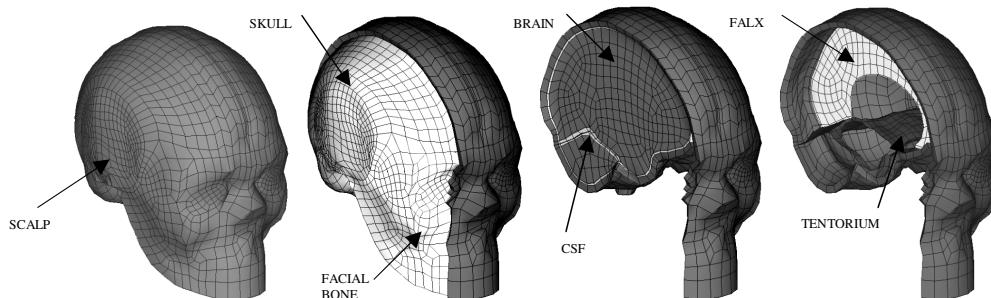


Figure 11. Illustration of the ULP finite element head model.

Tolerance limits for this model have been established by reconstructing 64 real world accident cases [7, 8] and summarized in Table 2. In order to evaluate the relevance of active protective panel on the windscreen, these limits will be used to predict the severity of head injuries and will be considered for further panel optimisation.

Table 2. Tolerance limits related to the ULP head FE model [8].

Mechanical parameter	Maximum strain energy in the CSF layer	Maximum Von Mises stress		Maximum strain energy in the skull
		Moderate DAI	Severe DAI	
Injury	Subdural or Subarachnoid haematoma	Moderate DAI	Severe DAI	Skull fractures
Tolerance limit	4211 mJ	27 kPa	39 kPa	833 mJ

Windscreen Modelling

FEM Model

The windscreen consists of three layers (two glass layers and a PVB layer) whose characteristics are given in Table 3. Each material is supposed to have an elastic brittle behaviour [9]. The A-pillars have been considered as rigid bodies.

The damping material is represented by four layers of eight-node bricks (11.740 bricks with a total thickness of 30 mm). The chosen damping material is expanded polystyrene with an 85 kg.m^{-3} density whose behaviour law has been established through experimental compression tests. The stress strain behaviour in compression is illustrated Figure 12.

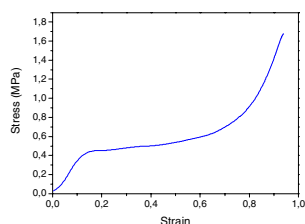


Figure 12. Stress strain curve of expanded polystyrene.

Table 3. Mechanical properties of the windscreen.

	ρ (kg.m^{-3})	E (GPa)	ν	ϵ_{t1}	ϵ_{m1}	t (mm)
Glass	2400	65	0.22	6.15×10^{-4}	1.23×10^{-3}	2.2
PVB	950	50	0.21	0	0	2

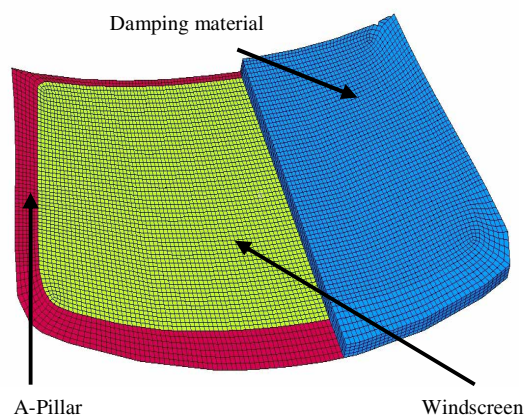


Figure 13. General view of pillar, windscreen and protective panel mode. Protective panel is only partially represented.

Head Impact Conditions

Head impacts have been carried out to evaluate the new protective system first in terms of HIC with the pedestrian head model and then in terms of biomechanical criteria with the ULP head model. The chosen initial conditions for the simulations are close to a typical pedestrian head impact condition as defined here after. The model was impacted at the junction between the windscreen and the A-pillar, with an impact angle of 65° and an initial velocity of 5 m.s^{-1} . Figure 14 represents the head before the impact. This impact condition is considered to be the most significant as it considers a quite critical situation.

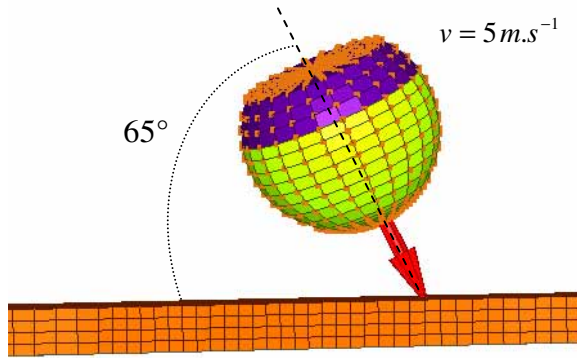


Figure 14. Illustration of the pedestrian standard head impact initial condition on the windscreen or protective panel: the standard head has an initial velocity of 5 m.s^{-1} with an impact angle of 65° with the windscreen.

Bonnet Modelling

FEM Model

The numerical model of the bonnet is characterised by the following components: the upper panel represented by 4032 four nodes shell, the protective panel represented by three layers of eight-nodes brick (12 096 bricks with a total thickness of 30 mm) and the engine block modelled with 4019 four nodes shell elements and 2664 eight-nodes brick elements. The different parts of the bonnet model are illustrated in Figure 15.

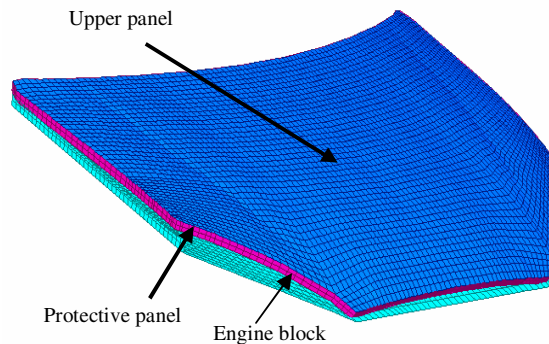


Figure 15. General view of upper panel (blue), protective panel (magenta) and engine block (green).

The chosen material for the upper panel is aluminium which is supposed to have an elastic plastic behaviour, the characteristics of which are given in Table 4. The protective panel material is expanded polystyrene, the characteristics of which are the same as those used for the windscreen model. The engine block has been considered as rigid body.

The boundary conditions are one of the most important parameters that influence the behaviour of the bonnet. The upper panel of the bonnet FEM

model is fixed in two points in the front of the bonnet and the engine block is fixed.

Table 4. Mechanical properties of the bonnet upper panel.

ρ (kg.m^{-3})	E (MPa)	ν	σ_e (MPa)	b (MPa)	n	σ_m (MPa)
2700	65000	0.3		567	0.623	345

Head Impact Conditions

The chosen initial conditions for the simulations are those prescribed by the EuroNCAP Pedestrian Testing Protocol. The head was impacted in the middle of the bonnet, with an initial velocity equal to 11.1 m.s^{-1} and an impact angle measured from the ground reference equal to 65° . The position of the head before the impact is represented in Figure 16.

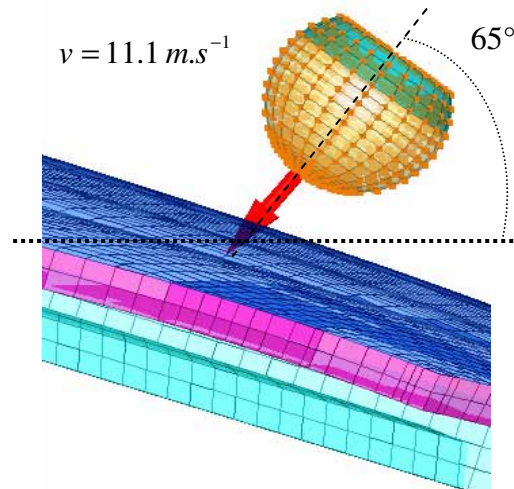


Figure 16. Illustration of the initial impact conditions of the standard head model on the bonnet: the initial velocity is equal to 11.1 m.s^{-1} and the impact angle is 65° measured from the ground reference.

Bonnet Evaluation Method

Based on 425 EuroNCAP tests, procedures have been defined to built stiffness corridors for the different vehicle front parts area (bumper, bonnet and windscreen). These corridors have been obtained by recording the normal acceleration of the centre of gravity of the head: this acceleration is integrated twice to get the displacement and multiplied with the impactor mass to get the normal impact force. All the obtained force-displacement curves have been classified into three categories defined by EuroNCAP [11]. The bonnet FEM model is considered as “yellow bonnet”, i.e. its HIC is between 1000 and 1350 and its force-displacement curve is inside the corridor represented in Figure 17.

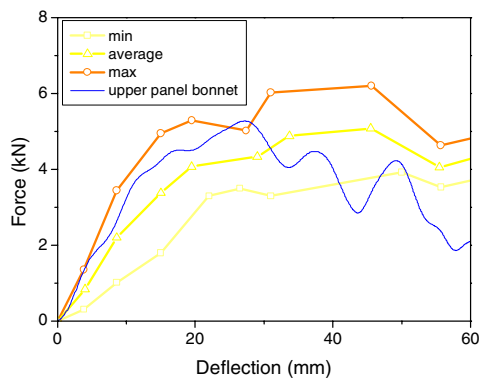


Figure 17. Simplified stiffness corridor for a “yellow bonnet” (HIC between 1000 and 1350) and proposed upper panel stiffness.

RESULTS

Windscreen Results

In order to demonstrate the improvement brought by this new system all simulations have been done with and without the protective panel. Radioss code has been used for this purpose. The simulations have been carried out first with regards to standards in terms of HIC and maximal linear acceleration. The results are given in Figure 18 and Figure 20. These results demonstrate the real improvement brought by the proposed system: as the HIC value decreases significantly when a protective panel is added to the windscreen and the A-pillars. The same improvement can be observed in terms of maximal linear acceleration of the centre of gravity as a whole HIC value has been divided by about 8 and remains under tolerance level when the protective panel is activated.

Same simulations have been carried out with the ULP model in order to predict the potential injuries during the impact of the head against the windscreen alone and the windscreen with the protective panel. The results are reported in Figure 21 in terms of maximum strain energy in the skull and in terms of maximum strain energy in the CSF layer and intracranial Von Mises shearing stress. The recommended tolerance limit for the maximum strain in the CSF layer is 4211 mJ, which is equivalent to an injury risk of 50% of subdural haematoma.

The results show that, without damping material, the maximum strain energy in the CSF layer reaches 7370 mJ (this implies a significant risk of subarachnoid or subdural haematoma) whereas this value decrease to 755 mJ with the protective panel, eliminating the SDH risk.

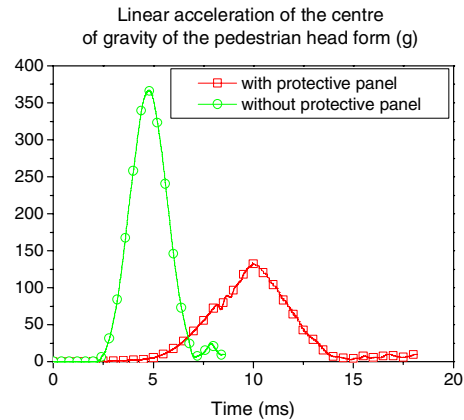


Figure 18. Evolution of the linear acceleration of the standard head form centre of gravity during impact with and without protective panel over the windscreen.

The same trend can be observed for the maximum strain energy in the skull as the initial value of 2038 mJ without damping material decreases to 95 mJ when adding the panel, eliminating thus the skull fracture risk.

The results in terms of Von Mises stress are given Figure 21 (c). Here again the risk of moderate neurological injury has been eliminated by the protective system.

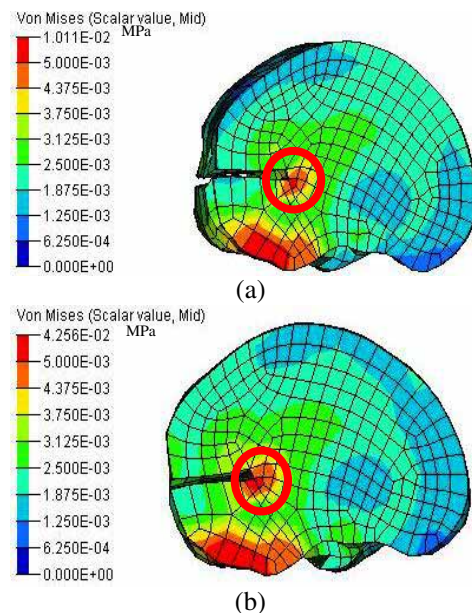


Figure 19. Localisation in sagittal section of the maximum Von Mises stress response computed with the ULP head model impacting the windscreen (a) and the windscreen with protective panel (b).

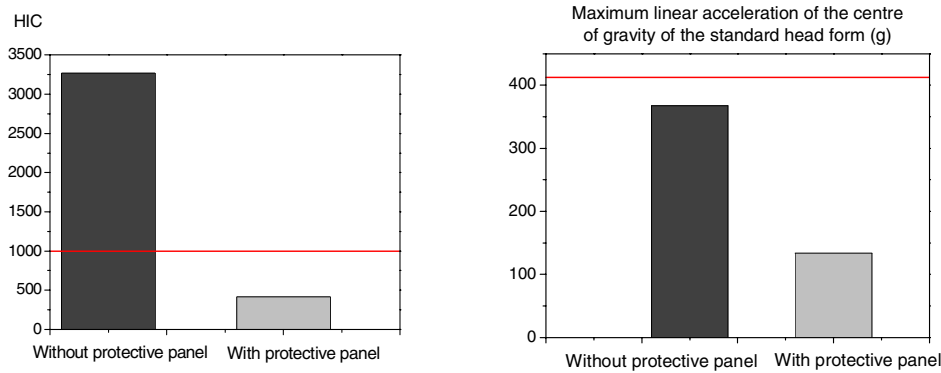


Figure 20. HIC and γ_{\max} results for the two cases (with and without damping material).

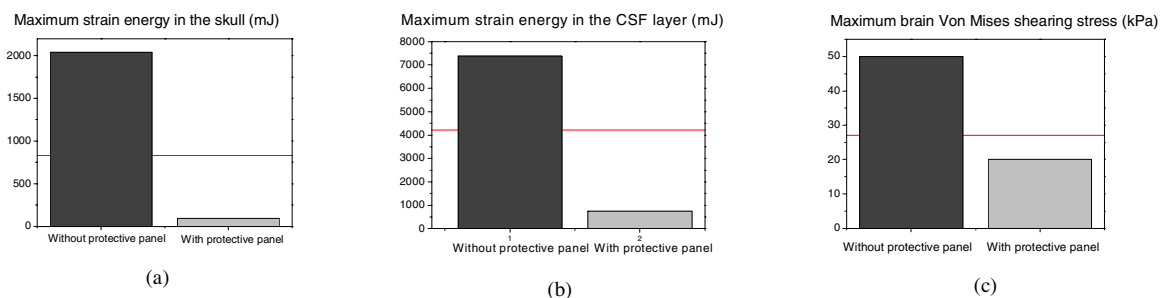


Figure 21. Intracranial head response computed with the ULP head model impact against the windscreen (black) and the windscreen with the protective panel (grey) in terms of strain energy in the skull (a), strain energy in the CSF layer (b) and in term of maximum brain Von Mises shear stress (c).

In Figure 19 the distribution of the intracranial Von Mises stress is shown. The maximum area is situated at the same place and only the maximum values vary.

Bonnet Results

In the same way as for the windscreen, all the simulations have been done with and without the protective panel. The bonnet has first been evaluated with regards to standards in terms of HIC and maximal linear acceleration. The results are given in Figure 22. The results in terms of HIC show the improvement due to the adding of a protective panel under the bonnet: with the panel the HIC value is 989 and is under the recommended limit of 1000. The same trend can be observed in terms of maximal linear acceleration of the centre of gravity of the head.

The two situations (with and without protective panel) have always been simulated with regards to biomechanical criteria. The results are reported in Figure 23 in terms of maximal strain energy in the skull, maximal strain energy in the CSF layer and in terms of maximum brain Von Mises shear stress. In the case of an upper panel without the protective panel, all the results are over the tolerance limits. The maximum strain energy in the skull reaches

13667 mJ, the limit being 833 mJ (Figure 23 (a)), so there is a very high risk of skull fracture. The maximum strain energy in the CSF layer is 6282 mJ whereas the limit is 4211 mJ (Figure 23 (b)) which corresponds to a high risk of subdural or subarachnoidal haematoma. Finally the maximum brain Von Mises shear stress reaches the value of 42 kPa (limit being 39 kPa) for severe neurological injuries (Figure 23 (c)). All these values decrease significantly when adding the protective panel under the bonnet: the maximum strain energy in the skull and in the CSF layer stays under the tolerance limits, and in the skull, even though the value of the maximum strain energy has significantly decreased, it remains slightly above the limit. Figure 24 shows the distribution of the intracranial Von Mises stress. The area of the maximum Von Mises stress varies when adding the protective panel: this area is situated on the top of the brain for simulations without the protective panel and inside the brain with the protective panel.

The numerical study of the proposed solution showed a real improvement when adding a damping panel on the windscreen or under the bonnet, in terms of HIC and maximum linear acceleration as well as in terms of biomechanical criteria.

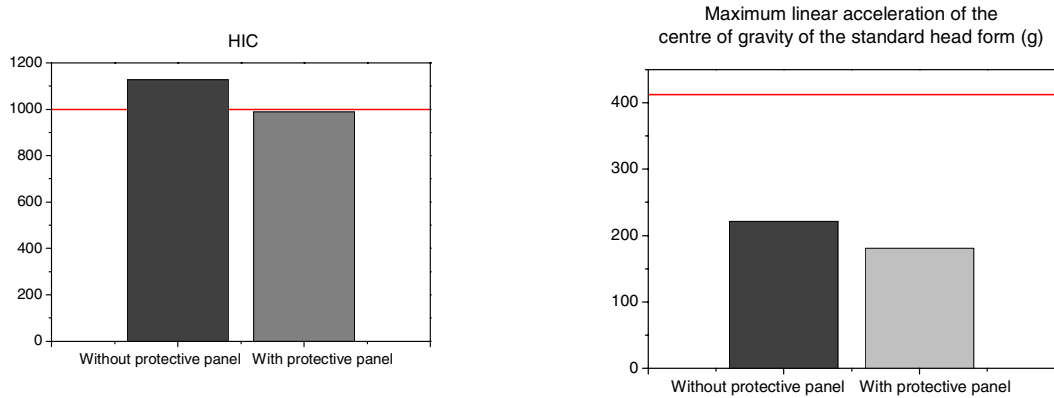


Figure 22. HIC and γ_{\max} results for the two cases (with and without damping material).

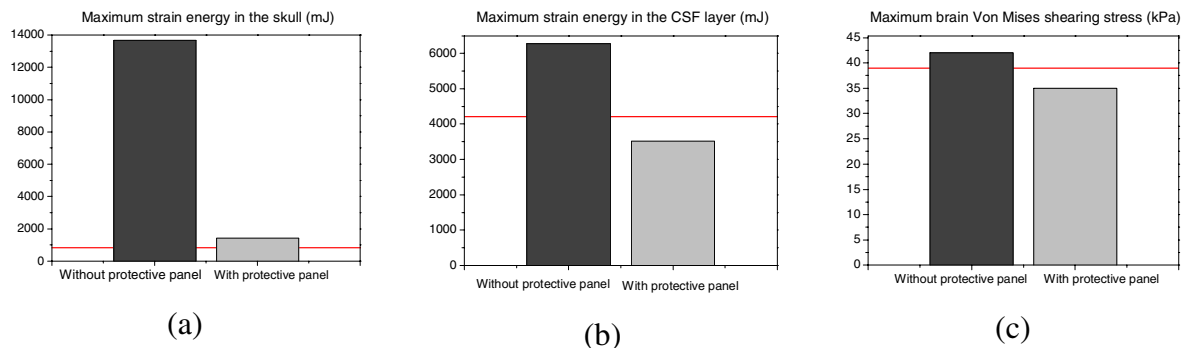


Figure 23. Intracranial head response computed with the ULP head model impact against the bonnet (black) and the bonnet with the protective panel (grey) in terms of strain energy in the skull (a), strain energy in the CSF layer (b) and in term of maximum brain Von Mises shearing stress (c).

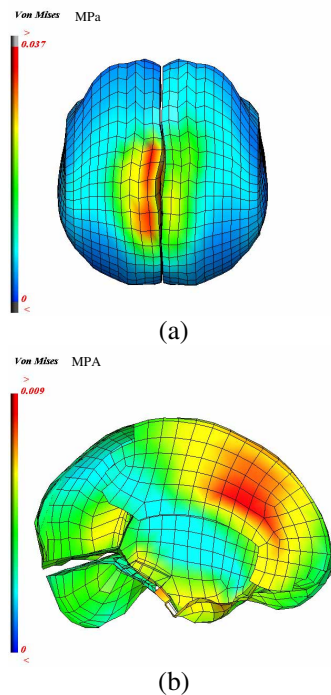


Figure 24. Localisation of the maximum Von Mises stress response computed with the ULP head model against the bonnet (a) and the bonnet with protective panel (b).

CONCLUSION AND DISCUSSION

The proposed innovative solution for protection of the pedestrian head during impacts on the windscreen or the pillars has been shown to be efficient if propelled in the 100 – 250 ms time frame. It decreases significantly the risk of head trauma for these pedestrians, in terms of HIC criteria as well as with regards to biomechanical criteria. The same improvements have been obtained with the new bonnet solution: when adding a protective panel under the bonnet, the risk of head injuries decreases importantly. Moreover these inventions have a huge economical and social interest as safety is a society priority but also an important sale argument.

REFERENCES

- [1] Otte, D: Possibilities of head protection analysis on the basis of accident data, Medical University Hannover.
- [2] Directive 2003/102/EC of the European Parliament and of the Council, 17th November 2003.

- [3] Kuehn, M: Assessment of vehicle related pedestrian safety, Paper Number 05-0044.
- [4] Kerkeling, Christoph: Structural hood and hinge concepts for pedestrian protection, GM Europe, Paper number 05-0304.
- [5] Scherf, Oliver: Development and performance of contact sensors for active pedestrian protection systems, Siemens restraint systems GmbH, Paper number 05-0021.
- [6] Kang HS, Willinger R, Diaw B, Chinn B (1997) Validation of a 3D anatomic human head model and replication of head impact in motorcycle accident by finite element modelling. Proceedings of the 41st STAPP Car Crash Conference, Lake Buena Vista, USA, November 1997, pp 329–338
- [7] Willinger R., Baumgartner D., Human head tolerance limits to specific injury mechanisms, International journal of Crashworthiness, Vol 8, No 6, 2003, pp.605-617.
- [8] Marjoux D. et al : Head injury prediction capability of the HIC, HIP, Simon and ULP criteria, IRCOBI Conference, Madrid (Spain), September 2006.
- [9] Mukherjee, S.: Modelling of head impact on; laminated glass windshields, IRCOBI 2000.
- [10] EuroNCAP, Assessment protocol and biomechanical limits, Version 4.1, March 2004.